

ION CYCLOTRON RESONANCE INVESTIGATIONS
OF NEGATIVE ION-MOLECULE REACTIONS

Thesis by

Sally Anne Sullivan

In Partial Fulfillment of the Requirements
For the Degree of
Doctor of Philosophy

California Institute of Technology
Pasadena, California

1978

(Submitted August 11, 1977)

For Mom - a beautiful lady, who deserves the best.

Acknowledgment

I want to thank Jack Beauchamp for his assistance and interest. Jack and the other group members (past and present) have become friends rather than just coworkers. I thank them all for fun and games, sympathy, insight, enthusiasm and caring. In particular, Frances Houle has become a close friend and aided me in numerous ways, thanks for being there. Wally, Pete, David, Amy, Pat and Glen have been particularly helpful by providing me with entertainment and distraction during the last few months, thanks. There are special bonds between those who arrive here together, suffering through candidacy and thesis writing, so thanks Reed Corderman and Ron Hodges for four years of commiseration. I also thank Caltech for four years of financial support. There are many people who have been part of my experience at Caltech, but Cindy, you have been here from the beginning with friendship and a talent for listening. Thanks for late-night talks and shelter when things got rough.

Abstract

Chapter I

Ion cyclotron resonance techniques are employed in the examination of the gas phase reactions of PF_3 and OPF_3 with anionic bases, including NH_2^- , OH^- , $\text{CH}_3\text{CH}_2\text{O}^-$, HNO^- , HS^- , SF_6^- , and SF_5^- . Evidence is presented which suggests that all reactions proceed by initial attack at phosphorous, with products resulting from decomposition of chemically activated intermediates. The energetics of intermediates inferred in these processes are related to the Lewis acidities of OPF_3 and PF_3 . With fluoride ion as a reference base, OPF_3 is found to be more acidic than PF_3 , with $D(\text{OPF}_3-\text{F}^-) = 58.9 \pm 0.4$ kcal/mole and $D(\text{PF}_3-\text{F}^-) = 50 \pm 5$ kcal/mol.

Chapter II

Ion cyclotron resonance techniques are employed to determine the gas phase Brönsted and Lewis acidities as well as the Brönsted basicity of 1-methyl-1,4 dihydroborabenzene, $\text{CH}_3\text{BC}_5\text{H}_6$. The ring proton is found to be highly acidic with $\text{PA}(\text{CH}_3\text{BC}_5\text{H}_5) = 337 \pm 3$ kcal/mol. This acidity results from the formation of 6π electron aromatic anion $\text{CH}_3\text{BC}_5\text{H}_5^-$, which is isoelectronic with toluene. Both the Lewis acidity and proton basicity of the parent molecule suggest that there is little interaction between the diene π system and the electron deficient boron. This is further confirmed by the similarity of both negative and positive ion chemistry of the borabenzene to that of aliphatic boranes.

Chapter III

Ion cyclotron resonance techniques are employed in the investigation of positive and negative ion formation and ion molecule reactions in sulfuryl halides SO_2XY ($\text{X}, \text{Y} = \text{Cl}, \text{F}$). Positive ion reactivity is discussed in terms of the relative Cl and F bond strengths in these species and possible structures of ionic intermediates and products. Electron attachment processes generate halide ion donors such as F_2^- , Cl_2^- , SO_2F^- and SO_2Cl^- from sulfuryl halides. Negative ion reactivity is dominated by halide transfer reactions. Halide transfer reactions in mixtures with HCN and HCl are examined in an attempt to quantify $\text{D}(\text{SO}_2-\text{F}^-)$ and $\text{D}(\text{SO}_2-\text{Cl}^-)$.

TABLE OF CONTENTS

	<u>Page</u>
INTRODUCTION	1
CHAPTER I Nucleophilic Reactions of Anions with PF_3 and OPF_3 in the Gas Phase Using Ion Cyclotron Resonance Spectroscopy	11
CHAPTER II Acid-Base Properties of 1-Methyl-1,4 Dihydroborabenzene, $\text{CH}_3\text{BC}_5\text{H}_6$	52
CHAPTER III Positive and Negative Ion-Molecule Reactions of Sulfuryl Halides	81
APPENDIX I Negative Ion Formation and Ion-Molecule Reactions in Alkyl Nitrites	110
APPENDIX II Reactions of HNO^-	125
APPENDIX III Tables of Gas Phase Acidities	127

Introduction

Ionic species have long been postulated as reaction intermediates in solution.¹ Consequently, reactivity is often described in terms of the stabilities and charge distributions of such intermediates. There is much evidence that solution effects may strongly modify the properties of these species. For this reason, ion cyclotron resonance techniques have been a valuable tool in the investigation of intrinsic molecular properties and reactivity.²

A broad and important class of solution reactions initiated by nucleophilic attack are proposed to proceed through anionic intermediates.¹ Gas phase anion reactions not only provide models for solution reactions but provide thermochemical properties (proton and Lewis acidities) which are not modified by solvation effects. In part because of the difficulties in generation of ionic reagents, anionic reactions have not been studied as extensively as positive ion reactivity. Gas phase studies performed relate to the interaction of bases with acidic protons,^{4,5,6} anionic nucleophilic attack^{7,8,9} and anion exchange reactions.^{10,11}

The predominant reaction of an anionic base with an acidic neutral is simple proton transfer. Gas phase proton acidities are inversely related to the proton affinities of the anionic conjugate bases (B^-). The proton affinity $PA(B^-)$ is defined as the enthalpy for reaction 1. Relative proton affinities are measured by determining the



preferred direction of proton transfer (eq 2) in mixtures of neutrals.²

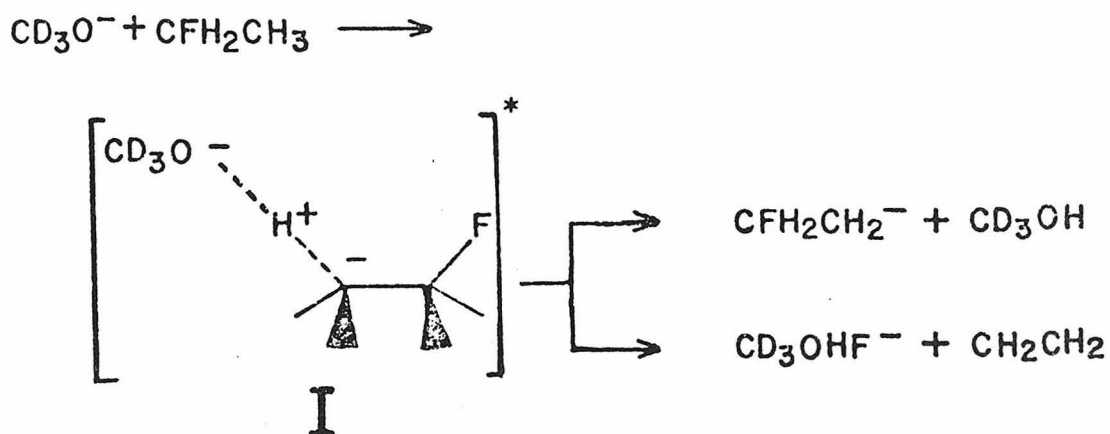


Ion cyclotron resonance techniques are particularly useful in this regard.² Quantitative relative proton affinities result from measurements of K_{eq} (eq 2) using either icr trapping studies¹² or high pressure mass spectrometry.¹³ Appendix III provides several tables of relative gas phase acidities of representative compounds including carbon, oxygen and inorganic acids. References included in this appendix provide both discussions of trends in acidities and comparisons to solution results. An interesting reversal is found in the acidities of alcohols. In solution, the acidities of alkyl alcohols generally decrease with increased alkylation $CH_3OH > CH_3CH_2OH > t-C_4H_9OH$.¹ This is explained in terms of increasing electron donation by the alkyl group.^{1,14} The gas phase ordering $tC_4H_9OH > C_7H_5OH > CH_3OH$ ^{14,15} suggests induced dipole effects (which increase with the polarizability of the alkyl group) provide anion stabilization.¹⁴ Comparisons of gas phase and solution acidities provide information on both intrinsic molecular properties and solvation effects.

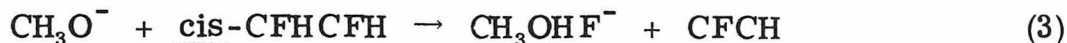
Strong hydrogen bonds may result from interaction of anionic bases with acidic species. For example, the interaction of alkoxide ions with fluoroalkanes^{5,6,7} results in energetic hydrogen bonded intermediates which decompose resulting in proton transfer or HF elimination as in Scheme 1 for CH_3O^- with CH_3CH_2F . The energy to

eliminate HF from the alkane is provided by the formation of the hydrogen bond ($\sim 40 \text{ kcal mole}^{-1}$) in the intermediate. There is a general trend favoring elimination as base strength decreases.

Scheme 1

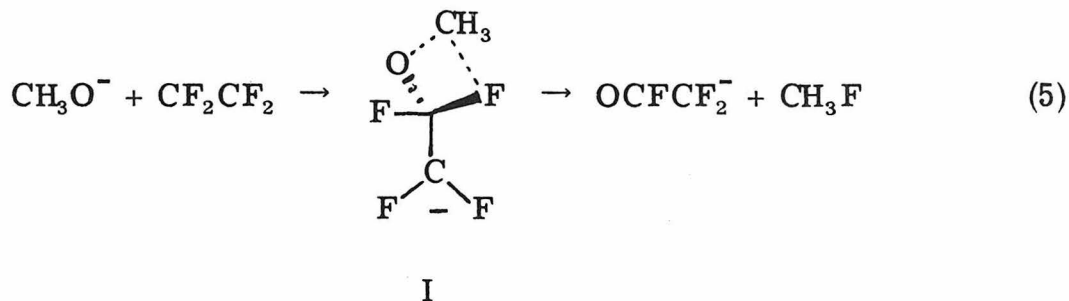
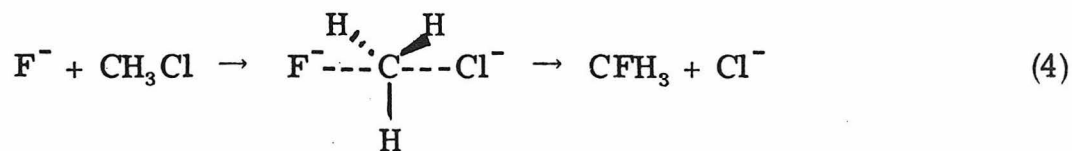


Although the formation of the hydrogen bound anion CH_3OHF^- suggests a cis HF elimination from the energetic intermediate (Scheme I), the reactions of fluoroethylenes with gas phase bases suggest a more complicated mechanism.⁷ When both cis 1,2-difluoroethylene and trans 1,2-difluoroethylene were treated with CH_3O^- , elimination of HF was observed only from the cis olefin (eq 3).



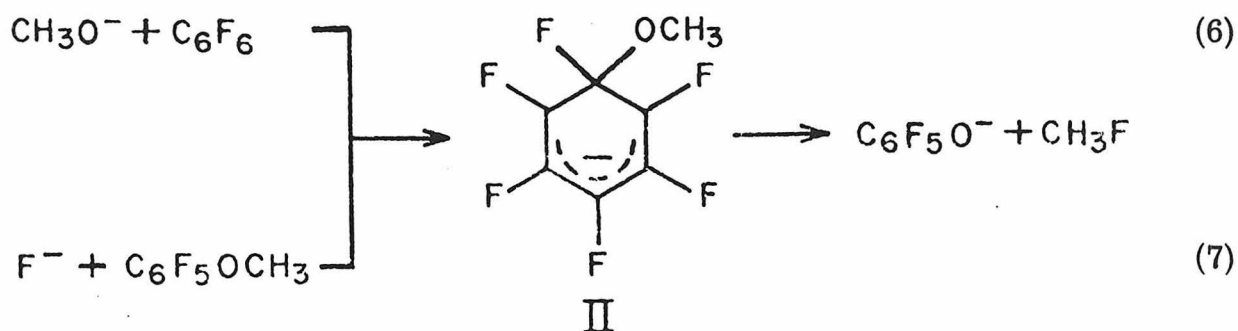
Although there is no thermochemical basis for a differences in reactivity of the isomers, solution results suggest that the F trans to the site of negative charge will have a larger portion of distributed electron density.¹⁶ In this case, the formation of CH_3OHF^- is facilitated by the stronger interaction of ions with polar molecules.¹⁷ Such interactions may result in multiple encounters, which would explain formation of CH_3OHF^- through an apparent trans-elimination.

Nucleophilic anionic attack results in direct substitution reactions (eq 4, for Cl^- with CH_3Cl) and more complicated rearrangement processes, exemplified by the generation of the fluoroenolate anion OCFCF_2^- on reaction of CH_3O^- with CF_2CF_2 (eq 5).⁷ Since a compre-

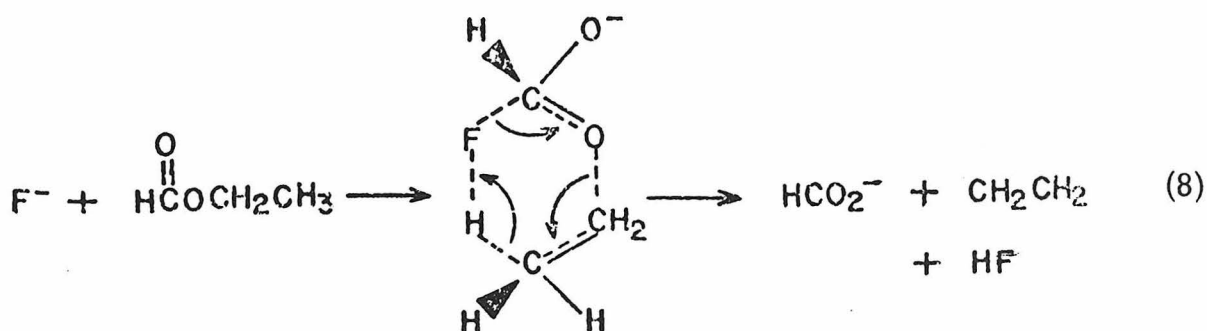


hensive discussion of the mechanism of nucleophilic substitution reactions has been provided recently by Olmstead and Brauman,¹⁸ these reactions will not be discussed further.

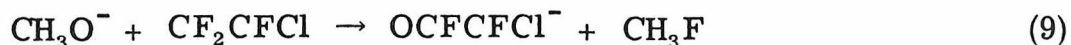
Reaction (4) exemplifies what now appears to be a general reaction of negative ions with a variety of substrates. In this reaction, products apparently result from initial attack at the electropositive carbon (as in I), followed by a 4-center rearrangement to lose CH_3F . A similar mechanism is suggested for alkoxide attack on fluoro-benzenes.⁸ The formation of the same ionic product on reaction of F^- with the pentafluoro anisole (eq 6)⁸ and reaction of CH_3O^- with pentafluorobenzene (eq 7),⁷ indicates that species II is intermediate



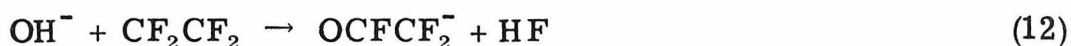
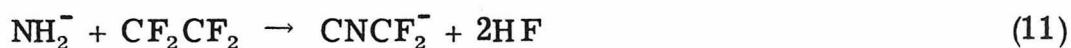
in both cases. Rate measurements of the reactions of F^- with alkyl formates HCO_2R (eq 8, $\text{R} = \text{C}_2\text{H}_5$) as a function of R group, indicate



that reaction results from the decomposition of a 6-center intermediate to form HF and olefin.⁹ In all of the above reactions direct elimination of the basic F^- or OR^- anions does not occur. Rearrangements proceed to eliminate an energetically favorable neutral (HF or CH_3F). It might be expected that elimination of a good leaving group (Cl^- , Br^-) might predominate over this rearrangement process. Interestingly, the only products observed on reaction of CF_2CFCl and CF_2CFBr with CH_3O^- are the chloro and bromoenolate anions (eq 9, 10).⁷ Reactions of this



type also occur with NH_2^- and OH^- with CF_2CF_2 (eq 11 and 12).⁷ In the



latter case loss of 2HF occurs directly, with no detection of $HNCFCF_2^-$.

Investigations of anion transfer reactions have provided relative gas phase Lewis acidities,^{10,11} and hydrogen bond strengths in proton-bound anionic¹⁹ species. As for gas phase proton acidities, Lewis acidities of neutrals toward an anionic base can be determined by examination of the preferred direction of anion transfer (eq 13).



At present, F^- transfers have been the most extensively investigated. Murphy and Beauchamp have examined F^- transfers to determine the relative Lewis acidities of a variety of boron^{10,11} and silicon compounds.¹¹ For example, the Lewis acidities of alkyl boranes are found to increase with alkylation $(CH_3)_3B < (CH_3CH_2)_3B < (i-C_3H_7)_3B$. This suggests, as with the acidities of alcohols, that the increased polarizability of the larger alkyl groups allows better anion stabilization. It is well known from solution studies that relative Lewis acidities are dependent on the reference base, for this reason further investigation of other anion adducts is important.

Bihalide ions, with unusually strong hydrogen bonds (XHY^-) can be produced by elimination reactions⁶ or by halide transfer to hydrogen halides¹⁰ (eq 14). Yamdagni and Kekarle have proposed that the



hydrogen bonds $D(XH-Y^-)$ will increase with the acidity of XH and the basicity Y^- .²⁰ These trends have been confirmed by icr investigations of halide¹⁹ transfer reactions. Quantitative values for these bond strengths may eventually be available from these studies by comparisons to reference anions (i.e., F_2^- , Cl_2^- or FHF^-).

This thesis describes further investigations of negative ion chemistry related to nucleophilic reactivity, acidity studies and halide transfer reactions. Chapter I deals with nucleophilic attack at phosphorous in OPF_3 and PF_3 . Rearrangements to lose HF , similar to those noted above, predominate. In Chapter II the acid-base

properties of methyl 1,4-dihydroborabenzene are discussed. Using acidity measurements the resonance energy of the 6π aromatic anion formed by proton abstraction from the borabenzene is determined. Finally, Chapter III describes the positive and negative ion chemistry of sulfonyl halides. The most important feature of these investigations is the copious formation of SO_2F^- in low pressures of SO_2FCl . This ion has been shown to be a good F^- donor, so that SO_2FCl appears to be an excellent reagent for negative chemical ionization spectroscopy.

References

1. See discussions in J. March "Advanced Organic Chemistry: Reactions, Mechanisms and Structure," McGraw-Hill, New York, N.Y., 1968.
2. J. L. Beauchamp, Ann. Rev. Phys. Chem., 22, 527 (1972) and J. L. Beauchamp "Reaction Mechanisms of Organic and Inorganic Ions in the Gas Phase," in Interactions Between Ions and Molecules, P. Ausloos, Ed., Plenum Press, New York, 1975, p. 413.
3. A review of negative ion generation is provided in J. G. Dillard, Chem. Rev., 73, 589 (1973).
4. See Appendix III for references to gas phase acidity measurements.
5. D. P. Ridge and J. L. Beauchamp, J. Amer. Chem. Soc., 96, 637 (1974) and D. P. Ridge and J. L. Beauchamp, ibid., 3595 (1974).
6. S. A. Sullivan and J. L. Beauchamp, J. Amer. Chem. Soc., 98, 1060 (1976).
7. S. A. Sullivan and J. L. Beauchamp, J. Amer. Chem. Soc., accepted for publication and unpublished results.
8. S. M. Jose Briscese and J. M. Riveros, J. Amer. Chem. Soc., 97, 230 (1975).
9. J. F. G. Fargle, P. C. Isolani and J. M. Riveros, J. Amer. Chem. Soc., 98, 2049 (1976) and S. M. Jose and J. M. Riveros, Nouveau J. Chimie, 1, 113 (1977).

References (continued)

10. M. K. Murphy and J. L. Beauchamp, J. Amer. Chem. Soc., 98, 1433 (1976).
11. M. K. Murphy and J. L. Beauchamp, submitted for publication.
12. For example, see R. T. McIver, Jr., and J. H. Silvers, J. Amer. Chem. Soc., 95, 8462 (1973).
13. T. B. McMahon and P. Kebarle, J. Amer. Chem. Soc., 98, 3399 (1976).
14. J. I. Brauman and L. K. Blair, J. Amer. Chem. Soc., 90, 6561 (1968).
15. J. S. Miller and R. T. McIver, Jr., J. Amer. Chem. Soc., 96, 4323 (1974).
16. S. Y. Delavarenne and H. G. Vielhe, "Abstracts, Fourth Int. Symp on Fluorine Chemistry," Estes Park (Am. Chem. Soc.), 1967, p. 122.
17. J. V. Dugan, Jr., J. H. Rice and J. L. Magee, Chem. Phys. Lett., 3, 323 (1969).
18. W. H. Olmstead and J. I. Brauman, J. Amer. Chem. Soc., 99, 4219 (1977).
19. M. S. Foster and J. L. Beauchamp, submitted for publication.
20. R. Yamdagni and P. Kebarle, J. Amer. Chem. Soc., 93, 7139 (1971).

CHAPTER I

Nucleophilic Reactions of Anions with PF_3 and OPF_3 in the
Gas Phase Using Ion Cyclotron Resonance Spectroscopy.

Mechanism and Energetics of Anionic
Adduct (OPF_4^- and PF_4^-) Formation.

S. A. Sullivan and J. L. Beauchamp

Contribution No. 5629 from the Arthur Amos Noyes
Laboratory of Chemical Physics, California Institute
of Technology, Pasadena, California 91125

ABSTRACT

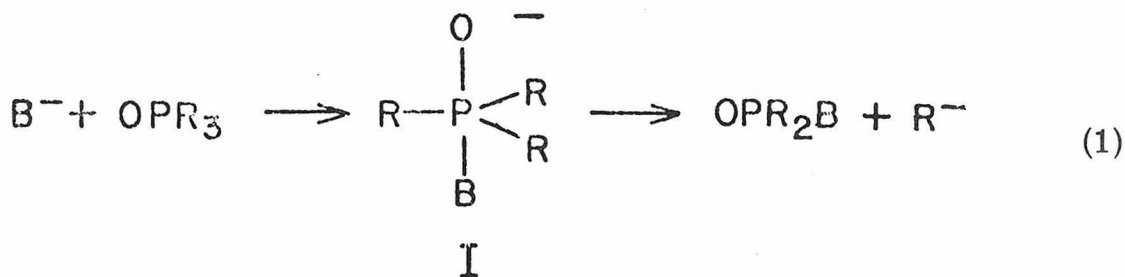
Ion cyclotron resonance techniques are employed in the examination of the gas phase reactions of PF_3 and OPF_3 with anionic bases, including NH_2^- , OH^- , $\text{CH}_3\text{CH}_2\text{O}^-$, HNO^- , HS^- , SF_6^- , and SF_5^- .

Evidence is presented which suggests that all reactions proceed by initial attack at phosphorous, with products resulting from decomposition of chemically activated intermediates. The energetics of intermediates inferred in these processes are related to the Lewis acidities of OPF_3 and PF_3 . With fluoride ion as a reference base, OPF_3 is found to be more acidic than PF_3 , with $D(\text{OPF}_3-\text{F}^-) = 58.9 \pm 0.4$ kcal/mol and $D(\text{PF}_3-\text{F}^-) = 50 \pm 5$ kcal/mol.

Introduction

Phosphorous, like other second row elements, is capable of hypervalent bonding¹ as shown by the existence of pentavalent phosphoranes PR_5 and phosphoryl compounds OPR_3 in addition to the expected trivalent phosphines PR_3 . Many studies of these compounds have focussed on processes involving nucleophilic attack at phosphorous.^{1, 2ab} Both P (III) and P (V) are susceptible to nucleophilic attack in solution. The reactions of tetracoordinate P(V) compounds, phosphate esters in particular, have been examined more extensively because of their relationship to processes in biological systems.³

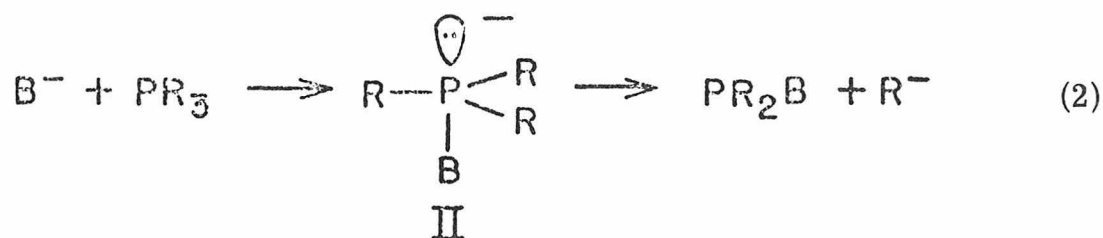
A somewhat complex situation is suggested by mechanistic studies of nucleophilic substitution at P(V). Isotopic exchange during hydrolysis of alkyl phosphoryl compounds by bases B^- implicates the formation of pentavalent P(V) anionic intermediates^{1, 4} (I). Similar experiments, with phosphorous bearing more electronegative



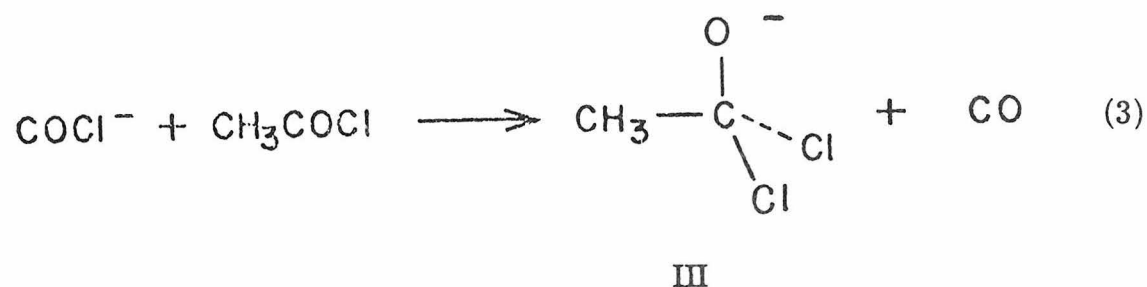
substituents (e.g., $\text{R} = \text{CH}_3\text{O}$, Cl), are consistent with a direct displacement mechanism through a transition state like I.^{1, 5} The inference of reaction mechanisms in these systems is complicated⁶ by the presence of two distinct ligand sites in the proposed intermediates. Analogous to PF_5 ,⁷ the intermediates are expected to have trigonal

bipyramidal structure, with a preference for axial binding of electro-negative substituents.¹ Structures and the mode of decomposition of reaction intermediates or transition states may thus be strongly moderated by the substituents on phosphorous.

Direct displacement mechanisms involving tetracoordinate transition states (II) have been proposed for nucleophilic attack at P(III) (eq 2). Recent results indicating complete inversion at P(III) on nucleophilic attack are consistent with a direct displacement.⁸



Recent ion cyclotron resonance (ICR) studies have considered gas phase reactions of anionic bases with fluorinated alkenes,⁹ alkyl formates¹⁰ and other halogenated carbonyls.¹¹ Observed products are rationalized as the results of multiple bond rearrangements and dissociation of chemically activated anionic intermediates. Often it is possible to separately study the energetics of the reaction intermediates in these processes. For example, the tetrahedral adduct III is formed in eq 3 by chloride transfer.¹²

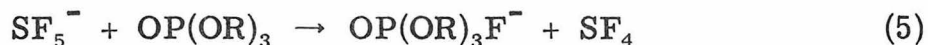


In this laboratory we are extending our continuing investigation of negative ion reaction mechanisms by examining the interaction of anions with phosphorous compounds. Preliminary studies of the reactions of strong bases with trimethylphosphate¹³ indicate that reaction 4 is the major process with CD_3O^- . The absence of



deuterium incorporation into the ionic product in reaction 4 suggests that nucleophilic attack occurs at carbon rather than phosphorous. This somewhat surprising result is in contrast to solution reactions in which strong bases preferentially attack phosphorous.¹⁴

By analogy with the gas phase reactions of fluoroalkyl silanes (i.e., CH_3SiF_3) in mixtures with SF_6 ,¹⁵ it was expected that F^- transfer adducts could also be formed with phosphate esters by transfer from F^- donors, for example, eq 5. Formation of such adducts may be



important as a method of soft ionization useful in chemical ionization mass spectrometry.¹⁶ All attempts to form F^- adducts with phosphate esters have failed.¹³ This suggests that these compounds are very weak Lewis acids.

In the present study we have examined the nucleophilic reactions of anionic bases including NH_2^- , OH^- , $\text{CH}_3\text{CH}_2\text{O}^-$, HNO^- , and HS^- , with OPF_3 and PF_3 . The electronegative fluorine ligands should decrease electron density at phosphorous significantly enhancing its

susceptibility to nucleophilic attack. Similarly, the stability of fluoride adducts OPF_4^- and PF_4^- should be considerably greater compared to adducts of phosphorous esters.

Experimental

Experiments were performed using an ICR spectrometer built in this laboratory, incorporating a 15' magnetic capable of observing up to m/e 800. Instrumentation and experimental techniques of icr spectroscopy have been described in detail previously.^{17, 18} Pressure was measured using a Schulz-Phelp ion gauge calibrated against a MKS Baratron Model 90-H1 capacitance manometer at higher pressures. Pressure measurements are the major source of error ($\pm 20\%$) in reaction rate constants.

Negative ion trapping techniques have been described elsewhere.¹⁹ In a typical trapped ion experiment, the precursor to the reagent base was admitted to the analyzer, followed by addition of one or two other compounds to be investigated. Independent pressure control allows for variation of the partial pressures of each component. Total pressures normally were below 5×10^{-6} torr, to minimize ion loss. Reaction rate constants are determined from limiting slopes for the disappearance of reactant ions in semi-log plots of the variation of ion abundance with time.

Reactivity of ions in mixtures of neutrals may also be examined by observation of the variation of single resonance ion intensities as a function of component partial pressure. Analytical methods for the

calculation of reaction rates using icr pressure studies have been described.²⁰

The major ions produced by thermalized electron attachment in SF_6 are SF_6^- (95%) and SF_5^- (5%). Both ions are unreactive toward SF_6 .²¹ In a similar manner, the alkoxide ion $\text{C}_2\text{H}_5\text{O}^-$ is produced in $\text{CH}_3\text{CH}_3\text{ONO}$.²² Primary ions CH_2CHO^- (17%) and HNO^- (10%) are also formed by electron attachment. The only reaction product ion detected is NO_2^- , which is formed on reaction of $\text{CH}_3\text{CH}_2\text{O}^-$ with the precursor nitrite. This reaction is minimized by maintaining low partial pressure of nitrites.

Reagent negative ions NH_2^- , HO^- and HS^- are formed in NH_3 , H_2O and H_2S , respectively.^{23, 24} Resonance electron capture processes (4.0-6.0 eV) initiate NH_2^- and OH^- formation. Near zero energy electrons are required for formation of HS^- . In all three cases, high pressures ($\sim 10^{-5}$ torr) of precursor were necessary to produce reagent negative ion intensities adequate for study. Only drift mode studies were performed in these cases.

Nitrites were prepared from CD_3OD and $\text{C}_2\text{H}_5\text{OH}$ using standard methods.²⁵ Both PF_3 and OPF_3 were obtained from PCR. An impurity found in OPF_3 at m/e 155 was removed by trap-to-trap vacuum distillation. All other compounds used in these studies were obtained from commercial sources and used without further purification except for repeated freeze-pump-thaw cycles to remove noncondensable impurities.

Results

Negative Ions in OPF_3 and PF_3 . In OPF_3 at low pressures (10^{-6} torr) the negative ions O^- , F^- and a small amount of OPF_2^- have been observed in previous studies.²⁶ These ions are formed by dissociative electron attachment processes, with resonance maxima between 10-15 eV electron energy. Similarly, the ions F^- , F_2^- , PF^- , and PF_2^- have been produced in PF_3 at electron energies above 10 eV.²⁷ In both cases, cross sections for negative ion formation are small. With pressure, emission current, and electron energy conditions used in experiments described below, the negative ions noted above are not observed in samples of OPF_3 and PF_3 .

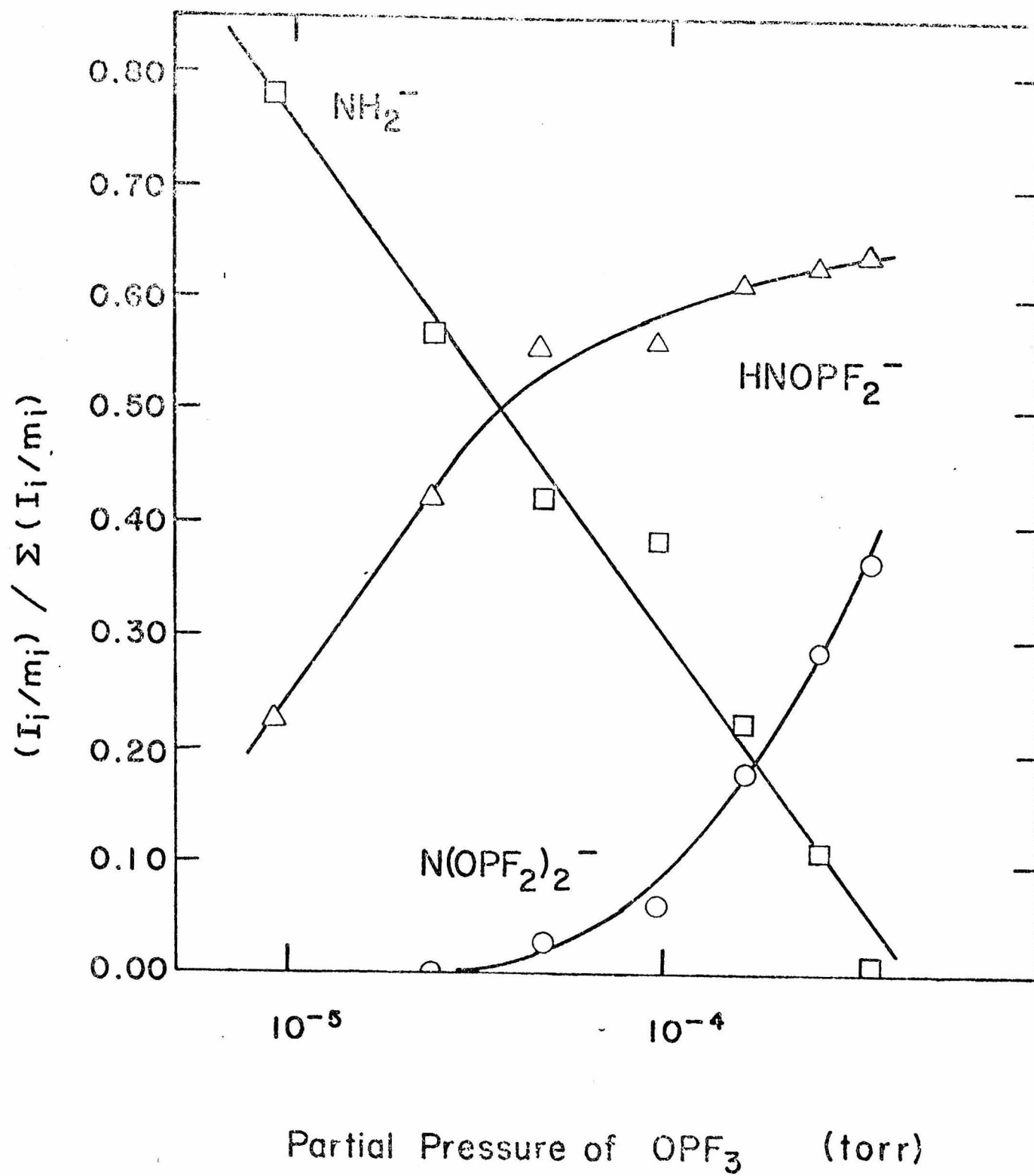
Only in the case of OPF_3 at pressures above 10^{-5} torr was the negative ion O_2PF_2^- (m/e 101) observed with a resonance maxima for ion formation at 7.2 eV electron energy. No other ions are detected with increased pressure. Mass spectral analysis indicates the presence of no other neutrals in the OPF_3 .²⁸

In mixtures of OPF_3 and PF_3 with both H_2O and NH_3 , ions are produced which show no double resonance from OH^- and NH_2^- . These ions (PF_2^- in PF_3 and OPF_2^- in OPF_3) are formed only in the presence of the second neutral. Double resonance results eliminate the possibility of ion generation from ion molecule reactions.²⁹ Surface reactions²⁸ or reactions on the electron filament³⁰ are possible. Neither of these ions is included in the figures presented.

Reactions of Nucleophiles with OPF_3 . Figure 1 presents the variation of normalized ion intensity as a function of OPF_3 pressure

FIGURE 1

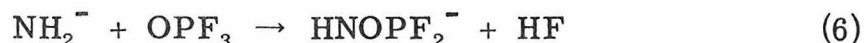
Variation of normalized negative ion intensity as a function of the partial pressure of OPF_3 in a mixture with 10^{-5} torr NH_3 at 4.8 eV electron energy.



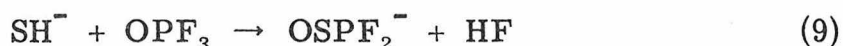
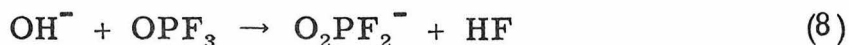
in a mixture with 10^{-5} torr NH_3 . As NH_2^- ($\underline{\text{m/e}}$ 16) decreases, ions appear corresponding to HNOPF_2^- ($\underline{\text{m/e}}$ 100) and $\text{N(OPF}_2)_2^-$ ($\underline{\text{m/e}}$ 185). As noted above OPF_2^- ($\underline{\text{m/e}}$ 85) is also detected in this mixture. Since it is not formed by reaction of NH_2^- , it is not included in Figure 1.

Double resonance experiments indicate that NH_2^- is the precursor to both product ions and further that HNOPF_2^- reacts to form $\text{N(OPF}_2)_2^-$.

There is no indication that HNOPF_2^- and OPF_2^- are reactively coupled. Reactions 6 and 7 are consistent with these results.



Analogous nucleophilic reactions occur in mixtures of H_2O , (eq 8) and H_2S (eq 9) with OPF_3 . Although, as noted above, O_2PF_2^- is



formed in OPF_3 alone, double resonance indicates the $\sim 30\%$ of the observed O_2PF_2^- is formed by reaction with OH^- . Neither of the product ions react further with the neutrals present. Rates for reactions 6, 7, and 9, determined from single resonance pressure studies are presented in Table I. Because of complications due to other sources of O_2PF_2^- , a reaction rate for eq 8 could not be measured.

Figure 2 presents the temporal variation of ion intensity as a function of reaction time in a mixture of 1×10^{-7} torr, $\text{CH}_3\text{CH}_2\text{ONO}$ with 1.76×10^{-6} torr OPF_3 . Product ions OPF_2^- ($\underline{\text{m/e}}$ 85), O_2PF_2^-

Table I. Summary of Gas Phase Nucleophilic Reactions of OPF_3 and PF_3

Reaction	Equation Number	k_{ex}^a	k_{ado}^b	$k_{\text{ex}}^c/k_{\text{ado}}$
$\text{NH}_2^- + \text{OPF}_3 \rightarrow \text{NHOPF}_2^- + \text{HF}$	6	16.5	20.6	0.80
$\text{NHOPF}_2^- + \text{OPF}_3 \rightarrow \text{N(POF}_2)_2^- + \text{HF}$	7	2.0	10.8	0.19
$\text{OH}^- + \text{OPF}_3 \rightarrow \text{O}_2\text{PF}_2^- + \text{HF}$	8	-	20.0	-
$\text{CH}_3\text{CH}_2\text{O}^- + \text{OPF}_3 \rightarrow \text{O}_2\text{PF}_2^- + \text{CH}_3\text{CH}_2\text{F}$	10	11.6	13.7	0.85
$\text{HNO}^- + \text{OPF}_3 \rightarrow \text{OPF}_2^- + \text{HF} + \text{NO}$	11	11.9	15.7	0.76
$\text{CH}_2\text{CHO}^- + \text{OPF}_3 \rightarrow \text{C}_2\text{H}_2\text{OPF}_2^- + \text{HF}$	12	5.0	13.9	0.36
$\text{SH}^- + \text{OPF}_3 \rightarrow \text{OSP}_2\text{F}_2^- + \text{HF}$	9	1.2	15.4	0.08
$\text{NH}_2^- + \text{PF}_3 \begin{cases} \rightarrow \text{NHPF}_2^- + \text{HF} \\ \rightarrow \text{NPF}^- + 2\text{HF} \end{cases}$	13 14	7.9 6.6	15.1	0.96
$\text{OH}^- + \text{PF}_3 \rightarrow \text{OPF}_2^- + \text{HF}$	15	-	14.8	-
$\text{CH}_3\text{CH}_2\text{O}^- + \text{PF}_3 \rightarrow \text{OPF}_2^- + \text{CH}_3\text{CH}_2\text{F}$	17	5.6	9.2	0.61
$\text{HNO}^- + \text{PF}_3 \rightarrow \text{NOPF}_2^- + \text{HF}$	18	5.0	11.8	0.42
$\text{PF}_2^- + \text{H}_2\text{O} \rightarrow \text{OPF}_2^- + \text{OH}$	16	-	18.0	-

^aExperimental rate is determined as noted in text; in units $10^{-10} \text{ cm}^3 \text{ mol}^{-1} \text{ sec}^{-1}$.^bRate, in units $10^{-10} \text{ cm}^3 \text{ mol}^{-1} \text{ sec}^{-1}$ is calculated using the average dipole orientation model.

Table I - Continued

equation:

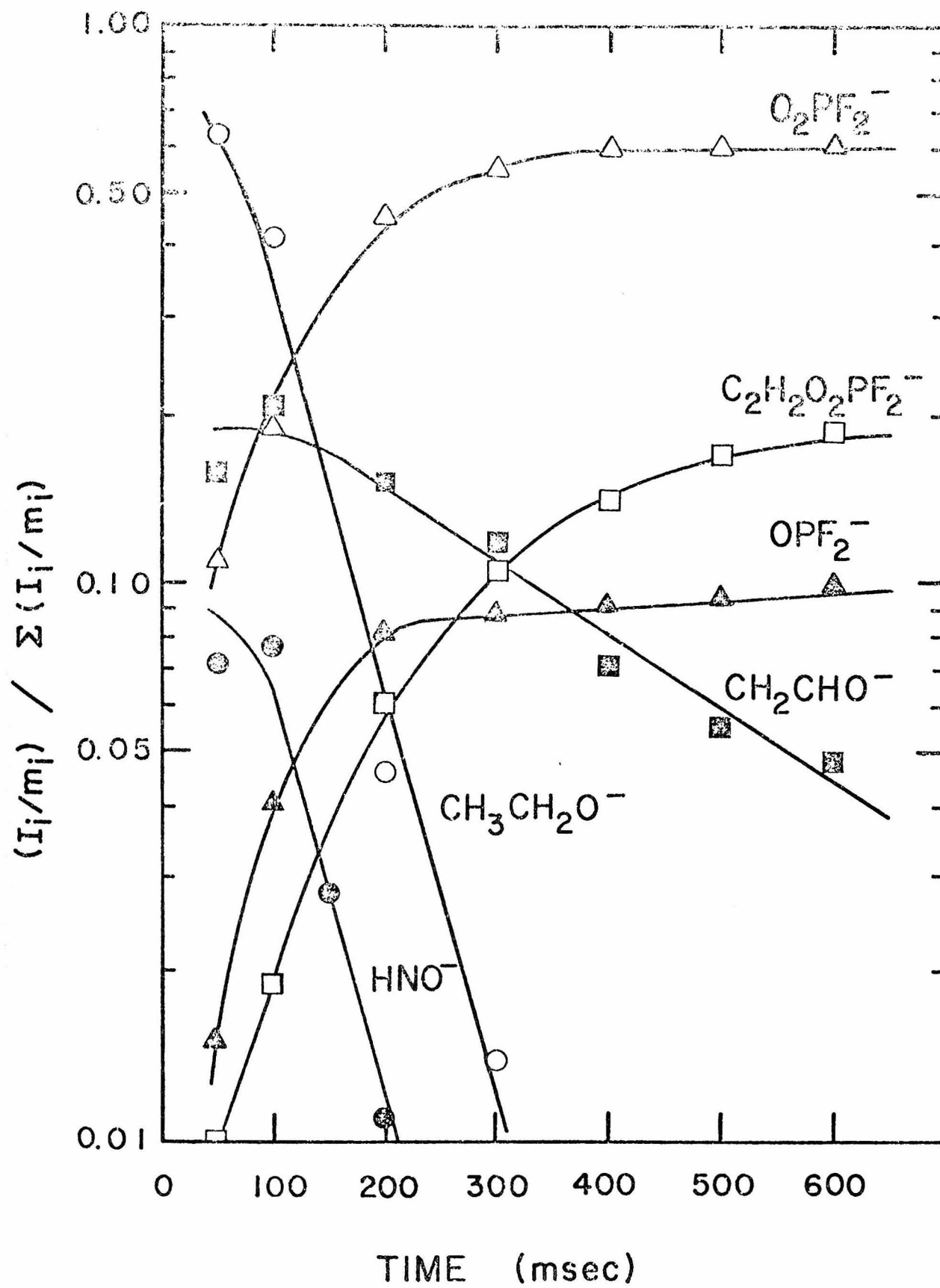
$$k_{\text{ado}} = [2\pi e / \mu^{\frac{1}{2}}] [\alpha^{\frac{1}{2}} + c \mu_{\text{d}} (2/\pi kT)^{\frac{1}{2}}]$$

in which μ = reduced mass of the ion molecule collision pair, α = polarizability of the neutral, μ_{d} = dipole moment of the neutral and c = constant estimated as noted in reference 36. Polarizabilities for OPF_3 and PF_3 are taken as 33.0 and $29.0 \times 10^{-25} \text{ cm}^3$, respectively, see reference 41. Dipole moments for OPF_3 and PF_3 are taken as 1.74 D and 1.03 D, respectively, from R. R. C. Carlson and D. W. Meck, Inorg. Chem., 13, 1941 (1974).

^cIn those cases where two reaction pathways occur, the total rate is compared to the ADO rate.

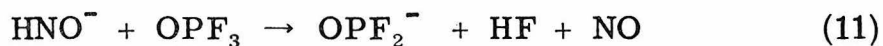
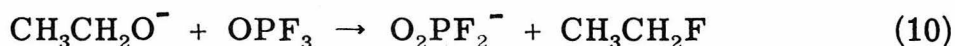
FIGURE 2

Temporal variation of normalized negative ion intensity in a mixture of $\text{CH}_3\text{CH}_2\text{ONO}$ (1.00×10^{-7} torr) and OPF_3 (1.76×10^{-6} torr) at 20.0 eV electron energy.



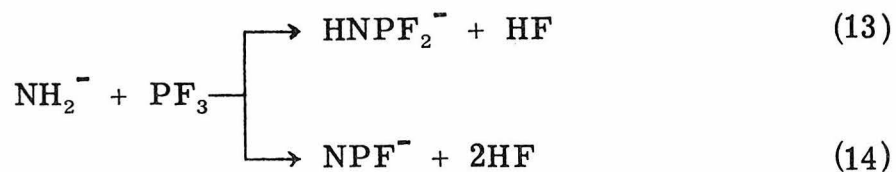
(m/e 101) and $\text{C}_2\text{H}_2\text{OPF}_2^-$ (m/e 127)³¹ appear as a function of time.

Double resonance experiments confirm that $\text{CH}_3\text{CH}_2\text{O}^-$ reacts to produce O_2PF_2^- (eq 10). It should be noted that at low pressures and 20 eV electron energy no O_2PF_2^- is generated in OPF_3 alone. The complete disappearance of OPF_2^- and $\text{C}_2\text{H}_2\text{OPF}_2^-$ on double resonance irradiation of HNO^- and CH_2CHO^- , respectively, indicate reactions 11 and 12 rates



for reactions 10-12 as determined from trapping studies are listed in Table I.

Reactions of Nucleophiles with PF_3 . On addition of PF_3 to 1×10^{-5} torr NH_3 at 4.8 eV electron energy, ions are detected at NH_2^- (m/e 16), NPF^- (m/e 64), PF_2^- (m/e 69), and HNPF_2^- (m/e 84). As noted above, PF_2^- is not formed by reaction of NH_2^- . Double resonance experiments confirm that NH_2^- reacts to form both HNPF_2^- and NPF^- as in eqs 13 and 14. No further reactions of these species are observed

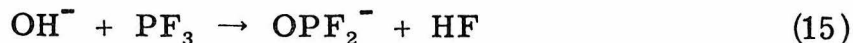


(14)

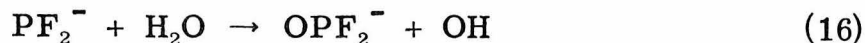
with the neutrals present.

Ions PF_2^- (m/e 69) and OPF_2^- (m/e 85) appear as PF_3 is added to a sample of H_2O (2×10^{-5} torr). Only the latter ion OPF_2^- is

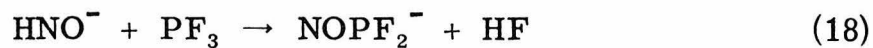
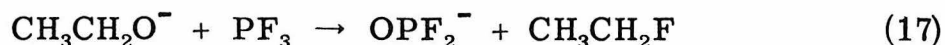
formed by reaction of PF_3 with OH^- (eq 15). Double resonance also



indicates that PF_2^- reacts to form OPF_2^- , possibly as in eq 16.



The temporal variation of ion intensity in a mixture of $\text{CH}_3\text{CH}_2\text{ONO}$ (1.20×10^{-7} torr) and PF_3 (2.44×10^{-7} torr) is presented in Figure 3. Product ions OPF_2^- (m/e 85) and NOPF_2^- (m/e 99) appear at longer times. Reactions 17 and 18 are consistent with double



resonance experiments, $\text{CH}_3\text{CH}_2\text{O}^-$ and HNO^- being the sold precursors of OPF_2^- and NOPF_2^- , respectively. The ion CH_2CHO^- (m/e 43) is unreactive in this mixture. Rates for reactions 13-18 are listed in Table I.

Fluoride Transfer Reactions and Lewis Acidity of OPF_3 .

Figure 4 presents the temporal variation of normalized ion intensity in a mixture of 3.50×10^{-7} torr OPF_3 with a trace amount ($< 10^{-7}$ torr) of SF_6 . Both primary ions SF_6^- (m/e 146) and SF_5^- (m/e 127) decrease as a product ion OPF_4^- (m/e 123) appears. Double resonance experiments link production of OPF_4^- directly to SF_6^- (eq 19). A slower F^- transfer from SF_5^- also occurs (eq 20).

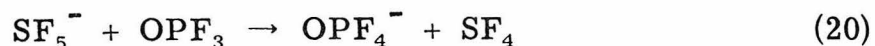
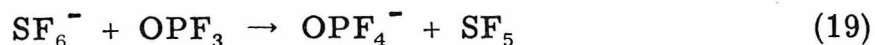


FIGURE 3

Temporal variation of normalized negative ion intensity in a mixture of $\text{CH}_3\text{CH}_2\text{ONO}$ (1.20×10^{-7} torr) and PF_3 (2.44×10^{-7} torr) at 20.0 eV electron energy.

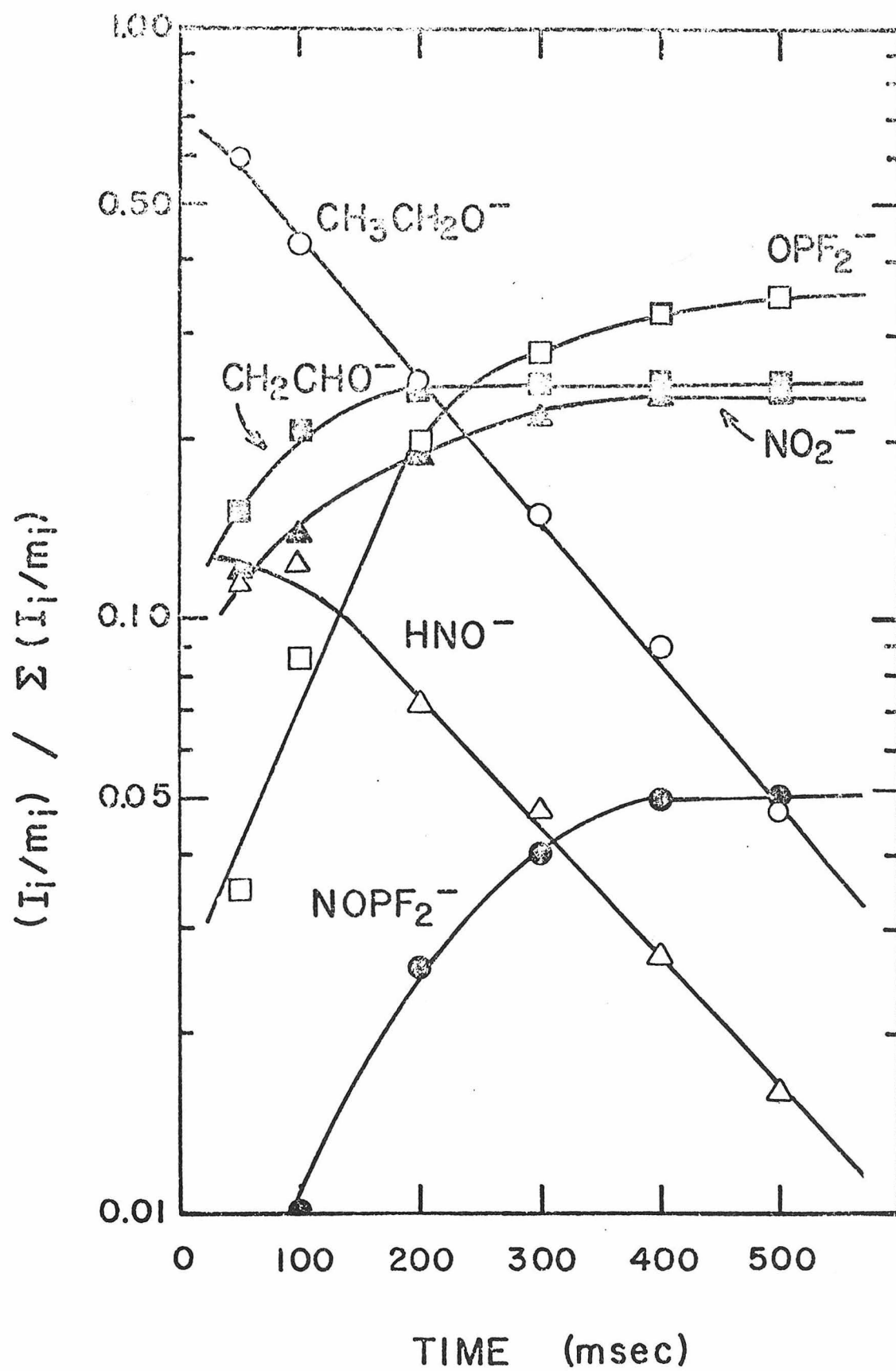
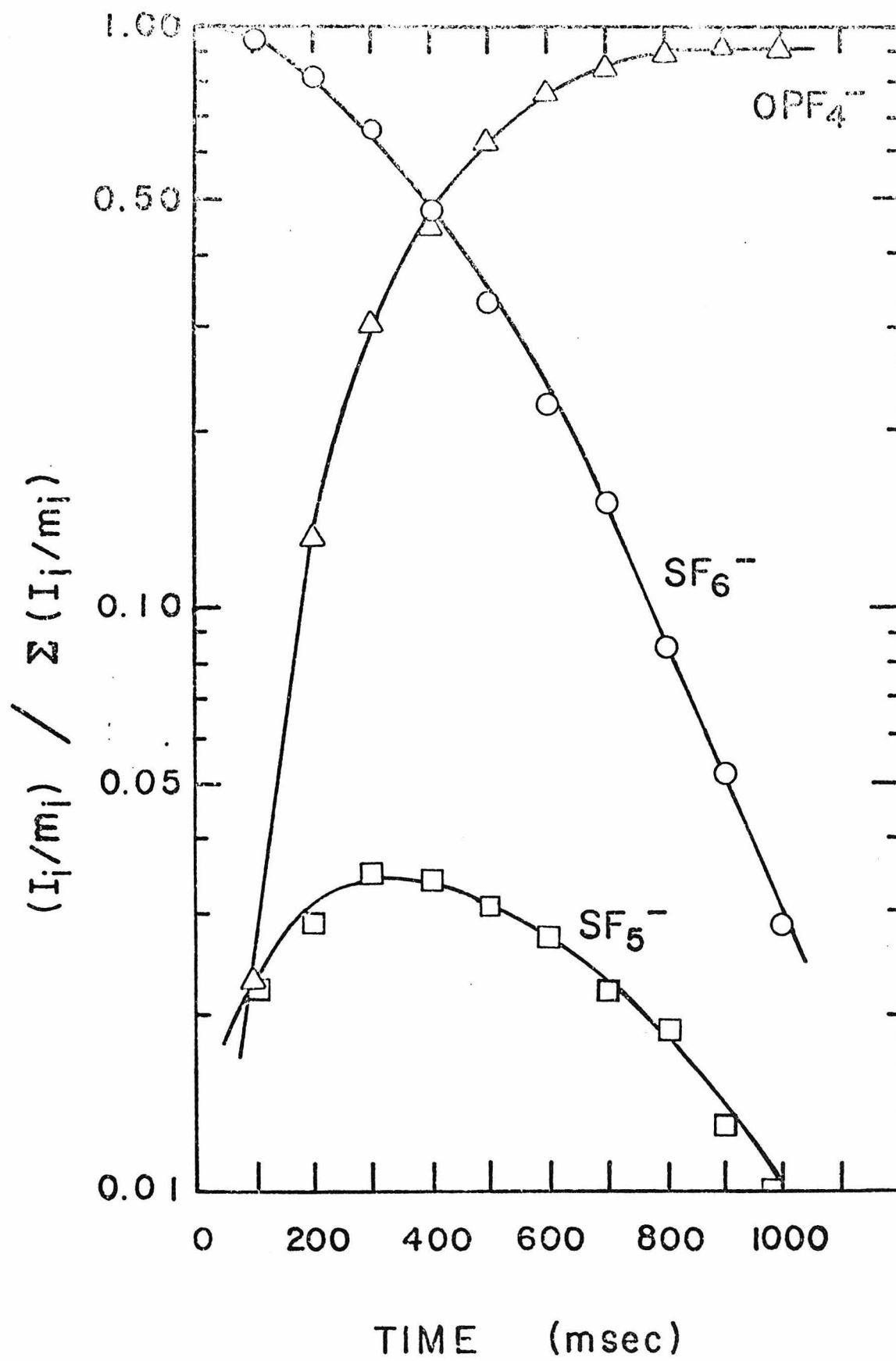
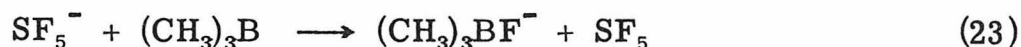
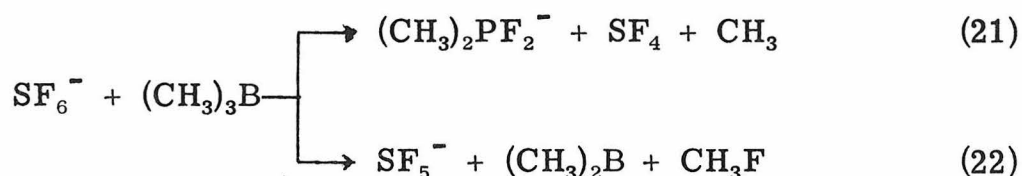


FIGURE 4

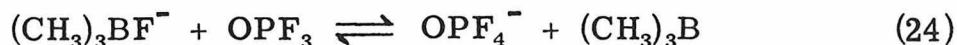
Temporal variation of normalized negative ion intensity in a mixture of OPF_3 (3.50×10^{-7} torr) with a trace of SF_6 at 20.0 eV.



Temporal variation of normalized ion intensity in a (1:1.9) mixture of OPF_3 and $(\text{CH}_3)_3\text{B}$ is presented in Figure 5. Ions $(\text{CH}_3)_3\text{BF}^-$ (m/e 75), $(\text{CH}_3)_2\text{BF}_2^-$ (m/e 79), OPF_4^- (m/e 123) and SF_5^- (m/e 127) appear and increase as SF_6^- (m/e 146) decays with time. Reactions 21-23 in addition to reactions 16 and 17, are consistent with observed double resonance. Reactions 21-23 have been investigated



previously.³² At long times equilibrium fluoride transfer occurs between OPF_4^- and $(\text{CH}_3)_3\text{BF}^-$ (eq 24). The equilibrium constant (K_{eq})



for reaction 21 as written is determined to be 1.9 ± 0.4 . Ion ejection techniques,³³ which allow measurement of the forward and reverse rate constants of reaction 24 (Table I), confirm this value for K_{eq} . Entropy contributions will be negligible,³⁴ so that $\Delta H \sim \Delta G$ and $D(\text{OPF}_3-\text{F}^-) - D[(\text{CH}_3)_3\text{B}-\text{F}^-] = 0.38 \pm 0.14$ kcal/mol. Using the estimated value of 58.5 ± 0.4 kcal/mol for the bond strength $D[(\text{CH}_3)_3\text{B}-\text{F}^-]$ (Table II). $D(\text{OPF}_3-\text{F}^-)$ is calculated as 58.9 ± 0.4 kcal/mol.

In the mixture of $(\text{CH}_3)_3\text{B}$ and OPF_3 , fluoride transfer does not occur from $(\text{CH}_3)_2\text{BF}_2^-$ to OPF_3 (Figure 5). Further, $(\text{CH}_3)_2\text{SiF}_3^-$

FIGURE 5

Temporal variation of normalized ion intensity in a
(1:1.9) mixture of OPF_3 and $(\text{CH}_3)_3\text{B}$ at total pressure
 6.6×10^{-7} torr.

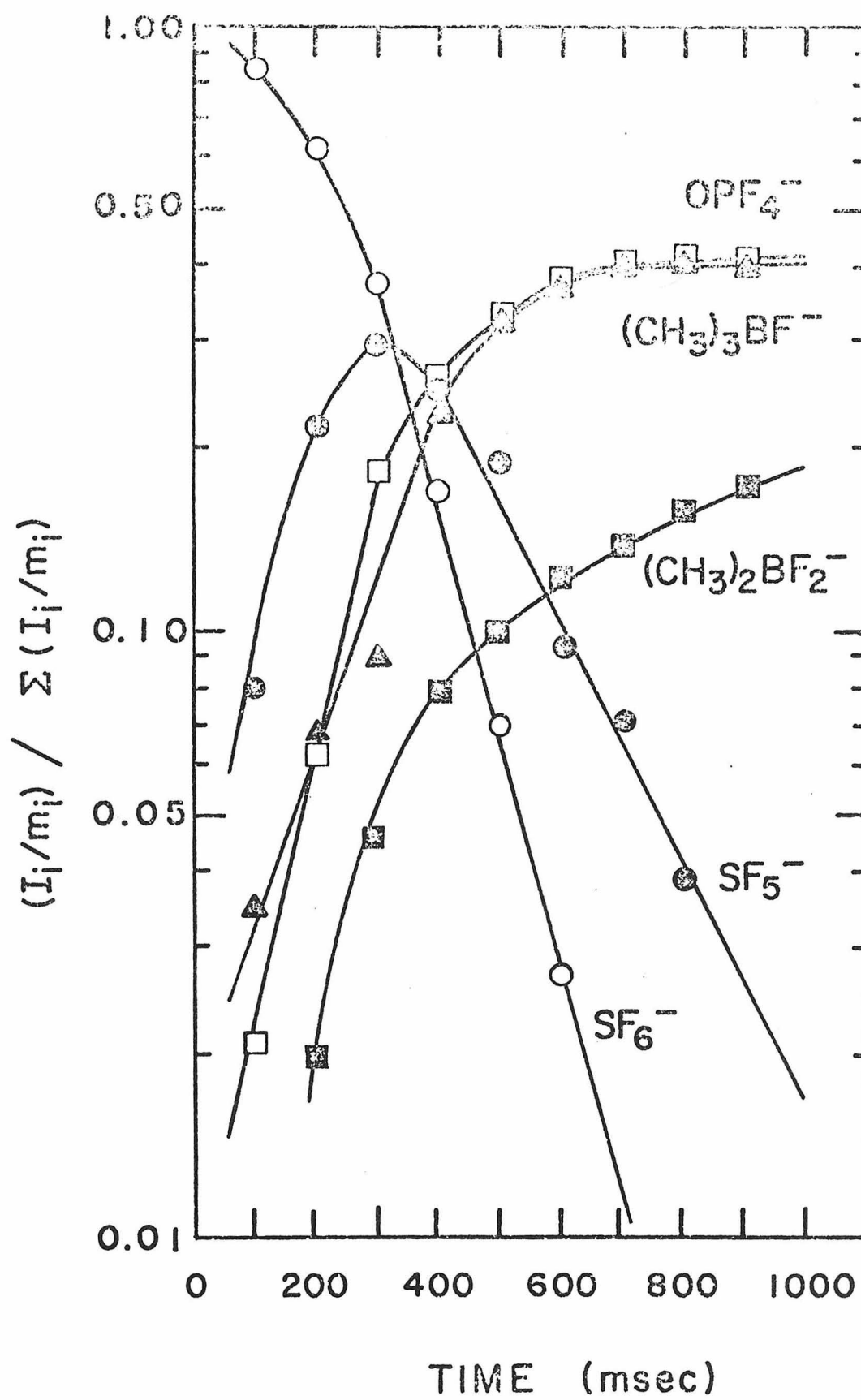


Table II. Fluoride Bond Strengths^a

M	D(M-F ⁻) ^b
PF ₅	> 71 ^c
BF ₃	71 ^c
SiF ₄	< 71 ^c
(CH ₃) ₂ BF	61.8
OPF ₃	58.9 ^d
(CH ₃) ₃ B	58.5
(CH ₃) ₂ SiF ₂	55.5
SF ₄	54 ± 12 ^e
(CH ₃) ₃ SiF	50 ± 10
PF ₃	50 ± 5 ^d
HCN	47 ± 3 ^f
SO ₂	< 45 ^f
F	29 ± 3.0 ^g
SF ₅	11 ± 8 ^e

^aAll values in kcal/mol at 298°K.

^bBinding energies of F⁻ to boron and silicon compounds are taken from reference 32 and 15, respectively.

^cJ. C. Haartz and D. H. McDaniel, J. Amer. Chem. Soc., 95, 3562 (1973).

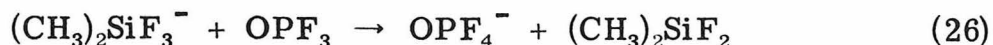
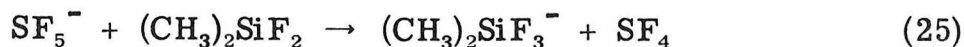
^dPresent study.

^eReference 19.

^fReference 35.

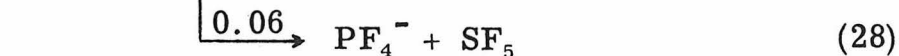
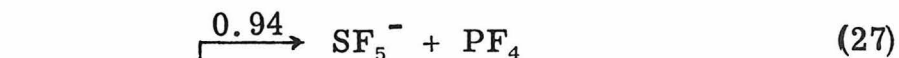
^gCalculated using EA(F₂) = 3.09 ± 0.1 eV from W. A. Chupka, J. Berkowitz, and D. Gutman, J. Chem. Phys., 55, 2724 (1971).

produced in a mixture of $(\text{CH}_3)_2\text{SiF}_2$ and SF_6 by reaction 25 reacts with OPF_3 to form OPF_4^- (eq 26). These results indicate limits for the



bonds strength in OPF_4^- , $61.8 \text{ kcal/mol} > D(\text{OPF}_3-\text{F}^-) > 55.5 \text{ kcal/mol}$, consistent with the measured bond strength noted above. Rates for F^- transfer reactions to OPF_3 are summarized in Table III.

Fluoride Transfer Reactions and Lewis Acidity of PF_3 . In Figure 6, the temporal variation of ion intensity in a mixture of 7.2×10^{-7} torr PF_3 with a trace of SF_6 is presented. As a function of reaction time, SF_6^- (m/e 146) decays as SF_5^- (m/e 127) and PF_4^- (m/e 107) appear. Reactions 27 and 28 are confirmed by double



resonance experiments. Fluoride transfer reaction 29 is effected by



irradiating SF_5^- in double resonance experiments, suggesting that this process is endothermic. In mixtures of OPF_3 , PF_3 and a trace of SF_6 , no PF_4^- is observed, due to the competing and much faster process 19.

Negative ions F^- (m/e 19, 60%), F_2^- (m/e 38, 11%) and SO_2F^- (m/e 85, 29%) are generated by electron impact in moderate pressures

Table III. Summary of Fluoride Transfer Reactions

Reaction	Equation Number	k_{ex}^a	k_{ado}^b	$k_{\text{ex}}/k_{\text{ado}}^c$	Thermochemical Inference
$\text{SF}_6^- + \text{OPF}_3 \rightarrow \text{OPF}_4^- + \text{SF}_5$	20	3.1	9.8	0.32	$\text{D}(\text{SF}_5-\text{F}^-) < \text{D}(\text{OPF}_3-\text{F}^-)$
$\text{SF}_5^- + \text{OPF}_3 \rightarrow \text{OPF}_4^- + \text{SF}_4$	20	2.1	10.4	0.20	$\text{D}(\text{SF}_4^+ \text{F}^-) < \text{D}(\text{OPF}_3-\text{F}^-)$
$\text{SF}_6^- + (\text{CH}_3)_3\text{B} \rightarrow (\text{CH}_3)_2\text{BF}_2^- + \text{SF}_4 + \text{CH}_3$	21	1.4	10.4	0.49	
$\text{SF}_5^- + (\text{CH}_3)_3\text{B} \rightarrow \text{SF}_5^- + (\text{CH}_3)_2\text{B} + \text{CH}_3\text{F}$	22	3.7			
$\text{SF}_5^- + (\text{CH}_3)_3\text{B} \rightarrow (\text{CH}_3)_3\text{BF}^- + \text{SF}_4$	23	2.8	10.6	0.26	
$(\text{CH}_3)_3\text{BF}^- + \text{OPF}_3 \rightarrow \text{OPF}_4^- + (\text{CH}_3)_3\text{B}$	24f	3.1	11.7	0.26	$\text{D}(\text{OPF}_3-\text{F}^-) =$
$\text{OPF}_4^- + (\text{CH}_3)_3\text{B} \rightarrow (\text{CH}_3)_3\text{BF}^- + \text{OPF}_3$	24r	1.7	10.7	0.16	$58.9 \pm 0.4 \text{ kcal/mol}$
$(\text{CH}_3)_2\text{SiF}_3^- + \text{OPF}_3 \rightarrow \text{OPF}_4^- + (\text{CH}_3)_2\text{SiF}_2$	26	2.87	10.4	0.27	$\text{D}[(\text{CH}_3)_2\text{SiF}_2-\text{F}^-] < \text{D}(\text{OPF}_3-\text{F}^-)$
$\text{SF}_6^- + \text{PF}_3 \rightarrow \text{SF}_5^- + \text{PF}_4$	27	0.95	7.7	0.13	$\text{D}(\text{SF}_5-\text{F}^-) < \text{D}(\text{PF}_3-\text{F}^-)$
$\text{PF}_4^- + \text{SF}_5 \rightarrow \text{PF}_4^- + \text{SF}_5$	28	0.04			
$\text{F}_2^- + \text{PF}_3 \rightarrow \text{PF}_4^- + \text{F}$	30	-	-	-	$\text{D}(\text{F}-\text{F}^-) < \text{D}(\text{PF}_3-\text{F}^-)$
$\text{SO}_2\text{F}^- + \text{PF}_3 \rightarrow \text{PF}_4^- + \text{SO}_2$	31	-	-	-	$\text{D}(\text{SO}_2-\text{F}^-) < \text{D}(\text{PF}_3-\text{F}^-)$

Table III. Continued

Reaction	Equation Number	k_{ex}^a	k_{ado}^b	$k_{\text{ex}}/k_{\text{ado}}^c$	Thermochemical Inference
$\text{PF}_4^- + \text{OPF}_3 \rightarrow \text{OPF}_4^- + \text{PF}_3$	32	- -	- -	- -	$\text{D}(\text{PF}_3-\text{F}^-) < \text{D}(\text{OPF}_3-\text{F}^-)$
$(\text{CH}_3)_3\text{SiF}_2^- + \text{PF}_3 \rightarrow \text{PF}_4^- + (\text{CH}_3)_3\text{SiF}$	33	- -	- -	- -	$\text{D}[(\text{CH}_3)_3\text{SiF}-\text{F}^-] < \text{D}(\text{PF}_3-\text{F}^-)$
$\text{FHCN}^- + \text{PF}_3 \rightarrow \text{PF}_4^- + \text{HCN}$	34	- -	- -	- -	$\text{D}(\text{CNH}-\text{F}^-) < \text{D}(\text{PF}_3-\text{F}^-)$

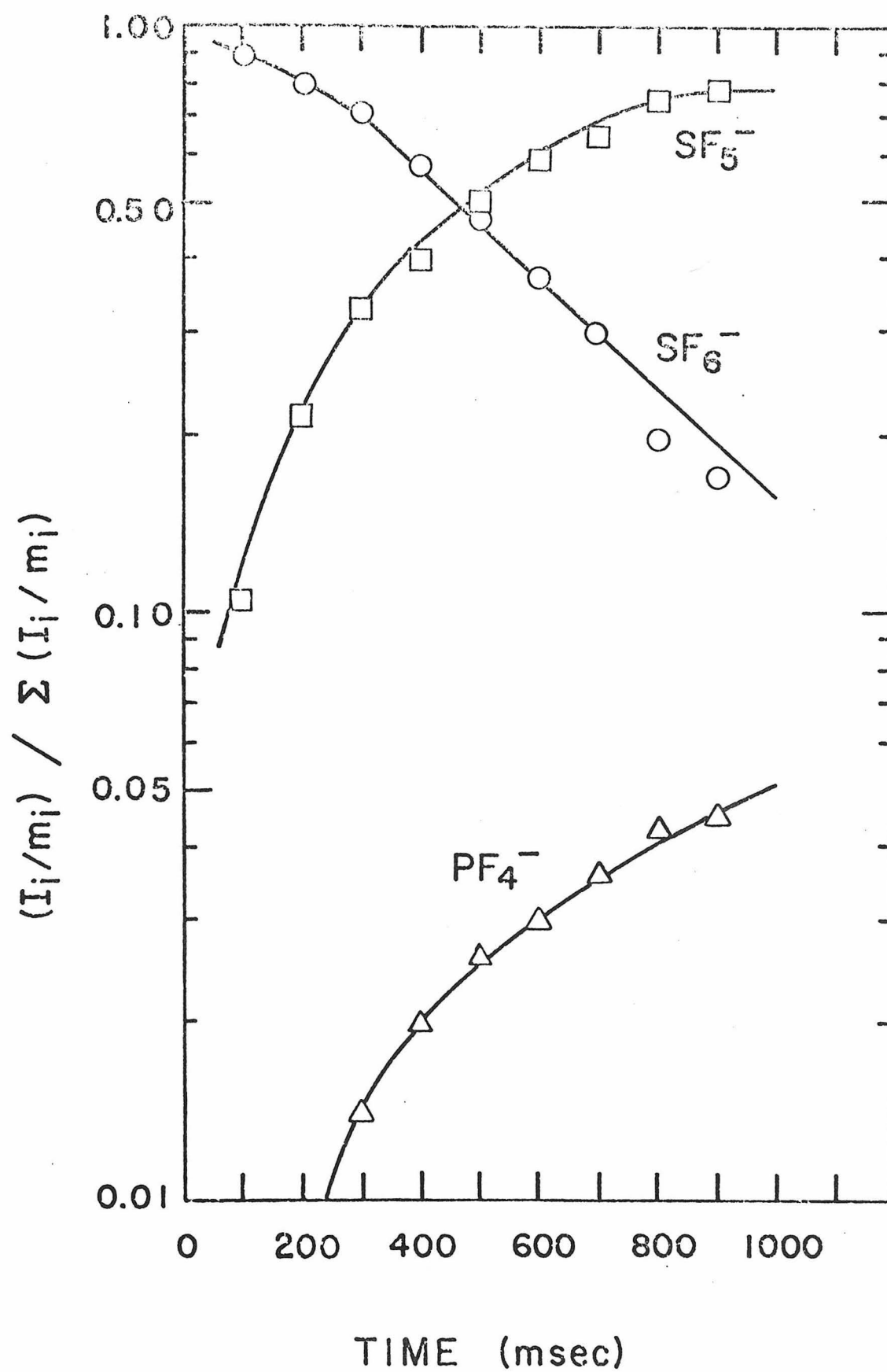
^aExperimental rate is determined as noted in the text; in units of $\text{cm}^3 \text{mol}^{-1} \text{sec}^{-1}$.

^bIn units $\text{cm}^3 \text{mol}^{-1} \text{sec}^{-1}$; calculated as noted in Table I. The Langevain rate equation is used for nonpolar molecules $[k_L = 2\pi e(\alpha/\mu)^{\frac{1}{2}}]$, $\alpha [(\text{CH}_3)_3\text{B}]$ was taken from reference 32.

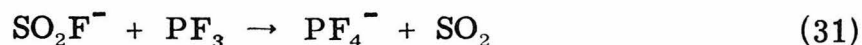
^cIn those cases in which two reaction pathways occur, the total rate is compared to the calculated rate.

FIGURE 6

Temporal variation of normalized ion intensity in a mixture of PF_3 (9.74×10^{-7} torr) with a trace of SF_6 at 20.0 eV.



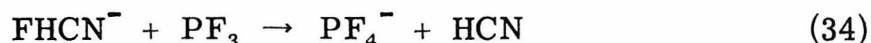
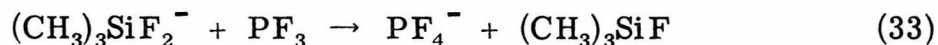
(5×10^{-6} torr) of SO_2F_2 .¹⁹ In a mixture of PF_3 with SO_2F_2 , PF_4^- (m/e 107) is produced by F^- transfer from F_2^- (eq 30) and SO_2F^- (eq 31).



On addition of OPF_3 and PF_3 to SO_2F_2 , OPF_4^- and PF_4^- can be observed. Double resonance confirms that F^- transfer occurs only from PF_4^- to OPF_3 (eq 32). In similar experiments using mixtures of SO_2F_2



with $(\text{CH}_3)_3\text{SiF}$ and HCN , F^- transfer processes generate $(\text{CH}_3)_3\text{SiF}_2^-$ (m/e 111) and FHCN^- (m/e 46), respectively. Both of these ions transfer F^- to PF_3 (eq 33 and 34). An ordering of F^- bond strengths



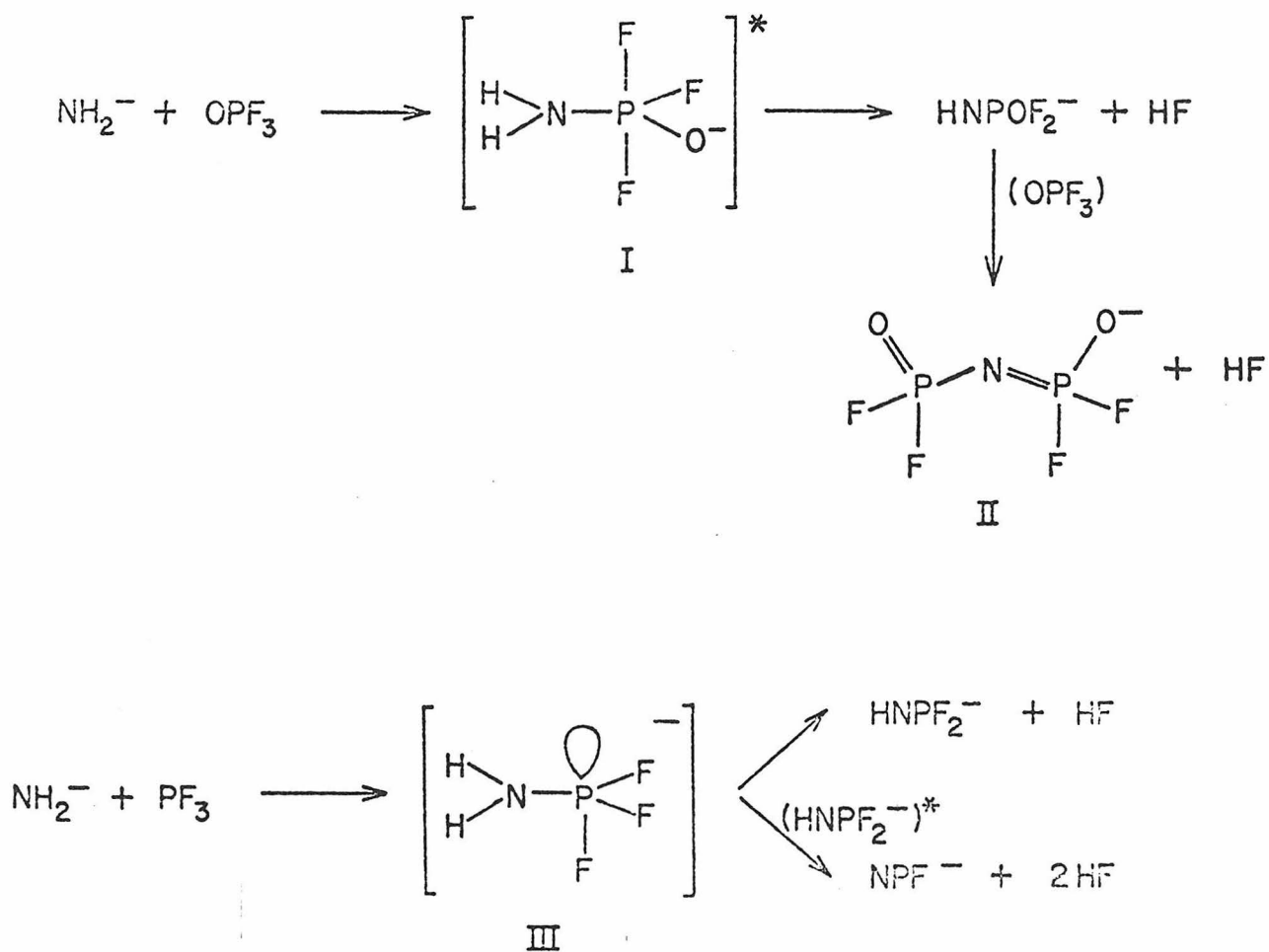
$\text{D}(\text{SO}_2-\text{F}^-) < \text{D}(\text{CNH}-\text{F}^-) < \text{D}(\text{PF}_3-\text{F}^-) < \text{D}(\text{SF}_4-\text{F}^-)$ is consistent with these results. Although $\text{D}(\text{SO}_2-\text{F}^-)$ and $\text{D}(\text{CNH}-\text{F}^-)$ are not well known, estimates³⁵ lead to limits of $45 \text{ kcal/mol} < \text{D}(\text{PF}_3-\text{F}^-) < 54 \text{ kcal/mol}$. Fluoride transfer reactions are summarized in Table II.

Discussion

Nucleophilic Reactivity. In Table I, rate constants for reactions of OPF_3 and PF_3 with gas phase bases are summarized. Experimental rates are compared to collision rates, calculated using the average dipole orientation (ADO) model³⁶ to account for the dipole moment of

the neutral reactants. There is a general trend of increased rate with increased base strength.

The reactions of OPF_3 and PF_3 with anionic bases can be described as the result of the decomposition of penta and tetra coordinate intermediates. In the reaction of NH_2^- with OPF_3 (Scheme I) the

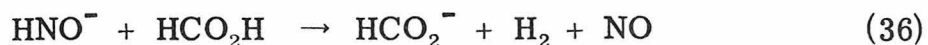


Scheme I

penta coordinate intermediate I dissociates by elimination of HF. The initial product HNOPF_2^- reacts further with OPF_3 to form $\text{N(OPF}_2)_2^-$, presumably a nitrogen bridged anion (II). In contrast, the reaction of NH_2^- with PF_3 results in two products HNPF_2^- and NPF^- (Scheme I). The intermediate in this case, III, also dissociates by elimination of HF. The product HNPF_2^- may be formed with sufficient internal excitation for further decomposition to occur leading to NPF^- .

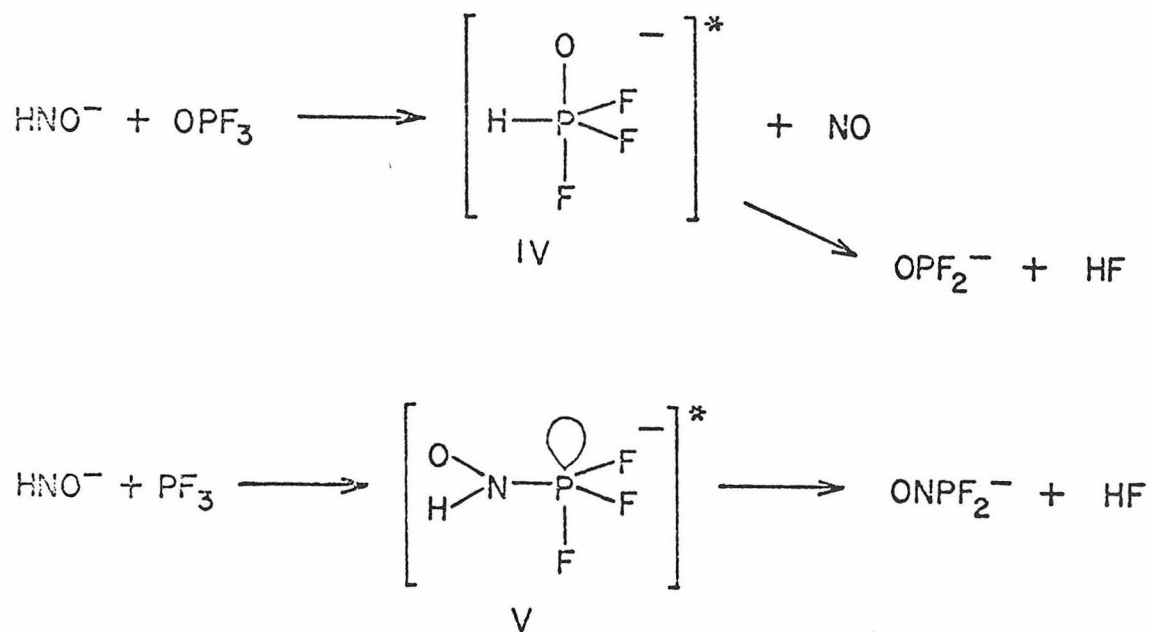
In the present study, O_2PF_2^- , OSPF_2^- , and OPF_2^- do not react further with the neutrals examined. In solution these ions are weakly nucleophilic, displacing halides from phosphoryl and carbonyl compounds.¹ Direct displacement of F^- in gas phase ion molecule reactions is very slow ($k \sim 10^{-12} \text{ cm}^3 \text{ mol}^{-1} \text{ s}^{-1}$).³⁷ Since the phosphorous anions noted above do not contain H or alkyl group to form an energetically favorable neutral leaving group (HF or RF), they are unreactive in these systems.

There are several interesting mechanistic possibilities for the reactions of HNO^- with OPF_3 and PF_3 (Scheme II). In reactions with alkyl boranes, for example with $(\text{CH}_3)_3\text{B}$ (eq 35), HNO^- acts as a hydride donor. With stronger acids such as HCO_2H , an apparent proton transfer occurs³⁸ (eq 36) with H_2 and NO assumed to be the neutral products.



Reaction 36 could proceed as a proton transfer or by decomposition of a chemically activated hydride transfer product $[\text{CH}_3\text{O}^-]^*$. In reaction

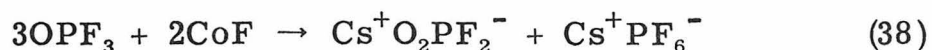
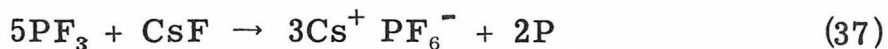
of OPF_3 with HNO^- , proton transfer is impossible. The formation of an energetic hydride transfer intermediate IV as in Scheme II is feasible however. This intermediate would then decompose by elimination of HF, as proposed for the intermediates in Scheme I. The formation of NOPF_2^- by reaction of HNO^- with PF_3 suggests a more



Scheme II

complicated process. Direct complexation of HNO^- to PF_3 as in intermediate V in Scheme II, followed by elimination of HF is a possible pathway to the observed ionic product.

Fluoride Transfer Reactions and Lewis Acidities. In solution, relative Lewis acidities are determined by measurement of the dissociation energies of acid-base complexes, such as $\text{R}_3\text{B}-\text{NR}_3$. A wide range of such complexes are formed with PF_5 acting as an acid. Trivalent phosphorus (III) compounds are generally considered as electron donors, but weakly bound complexes of PF_3 with tertiary amines have been reported.³⁹ Only acid-base complexes in which OPF_3 behaves as a base, with bonding through oxygen, have been observed.⁴⁰ A comparison of the relative abilities of OPF_3 , PF_3 and PF_5 to bind F^- is seen in their reaction with CsF in solution.⁴¹ With PF_5 , the salt Cs^+PF_6^- is readily produced on treatment of PF_5 with CsF . The species $\text{Cs}^+\text{OPF}_4^-$ and Cs^+PF_4^- have not been observed under similar conditions with OPF_3 and PF_3 . In these cases, more complicated reactions occur to form the more stable Cs^+PF_6^- (eq 37) and $\text{Cs}^+\text{O}_2\text{PF}_2^-$ (eq 38). These



solution results indicate that Lewis acidity should decrease in the order $\text{PF}_5 \gg \text{PF}_3 > \text{OPF}_3$.

Gas phase Lewis acidities toward F^- , as measured using icr techniques, decrease in the somewhat different order $\text{PF}_5 > \text{OPF}_3 > \text{PF}_3$ (Table III).⁴² The susceptibility of OPF_3 to nucleophilic attack is strong evidence that OPF_3 acts as an electron acceptor, consistent with the present results. Kinetic instability

rather than thermodynamic instability may prevent the observation of base complexes with OPF_3 in solution. Alternatively, differential solvation effects may cause the inversion of acidities in solution.

The relative acidities of PF_5 , OPF_3 and PF_3 toward F^- as a reference base reflect the decreasing electron density at phosphorous. The ordering observed in this study parallels the increase in Lewis acidities of fluorinated methyl silanes with increased number of fluorine ligands $(\text{CH}_3)_3\text{SiF} < (\text{CH}_3)_2\text{SiF}_2 < \text{CH}_3\text{SiF}_3$ ¹⁵ (Table II). The failure to observe F^- adduct formation with alkyl phosphate esters and the predominance of nucleophilic attack at carbon in these compounds, is then consistent with the lower electronegativity of alkoxide groups compared to fluorine. These results suggest that fluorinated phosphate esters (i.e., $\text{OPF}(\text{OCH}_3)_2$) may have moderate gas phase Lewis acidities toward F^- as a base. If this is true, anionic fluoride transfer will be a useful method for chemical ionization detection¹⁶ of these compounds.⁴³

In conclusion, anionic nucleophilic attack on OPF_3 and PF_3 occurs at phosphorous with anionic products the result of HF elimination from tetra and penta coordinated intermediates. Reaction is enhanced with increased basicity of the attacking anion. This is in contrast to the reactivity of alkyl phosphate esters, in which anionic attack occurs preferentially at carbon. Fluoride transfer reactions suggest that OPF_3 and PF_3 are considerably stronger Lewis acids than phosphorous esters. Both of these differences appear to be a consequence of the decreased electron density at phosphorous in OPF_3 and PF_3 which is imposed by the electronegative fluorine ligands.

Acknowledgment. This research was supported in part by the
U.S. Army Research Office under Grant No. DAAG29-76-G-0274.

References and Notes

- (1) A. J. Kirby and S. G. Warren, "The Organic Chemistry of Phosphorous", Elsevier, Amsterdam, 1967.
- (2) (a) G. M. Kosolapoff and L. Maier, "Organic Phosphorous Compounds", Wiley Interscience, New York, N.Y., 1972; (b) J. R. Van Wazer, "Phosphorous and Its Compounds", Interscience, New York, N.Y., 1958.
- (3) Attack and displacement at phosphoryl groups is important in biological energy transfer processes, see reference 2b.
- (4) D. B. Denny, A. K. Tsolis, and K. Mislow, J. Amer. Chem. Soc., 84, 4486 (1964).
- (5) I. Dostrovsky and M. Halmann, J. Chem. Soc., 1004 (1956).
- (6) D. Samuel and B. L. Silver, Adv. in Phys. Org. Chem., 3, 123 (1965).
- (7) K. W. Hausen and L. S. Bartell, Inorg. Chem., 4, 1775 (1965).
- (8) E. R. Kyba, J. Amer. Chem. Soc., 97, 2554 (1976).
- (9) S. A. Sullivan and J. L. Beauchamp, J. Amer. Chem. Soc., accepted for publication.
- (10) J. F. G. Faigle, P. C. Isolaini, and S. M. Riveros, J. Amer. Chem. Soc., 98, 2049 (1976).
- (11) J. A. Bowie and B. D. Williams, Aust. J. Chem., 27, 1923 (1974).
- (12) O. I. Asubiojo, L. K. Blair, and J. I. Brauman, J. Amer. Chem. Soc., 97, 6685 (1975).
- (13) R. V. Hodges, S. A. Sullivan, and J. L. Beauchamp, unpublished results.
- (14) N. T. Thuong, Bull. Soc. Chim. France, 928 (1971).

- (15) M. K. Murphy and J. L. Beauchamp, Inorg. Chem., accepted for publication.
- (16) See for example, H. P. Tannenbaum, J. D. Roberts, and R. C. Dougherty, Analytical Chem., 47, 49 (1975).
- (17) J. L. Beauchamp, Ann. Rev. Phys. Chem., 22, 527 (1972).
- (18) T. B. McMahon and J. L. Beauchamp, Rev. Sci. Instrum., 43, 509 (1972).
- (19) M. S. Foster and J. L. Beauchamp, unpublished results.
- (20) A. G. Marshall and S. E. Buttrill, Jr., J. Chem. Phys., 52, 2750 (1970) and T. B. McMahon, Ph.D. Thesis, California Institute of Technology, Pasadena, 1973, Chapter V.
- (21) R. W. Odom, D. L. Smith, and J. H. Futrell, Chem. Phys. Lett., 24, 227 (1974) and M. S. Foster and J. L. Beauchamp, Chem. Phys. Lett., 31, 482 (1975).
- (22) K. Jaeger and A. Heinglein, Z. Naturforsch A., 222, 700 (1967).
- (23) J. G. Dillard, Chem. Rev., 73, 590 (1973).
- (24) G. E. Melton and G. A. Neece, J. Amer. Chem. Soc., 93, 6757 (1971).
- (25) W. A. Noyes, Org. Synthesis, 2, 108 (1943).
- (26) T. C. Rhyne and J. G. Dillard, Int. J. Mass Spectrom. Ion Phys., 7, 371 (1971).
- (27) K. A. G. MacNeil and J. C. J. Thynne, J. Phys. Chem., 74, 2257 (1970).

- (28) These ionic species may be formed by electron attachment to trace impurities or neutral products of surface reactions. Similar processes may generate Cl_2^- in CF_2CFCl . See, S. A. Sullivan and J. L. Beauchamp, Chem. Phys. Lett., 48, 294 (1977).
- (29) Since OH^- is generated by a very fast reaction of H^- with H_2O , $\text{H}^- + \text{H}_2\text{O} \rightarrow \text{OH}^- + \text{HO}$ (see reference 24). Similar processes (i.e., $\text{H}^- + \text{PF}_3 \rightarrow \text{PF}_2^- + \text{HF}$) are possible in these systems. Double resonance experiments eliminate this possibility.
- (30) J. L. Beauchamp, J. Chem. Phys., 64, 929 (1976).
- (31) The chemical formula of this ion is inferred from its mass and precursor. The ion structure has not been established.
- (32) M. K. Murphy and J. L. Beauchamp, J. Amer. Chem. Soc., 98, 1433 (1976).
- (33) B. S. Freiser, T. B. McMahon, and J. L. Beauchamp, Int. J. Mass Spectrom. Ion Phys., 12, 249 (1973).
- (34) Entropy effects in equilibrium reaction 21 are estimated to be negligible by comparison of ΔS_{298} of OPF_3 , $(\text{CH}_3)_3\text{B}$, PF_5 , and $(\text{CH}_3)_3\text{CF}$. The latter two species are isoelectronic with the reactant ions OPF_4^- and $(\text{CH}_3)_3\text{BF}^-$, respectively. See S. W. Benson, "Thermochemical Kinetics", 2nd Ed., Wiley and Sons, New York, N.Y., 1976.
- (35) S. A. Sullivan and J. L. Beauchamp, "Positive and Negation Ion Chemistry of Sulfuryl Halides", Chapter III of this thesis.
- (36) L. Bass, T. Su, W. J. Chesnavich, and M. T. Bowers, Chem. Phys. Lett., 34, 119 (1975).

- (37) D. K. Bohme, G. J. Mackay, and J. D. Payzant, J. Amer. Chem. Soc., 96, 4027 (1974).
- (38) S. A. Sullivan and J. L. Beauchamp, unpublished results (see Appendix II of this thesis).
- (39) R. R. Holmes, W. P. Gallagher, and R. P. Carter, Jr., Inorg. Chem., 2, 437 (1963), and E. L. Muetterties and W. Mahler, Inorg. Chem., 4, 119 (1965).
- (40) R. R. Holmes and J. A. Forstner, Inorg. Chem., 2, 380 (1963), and R. R. Holmes, J. Amer. Chem. Soc., 82, 5285 (1960).
- (41) M. Lustig and J. K. Ruff, Inorg. Chem., 6, 2115 (1967).
- (42) A previous gas phase study suggests the relative F^- binding energies decrease $PF_5^- > PF_4^- > OPF_4^-$. T. C. Rhyne and J. G. Dillard, J. Amer. Chem. Soc., 91, 6521 (1969) and T. C. Rhyne and J. G. Dillard, Inorg. Chem., 10, 730 (1971). This ordering is based on relative cross sections for F^- transfer from SF_6^- . Rates do not necessarily reflect thermochemistry. See J. C. Haartz and D. H. McDaniel, J. Amer. Chem. Soc., 95, 3562 (1973).
- (43) Fluorophosphonates are used widely as pesticides. The high human toxicities of some of these compounds necessitates the development of sensitive and specific methods of detection. See, R. D. O'Brien "Toxic Phosphorous Esters: Chemistry, Metabolism and Biological Effects", Academic Press, New York, N.Y., 1960.

CHAPTER II

Acid-Base Properties of 1-Methyl-1, 4

Dihydroborabenzene, $\text{CH}_3\text{BC}_5\text{H}_6$

S. A. Sullivan, H. Sanford, J. L. Beauchamp, and A. J. Ashe III

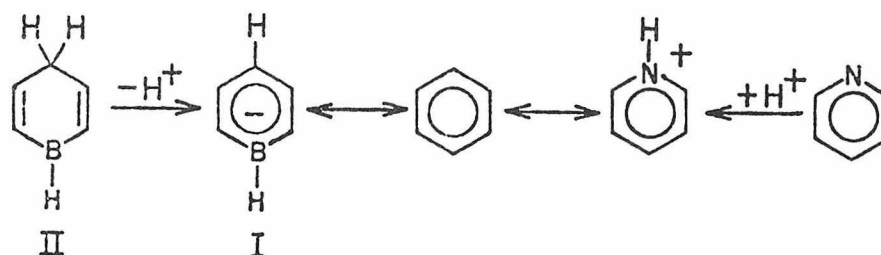
Contribution No. 5624 from the Arthur Amos Noyes
Laboratory of Chemical Physics, California Institute
of Technology, Pasadena, California 91125

ABSTRACT

Ion cyclotron resonance techniques are employed to determine the gas phase Brönsted and Lewis acidities as well as the Brönsted basicity of 1-methyl-1, 4 dihydroborabenzene, $\text{CH}_3\text{BC}_5\text{H}_6$. The ring proton is found to be highly acidic with $\text{PA}(\text{CH}_3\text{BC}_5\text{H}_5) = 337 \pm 3$ kcal/mol. This acidity results from the formation of a 6π electron aromatic anion $\text{CH}_3\text{BC}_5\text{H}_5^-$, which is isoelectronic with toluene. Both the Lewis acidity and proton basicity of the parent molecule suggest that there is little interaction between the diene π system and the electron deficient boron. This is further confirmed by the similarity of both negative and positive ion chemistry of the borabenzene to that of aliphatic boranes.

Introduction

Ionic 6π electron aromatic compounds isoelectronic with benzene can be generated and studied in the gas phase where their intrinsic properties and reactivities can be probed without interference from solvent effects. For example, on protonation of pyridine to form $C_5H_6N^+$ (Scheme I), the cation retains the aromatic properties of neutral pyridine. The low solution basicity of pyridine compared to

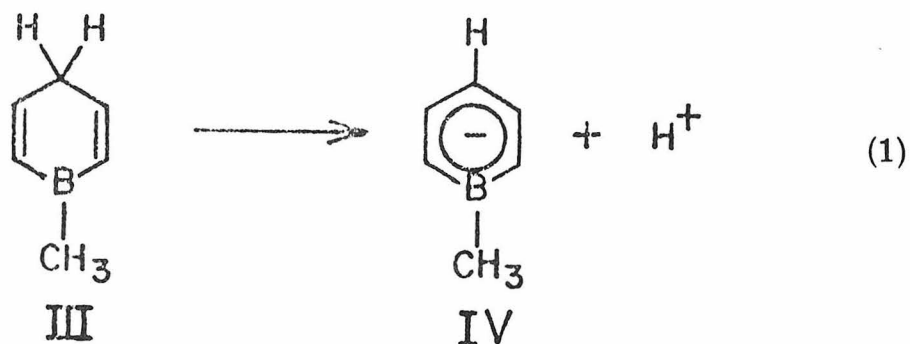


Scheme I

aliphatic amines has been interpreted as the result of increased s character in the nitrogen lone pair. This hybridization change is the result of the involvement of nitrogen in the planar π system. Ion cyclotron resonance measurements indicate that the gas phase basicity of pyridine is significantly greater than that of NH_3 and comparable to aliphatic amines.¹ Differential solvation is responsible for the discrepancy between gas phase and solution results.

An anionic analog of benzene can be generated by proton abstraction from dihydroborobenzene (II) (Scheme I). If boron

participates effectively in π bonding, the anion I will be resonance stabilized, imposing a high acidity on the ring protons of the conjugate acid precursor. Not surprisingly, solution studies in THF indicate that the methyl substituted 1,4-dihydroborabenzene (eq 1) (III)² is a very strong acid, considerably stronger than cyclopentadiene under the same








conditions.³

As with proton basicities, gas phase studies indicate that molecular acidities are strongly moderated by solvation effects. For example, the lower solution acidity of fluorene (pK 23) compared to cyclopentadiene (pK 14-15) has been explained as the result of decreased availability of the electrons to the five-membered ring (annellation) in the fluorenyl anion.⁴ In the gas phase, fluorene is slightly more acidic than cyclopentadiene (Table I).⁵ The solution acidities are apparently strongly moderated by decreased solvation of the larger fluorenyl anion.

In addition to extensive π delocalization in the anion (IV), it is possible that the electron rich diene system may donate electron density into the deficient boron in the neutral borane. The question of π

Table I. Gas Phase Acidities of Selected Compounds^a

MH	PA(M ⁻)	D(M-H)	EA(M)
CH ₃ CHCH ₂	388 ^{b, c}	87 ^g	12.7 ^j
	359.7 ± 0.4 ^d	67 ^b	20.4 ± 0.3 ^j
	352.7 ± 0.2 ^d	81.2 ^h	42.4 ± 0.7 ^k
	348.5 ^d	- -	- -
	335 ± 2.0 ^e	(74) ⁱ	(53) ^{b, i}
	363 ^e	- -	- -
(CH ₃) ₃ B	365 ± 5 ^f	- -	- -

^aAll values in kcal/mol at 298°K.^bCalculated using data in this table.^cJ. H. Richardson, L. M. Stephenson, and J. I. Brauman, J. Chem. Phys., 59, 5068 (1973).^dReference 5.^eThis study.^fReference 17.^gS. W. Benson, "Thermochemical Kinetics", Wiley Interscience, New York, N.Y., 1976.^hS. Furuyama, D. M. Golden, and S. W. Benson, Int. J. Chem. Kinetics, 3, 237 (1971).ⁱEstimated as the bond strength in cyclohexadiene, Reference 20.^jJ. I. Brauman, private communication.

delocalization in vinyl boranes has been examined by several spectroscopic techniques including uv,⁶ nmr,⁷ and photoelectron spectroscopy (PES).⁸ It has been reported that the photoelectron spectra of vinyl borane indicates little or no delocalization into the boron orbital.⁸ On the other hand, both ultraviolet⁶ spectra and nmr studies⁷ have been interpreted in terms of this delocalization. For example, a recent ¹³C-nmr study relates the large deshielding of the terminal carbons in vinyl boranes to π interactions with boron.⁷ This deshielding was considerably decreased in the Lewis acid-base complexes of the vinyl boranes, in which the boron orbital is bonded to a substituent base. By similar reasoning it is expected that the availability of the boron orbital for bonding to a base would be directly effected by π delocalization in the neutral.

Gas phase Lewis acidities of neutrals are determined by measuring bond strengths of neutrals to reference anionic bases such as F^- .⁹ Ion cyclotron resonance studies have provided Lewis acidities of a variety of S, Si, and B compounds toward F^- as a reference base (Table II).

In this study we have investigated the gas phase acid-base properties of $CH_3BC_5H_6$. The proton acidity as well as the Lewis acidity and proton basicity have been determined. By comparisons with appropriate model compounds the present results provide information relating to the degree of resonance stabilization in the anion and π delocalization in the neutral.

Table II. Gas Phase Fluoride Bond Strengths^a

M	D(M-F) ^b
BF ₃	71 ^c
SiF ₄	< 71 ^c
(C ₂ H ₅) ₂ FB	64.0
(C ₂ H ₅) ₃ B	62.0
(CH ₃) ₂ FB	61.8
CH ₃ SiF ₃	60.2 ^d
CH ₃ BC ₅ H ₆	~ 59 ^e
(CH ₃) ₃ B	58.5
(CH ₃) ₂ SiF ₂	56 ^d
SF ₄	54 ± 12 ^f
SF ₅	11 ± 8 ^f

^aAll values in kcal/mol at 298°K, listed in order of decreasing bond strengths.

^bBond strengths to boron species from M. K. Murphy and J. L. Beauchamp, Inorg. Chem., in press, and Reference 17.

^cJ. C. Haartz and D. M. McDaniel, J. Amer. Chem. Soc., 95, 8562 (1973).

^dEstimates based on order of strengths in Reference 9.

^eThis study.

^fM. S. Foster and J. L. Beauchamp, submitted for publication.

Experimental

ICR instrumentation and techniques have been detailed previously.^{10, 11} All experiments were performed on a spectrometer built in this laboratory, incorporating a 15" magnet capable of observing up to m/e 800. Pressure was measured using a Schulz-Phelp ion gauge, calibrated at higher pressures against an MKS Model 90-H1 baratron capacitance manometer. Pressure measurements are the major source of error ($\pm 20\%$) in reported reaction rate constants.

Double resonance techniques were employed to determine the preferred direction of proton transfer reactions in mixtures. Relative proton basicities and acidities result from these data. In acidity studies, the anionic conjugate bases of the neutrals to be compared were generated in proton abstraction reactions of the strong gas phase base CD_3O^- . In a similar manner, relative Lewis acidities toward the reference base F^- were determined in mixtures with SF_6 , in which fluoride donors are produced by electron attachment.

Near thermal electron attachment produces CD_3O^- (75%) and HNO^- (25%) in CD_3ONO .¹² The deuterated nitrite is used to distinguish between CH_3O^- and HNO^- which both appear at m/e 31. At moderate pressures of nitrite (5×10^{-5} torr), NO_2^- is formed on reaction of CD_3O^- with the nitrite. By variation of the partial pressures of the components of mixtures, NO_2^- can be generated in amounts adequate for study of its reactions. Electron attachment processes in SF_6 result in formation of SF_6^- (95%) and SF_5^- (5%).¹³ F^- is similarly generated from NF_3 .¹⁴

The methods of synthesis of the boron compounds used in this study have been described previously.² The purity and identities of $\text{CH}_3\text{BC}_5\text{H}_6$ and the dimethyl analog $\text{CH}_3\text{BC}_5\text{H}_4(\text{CH}_3)_2$ were checked by H-nmr and mass spectral analysis. The latter sample contained $\sim 5\%$ of an unidentified boron species at $\underline{m/e}$ 124-126. Since relative proton acidity studies were not affected by the impurity, no attempt was made to purify the sample. No trace of isotopic impurity was detected in the H-nmr or mass spectrum of the deuterated borabenzene $\text{CD}_3\text{BC}_5\text{H}_6$.

Preparation and use of alkyl nitrites has been described previously.¹⁵ All other compounds used in these experiments were from commercial sources and used without further purification except for repeated freeze-pump-thaw cycles to remove noncondensable impurities.

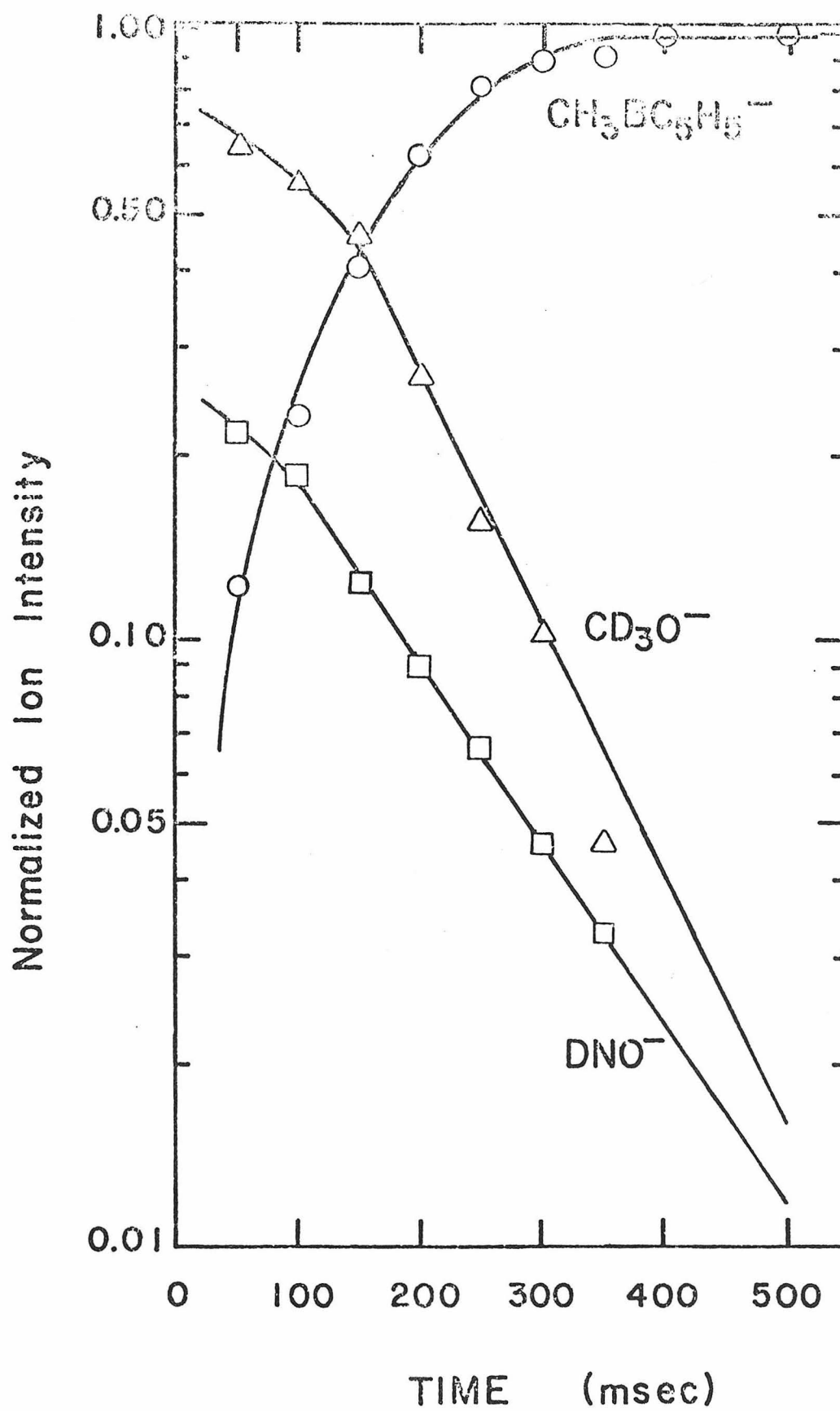
Normalized intensities of boron ions reported in tables and figures are the sum of ^{10}B and ^{11}B isotope intensities. In all cases, the naturally occurring isotope ratios were observed (^{10}B , 19.9% and ^{11}B , 80.1%). For simplicity, only the mass of the more abundant ^{11}B isotopes are included in the text and figures.

Results

Proton Acidity of $\text{CH}_3\text{BC}_5\text{H}_6$. Figure 1 presents the temporal variation of normalized ion intensity in a (1.3:1) mixture of $\text{CH}_3\text{BC}_5\text{H}_6$ and CD_3ONO at a total pressure of 8.0×10^{-7} torr. Double resonance experiments confirm that both CD_3O^- ($\underline{m/e}$ 34) and DNO^- ($\underline{m/e}$ 32) react with $\text{CH}_3\text{BC}_5\text{H}_6$ by proton transfer to form $\text{CH}_3\text{BC}_5\text{B}_5^-$ ($\underline{m/e}$ 91),

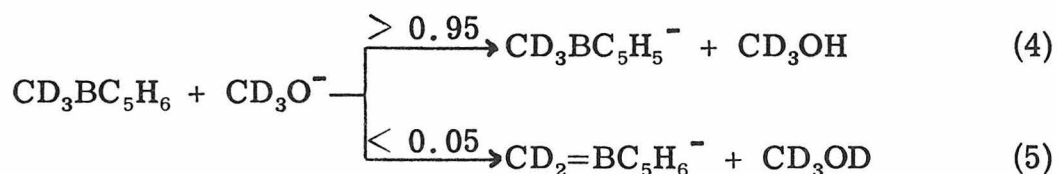
FIGURE 1

Temporal variation of normalized negative ion intensity in a (1.3:1) mixture of $\text{CH}_3\text{BC}_5\text{H}_6$ and CD_3ONO at total pressure 8.0×10^{-7} torr.





as in eqs 2 and 3, where neutrals are assumed. The ring proton is more acidic, as shown by the predominance of $\text{CD}_3\text{BC}_5\text{H}_5^-$ (m/e 94) in the reaction of CD_3O^- with $\text{CD}_3\text{BC}_5\text{H}_6$ as seen in eqs 4 and 5. Rates of



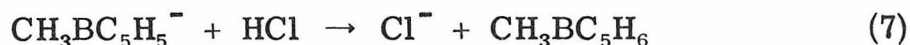
(5)

reactions 2 and 3 are listed in Table III.

Proton transfer processes were further examined in mixtures of CD_3ONO , $(\text{CH}_3)_3\text{B}$, HCO_2H , HCN , HCl , $\text{C}_6\text{H}_5\text{OH}$ and $\text{C}_6\text{H}_5\text{CO}_2\text{H}$ with $\text{CH}_3\text{BC}_5\text{H}_6$ to determine the acidity of the latter species. In each case, CD_3ONO was added to insure the formation of both anionic species, by reaction of the strong base CD_3O^- . The preferred direction of proton transfer in these mixtures was determined using double resonance techniques. Proton transfer reaction 6 is observed only in the direction noted with $\text{B}^- = (\text{CH}_3)_2\text{B}=\text{CH}_2^-$, CN^- , HCO_2^- and NO_2^- . In contrast,



$\text{CH}_3\text{BC}_5\text{H}_5$ reacts with HCl to form Cl^- (eq 7). Double resonance



irradiation of Cl^- results in a slight decrease in $\text{CH}_3\text{BC}_5\text{H}_5^-$ ion intensity, suggesting that reaction 7 may also occur in the reverse direction.

Table III. Summary of Measured Reaction Rates

Reaction	k_{ex}^a
$\text{CD}_3\text{O}^- + \text{CH}_3\text{BC}_5\text{H}_6 \longrightarrow \text{CH}_3\text{BC}_5\text{H}_5^- + \text{CD}_3\text{OH}$	11.1
$\text{DNO}^- + \text{CH}_3\text{BC}_5\text{H}_6 \longrightarrow \text{CH}_3\text{BC}_5\text{H}_5^- + \text{DH} + \text{NO}$	3.2
$\text{SF}_6^- + \text{CH}_3\text{BC}_5\text{H}_6 \begin{cases} \xrightarrow{0.75} \text{SF}_5^- + \text{HF} + \text{CH}_3\text{BC}_5\text{H}_5 \\ \xrightarrow{0.25} \text{F}_2\text{BC}_5\text{H}_6^- + \text{CH}_3 + \text{SF}_4 \end{cases}$	1.25
$\text{SF}_5^- + \text{CH}_3\text{BC}_5\text{H}_6 \longrightarrow \text{F}(\text{CH}_3)\text{BC}_5\text{H}_6^- + \text{SF}_4$	0.22
$\text{SF}_5^- + \text{CH}_3\text{BC}_5\text{H}_6 \longrightarrow \text{F}(\text{CH}_3)\text{BC}_5\text{H}_6^- + \text{SF}_4$	0.56
$\text{SF}_6^- + (\text{CH}_3)_3\text{B} \begin{cases} \longrightarrow \text{SF}_5^- + \text{HF} + (\text{CH}_3)_2\text{BCH}_2 \\ \longrightarrow \text{F}_2\text{B}(\text{CH}_3)_2^- + \text{SF}_4 + \text{CH}_3 \end{cases}$	3.7
$\text{SF}_5^- + (\text{CH}_3)_3\text{B} \longrightarrow \text{F}_2\text{B}(\text{CH}_3)_2^- + \text{SF}_4 + \text{CH}_3$	1.4
$\text{SF}_5^- + (\text{CH}_3)_3\text{B} \longrightarrow \text{FB}(\text{CH}_3)_2^- + \text{SF}_4$	2.8

$^a k_{\text{ex}}$ in units of $10^{-10} \text{ cm}^3 \text{ mol}^{-1} \text{ sec}^{-1}$.

However, equilibrium could not be achieved in this mixture by variation of the relative pressures of the neutrals. In mixtures of C_6H_5OH and $C_6H_5CO_2H$ with $CH_3BC_5H_6$, the conjugate bases were formed in abundance by proton transfer to CD_3O^- . In each case, no reactive coupling of the anions was detected by double resonance. This is not very surprising considering that reactions of conjugated anions are generally very slow.¹⁶ These experiments combined with literature data suggest that acidity increases in the order $(CH_3)_3B > HCO_2H > HCN > HNO_2 > CH_3BC_5H_6 > HCl$. The acidities of the reference compounds have been determined previously as listed in Table IV. Using these data, $PA(CH_3BC_5H_5^-)$ is estimated as 335 ± 2 kcal/mol.

Lewis Acidity of $CH_3BC_5H_6$. The bond strength $D(M-F^-)$ is a measure of the Lewis acidity of the species M. Relative fluoride bond strengths to a variety of neutrals have been measured previously and are listed in Table II. The acidity of a compound toward fluoride ion as a reference base can be measured by determining the preferred direction of F^- transfer in mixtures with neutrals of known acidity.⁹ Anionic F^- adducts are formed in these experiments by reactions of SF_6^- and/or SF_5^- .

Temporal variation of normalized ion intensity in a mixture of $CH_3BC_5H_6$ (7.16×10^{-7} torr) with a trace amount ($< 10^{-7}$ torr) of SF_6 is presented in Figure 2. Ionic products SF_5^- (m/e 127), $F(CH_3)BC_5H_6^-$ (m/e 111) and $F_2BC_5H_6^-$ (m/e 115) increase as SF_6^- (m/e 146) decays with time. Double resonance confirms that SF_6^- reacts to form SF_5^- (eq 8) and $F_2BC_5H_6^-$ (eq 9). The F^- adduct $F(CH_3)BC_5H_6^-$ is formed only

Table IV. Gas Phase Acidities of Selected Reference Acids^a

MH	PA(M ⁻)
CD ₃ OH	378.4 ^b
HF	371.3 ^c
CF ₃ CH ₂ OH	364 ± 5 ^d
AsH ₃	360 ± 10 ^e
HCN	348.9 ^c
C ₆ H ₅ OH	346.9 ^f
HCO ₂ H	342.2 ^g
C ₆ H ₅ CO ₂ H	336.7 ^g
HCl	333.3 ^c

^aAll values in kcal/mol at 298°K. Unless otherwise noted, error limits are ± 0.5 or less.

^bR. T. McIver, Jr. and J. S. Miller, J. Amer. Chem. Soc., 96, 4323 (1974) and J. E. Bartness and R. T. McIver, Jr., J. Amer. Chem. Soc., 99, 4163 (1977).

^cCalculated using thermochemical data from D. R. Stull and H. Prophet, "JANAF Thermochemical Tables", 2nd edition, U. S. Government Printing Office, Washington, D.C., 1971.

^dB. S. Freiser and J. L. Beauchamp, unpublished results.

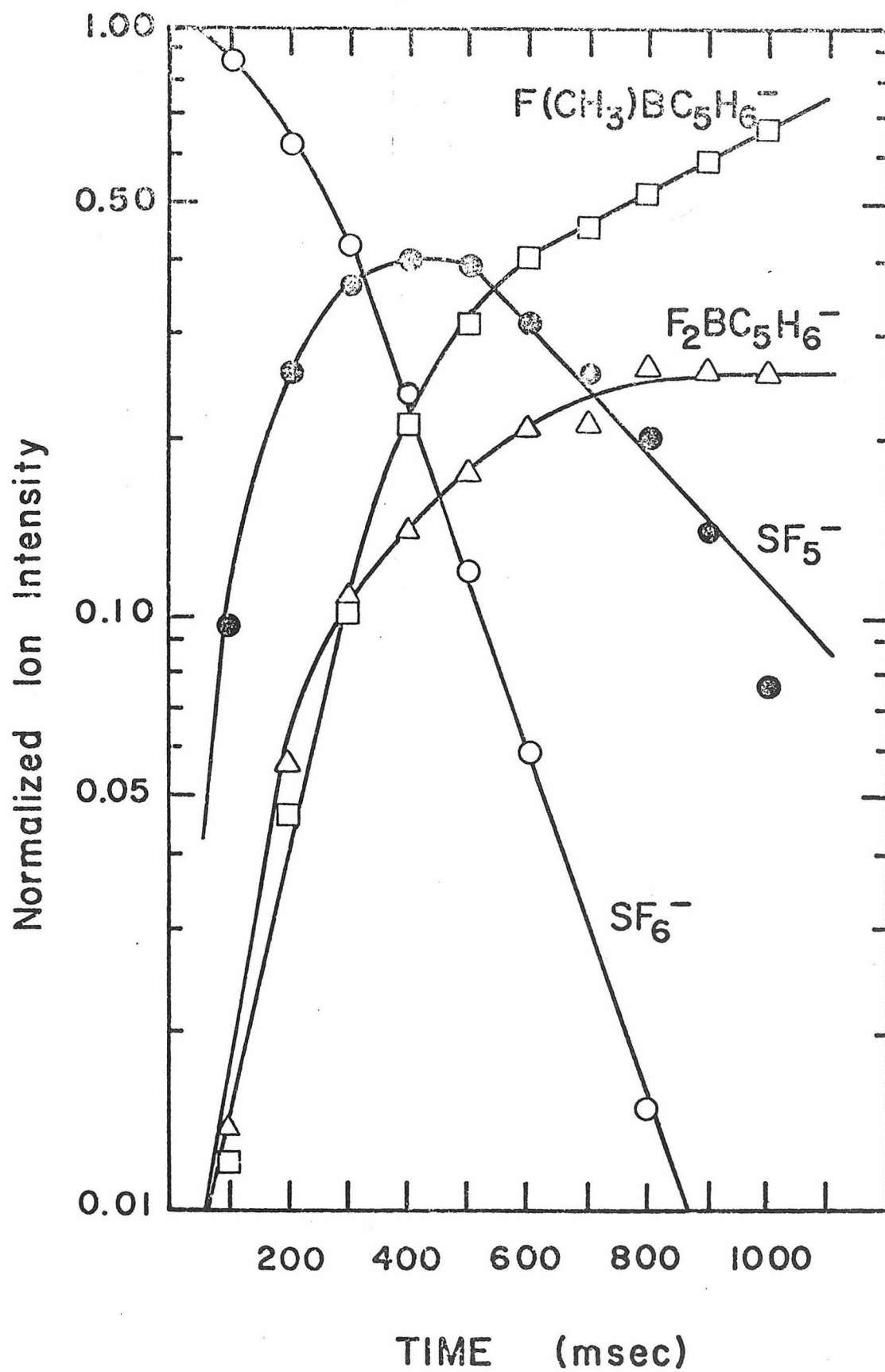
^eR. H. Wyatt, D. Holtz, T. B. McMahon, and J. L. Beauchamp, Inorg. Chem., 13, 1511 (1974).

^fR. T. McIver, Jr. and J. H. Silvers, J. Amer. Chem. Soc., 95, 8462 (1973).

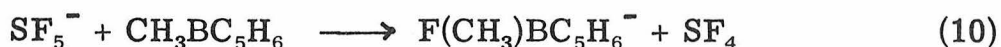
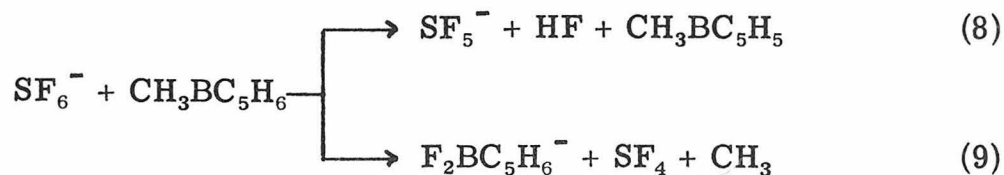
^gT. B. McMahon and P. Kebarle, J. Amer. Chem. Soc., 99, 2222 (1977) and references contained therein.

FIGURE 2

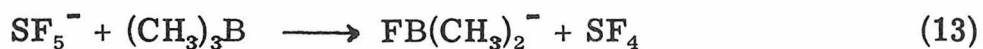
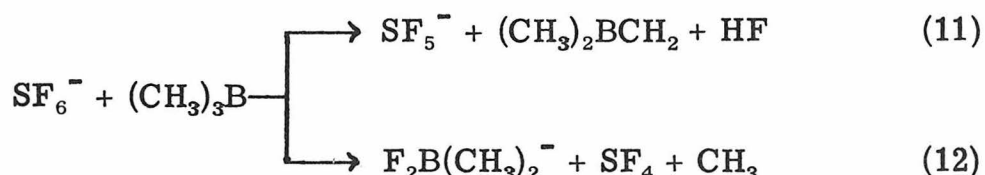
Temporal variation of normalized negative ion intensity in a mixture of 7.16×10^{-7} torr $\text{CH}_3\text{BC}_5\text{H}_6$ with a trace amount of SF_6 .



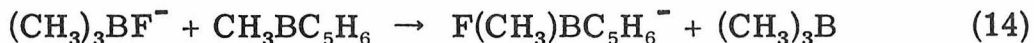
by reaction of SF_5^- (eq 10). Rates for these reactions (eqs 7-10) are summarized in Table III.



Fluoride transfers were examined in mixtures of $(\text{CH}_3)_3\text{B}$ and $(\text{CH}_3)_2\text{SiF}_2$ with $\text{CH}_3\text{BC}_5\text{H}_6$ and a trace amount of SF_6 . When $(\text{CH}_3)_3\text{B}$ is added to SF_6 , ¹⁷ product ions $(\text{CH}_3)_3\text{BF}^-$ (m/e 75) and $(\text{CH}_3)_2\text{BF}_2^-$ (m/e 79) and SF_5^- (m/e 127) result in reactions 11-13 analogous to

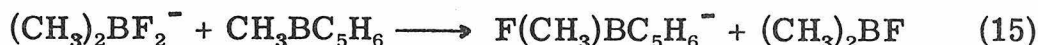


processes 8-10. These reactions are summarized in Table III with rates included for comparison to reactions of $\text{CH}_3\text{BC}_5\text{H}_6$. With addition of $\text{CH}_3\text{BC}_5\text{H}_6$, double resonance indicates that $(\text{CH}_3)_3\text{BF}^-$ reacts to form $\text{F}(\text{CH}_3)\text{BC}_5\text{H}_6^-$ (eq 14). Although there is some indication

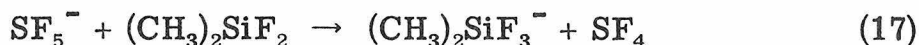
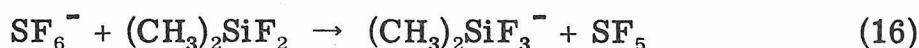


that the reverse reaction occurs, the slow rate of formation of $\text{F}(\text{CH}_3)\text{BC}_5\text{H}_6^-$ from SF_5^- hinders quantitative measurement of the equilibrium constant for F^- transfer in this reaction. The difluoride

ion $(\text{CH}_3)_2\text{BF}_2^-$ does not contribute to the formation of $\text{F}(\text{CH}_3)\text{BC}_5\text{H}_6^-$ suggesting that reaction 15 is endothermic.



Both SF_6^- (eq 16) and SF_5^- (eq 17) react to form $(\text{CH}_3)_2\text{SiF}_3^-$ (m/e 115) on electron impact of a mixture of $(\text{CH}_3)_2\text{SiF}_2$ and SF_6 .⁹



On addition of $\text{CH}_3\text{BC}_5\text{H}_6$, double resonance indicates that $(\text{CH}_3)_2\text{SiF}_3^-$ transfers F^- to $\text{CH}_3\text{BC}_5\text{H}_6$ (eq 18). These results suggest the Lewis



acidities increase $\text{SF}_5 < (\text{CH}_3)_2\text{SiF}_2 < (\text{CH}_3)_3\text{B} \sim \text{CH}_3\text{BC}_5\text{H}_6 < (\text{CH}_3)_2\text{BF}$. A value of 59 kcal/mol for $\text{D}(\text{CH}_3\text{BC}_5\text{H}_6 - \text{F}^-)$ is estimated from F^- bond strengths in Table II.

Proton Affinity of $\text{CH}_3\text{BC}_5\text{H}_6$. Proton transfer reactions were examined in mixtures of $\text{CH}_3\text{BC}_5\text{H}_6$ with CH_4 , $(\text{CH}_3)_2\text{CHCH}_2$, CH_3CHCH_2 , *c*- C_6H_{10} and CH_3COCH_3 to determine the basicity of the borabenzene. Protonation of $\text{CH}_3\text{BC}_5\text{H}_6$ to form $\text{CH}_3\text{BC}_5\text{H}_7^+$ (m/e 93) occurs with proton donors ($\text{MH}^+ = \text{CH}_5^+$, C_2H_5^+ and $(\text{CH}_3)_3\text{C}^+$) as in reaction 19.








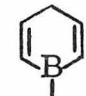
Double resonance indicates that reaction occurs in both directions with

M = isobutene. Failure to observe equilibrium in this case suggests that deprotonation of $\text{CH}_3\text{BC}_5\text{H}_7^+$ is slow.

Conclusive results were not obtained in other mixtures. In mixtures of $\text{CH}_3\text{BC}_5\text{H}_6$ with *c*- C_6H_{10} and CH_3CHCH_3 , the boron compound is preferentially protonated by the parent and fragment ions of the alkenes. In both cases, little or no protonated alkene is observed. The reverse situation obtains in mixtures of $\text{CH}_3\text{BC}_5\text{H}_6$ with CH_3COCH_3 , in which protonation of acetone predominates and proton transfer from this species to the neutral borane is not observed. These results suggest that proton affinities increase $\text{CH}_4 < \text{C}_2\text{H}_4 < \text{CH}_3\text{CHCH}_2 < (\text{CH}_3)_2\text{CCH}_2 \sim \text{CH}_3\text{BC}_5\text{H}_6 < \text{CH}_3\text{COCH}_3$, with $\text{PA}(\text{CH}_3\text{BC}_5\text{H}_6)$ estimated as 195 kcal/mol (Table V). From a limiting value for the ionization potential $\text{IP}(\text{CH}_3\text{BC}_5\text{H}_6) < 9.0 \pm 0.50$ eV obtained from appearance potential measurements,¹⁹ a hydrogen affinity¹⁰ $\text{HA}(\text{CH}_3\text{BC}_5\text{H}_6^+) = 89 \pm 11$ kcal/mol is estimated, somewhat higher than expected by analogy to trans-2-butene (Table V).

Positive Ion Chemistry of $\text{CH}_3\text{BC}_5\text{H}_6$. Three major ions represent $\sim 95\%$ of total ionization in the 70.0 eV electron impact mass spectrum of $\text{CH}_3\text{BC}_5\text{H}_6$, the parent ion $\text{CH}_3\text{BC}_5\text{H}_6^+$ (m/e 92, 12%), loss of methyl to give BC_5H_6^+ (m/e 77, 22%) and loss of hydrogen to yield $\text{CH}_3\text{BC}_5\text{H}_5^+$ (m/e 91, 61%). The latter ion, first detected at electron energies ~ 0.50 eV higher than the $\text{IP}(\text{CH}_3\text{BC}_5\text{H}_6)$,¹⁹ becomes the most abundant fragment above 10.0 eV. These three ions are unreactive with $\text{CH}_3\text{BC}_5\text{H}_6$. In particular, double resonance of the boron isotopes of BC_5H_6^+ indicate that the thermoneutral CH_3^- transfer (eq 20) does

Table V. Gas Phase Proton Affinities, Hydrogen Affinities, and Ionization Potentials of Selected Alkenes^a

M	PA(M) ^b	HA(M ⁺) ^b	IP(M)	$\Delta H_f(MH^+)$
CH ₂ CH ₂	161	89	242.4	219
CH ₃ CHCH ₂	181	92	224.6	191
	181	78	210.5	183
	182	79	210.5	183
	196	95	212.8	167
	200	84	197.6	199 ^c
	178	72	207.7	197 ^c
	195	88 ^d	$< 207 \pm 12^d$	- -

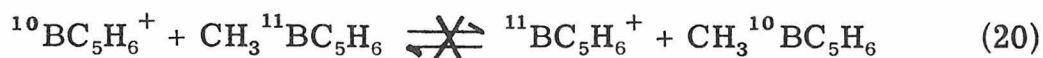
^aAll values in kcal/mol at 298°K. Unless otherwise noted, IP(M) and $\Delta H_f(MH^+)$ are taken from H. M. Rosenstock, K. Draxl, B. W. Steiner, and J. T. Herron, J. Phys. and Chem. Ref. Data, 6, Supplement 1 (1977).

^bCalculated from thermochemical data listed in this table.

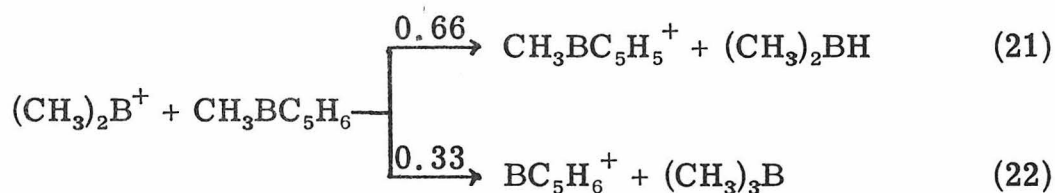
^cCalculated using data in F. P. Lossing and J. C. Traeger, J. Amer. Chem. Soc., 97, 1579 (1975).

^dSee text.

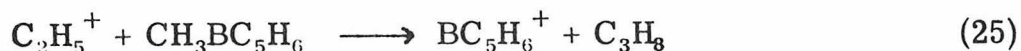
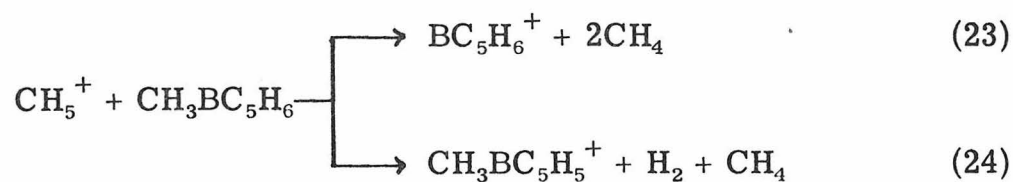
not occur in contrast to reactions in $(\text{CH}_3)_3\text{B}$.¹⁷



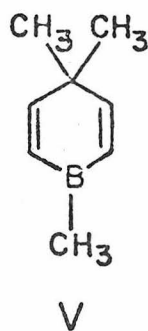
Positive Ion Chemistry in Mixtures of $(\text{CH}_3)_3\text{B}$ and CH_4 with $\text{CH}_3\text{BC}_5\text{H}_6$. In trapped ion studies of mixtures of $\text{CH}_3\text{BC}_5\text{H}_6$ and $(\text{CH}_3)_3\text{B}$, double resonance confirms that the major fragment ion of $(\text{CH}_3)_3\text{B}$, $(\text{CH}_3)_2\text{B}^+$, reacts with $\text{CH}_3\text{BC}_5\text{H}_6$ to form $\text{CH}_3\text{BC}_5\text{H}_5^+$ (eq 21) and BC_5H_6^+ (eq 22).



As described above, proton transfer reactions in mixtures of $\text{CH}_3\text{BC}_5\text{H}_6$ with a variety of proton donors were examined. With CH_4 , the reactivity of CH_5^+ and C_2H_5^+ were studied in more detail. In addition to proton transfer reactions (eq 5), both CH_5^+ (eq 23) and C_2H_5^+ (eq 24) react with $\text{CH}_3\text{BC}_5\text{H}_6$ to form BC_5H_6^+ . CH_5^+ also contributes to the formation of $\text{CH}_3\text{BC}_5\text{H}_5^+$ (eq 25). This reaction involves cleavage of the ring hydrogen, as determined by reaction with $\text{CD}_3\text{BC}_5\text{H}_6$ (eq 26).

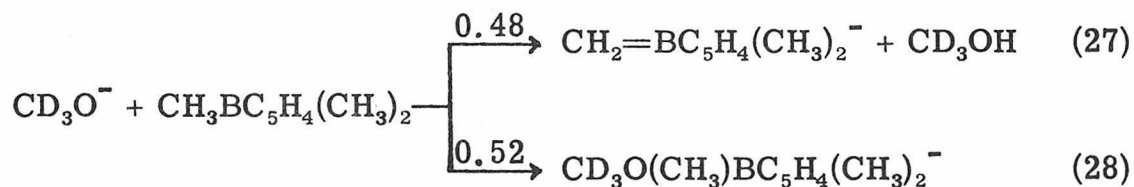


Negative Ion Chemistry. Proton transfer processes dominate the negative ion chemistry of $\text{CH}_3\text{BC}_5\text{H}_6$. To probe the interaction of negative ions with the vinyl borane moiety, chemistry in mixtures with $\text{CH}_3\text{BC}_5\text{H}_5(\text{CH}_3)_2$ (V) was examined. These studies also provide a

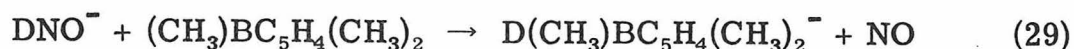


qualitative measure of the proton acidity of the boron methyl.

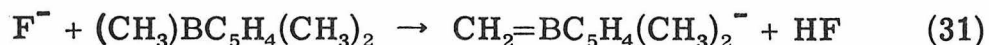
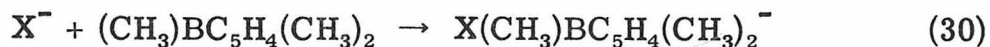
In a mixture of V with CD_3ONO , anionic products $\text{CH}_2=\text{BC}_5\text{H}_4(\text{CH}_3)_2^-$ ($\underline{\text{m/e}}$ 119), $\text{CD}_3\text{O}(\text{CH}_3)\text{BC}_5\text{H}_4(\text{CH}_3)_3^-$ ($\underline{\text{m/e}}$ 154) and $\text{D}(\text{CH}_3)\text{BC}_5\text{H}_4(\text{CH}_3)_2^-$ ($\underline{\text{m/e}}$ 122) appear. Double resonance indicates that CD_3O^- reacts with V by proton transfer (eq 27) and direct anion addition (28). Product distributions in eqs 27 and 28 are determined



from drift mode single resonance ion intensities at 1×10^{-5} torr of borane. The anion addition product (eq 28) increases markedly relative to proton transfer, as the borane pressure is increased. This is consistent with increased collisional stabilization of the adduct ion at higher pressures. In contrast to reactivity in $\text{CH}_3\text{BC}_5\text{H}_6$, DNO^- reacts with V to form only $\text{D}(\text{CH}_3)\text{BC}_5\text{H}_4(\text{CH}_3)_2^-$ by deutride transfer (eq 29).



Direct formation of anionic adducts (eq 30) is observed with anions $\text{X}^- = \text{CD}_3\text{O}^-$, NO_2^- , and Cl^- . In contrast, F^- reacts with V only by proton transfer (eq 31).



Attempts were made to determine the preferred direction of proton transfer in mixtures of V with AsH_3 and $\text{CF}_3\text{CH}_2\text{OH}$. Although the anionic conjugate bases were formed by proton transfer to CD_3O^- in both bases, no reactive coupling of AsH_2^- and $\text{CF}_3\text{CH}_2\text{O}^-$ with $\text{CH}_2=\text{BC}_5\text{H}_4(\text{CH}_3)_2^-$ was observed. Only rough limits $\sim 365 \text{ kcal/mol} < \text{PA}(\text{CH}_2\text{BC}_5\text{H}_4(\text{CH}_3)_2^-) < 370 \text{ kcal/mol}$ are suggested by reaction 30 and the failure to observe proton transfer to DNO^- (Table IV).¹⁸ The proton affinity $\text{PA}[(\text{CH}_3)_2\text{B}=\text{CH}_2^-]$ was determined previously in a similar manner to be $365 \pm 5 \text{ kcal/mol}$.¹⁹

Discussion

The acid-base properties of $\text{CH}_3\text{BC}_5\text{H}_6$ reflect the degree of interaction of the diene π system with the empty B orbital in both the neutral and conjugate base. The unusually high acidity of $\text{CH}_3\text{BC}_5\text{H}_6$, comparable to HCl, indicates that the anion is resonance stabilized with participation of the boron orbital to form a 6π aromatic anion. In contrast, no evidence is found for π delocalization in $\text{CH}_3\text{BC}_5\text{H}_6$.

Delocalization of π electron density into the B orbital in the neutral would be expected to decrease its availability for bonding, i.e.,

result in a low Lewis acidity or electron acceptor ability. There is no significant decrease in Lewis acidity of $\text{CH}_3\text{BC}_5\text{H}_6$ compared to $(\text{CH}_3)_3\text{B}$ or $(\text{C}_2\text{H}_5)_3\text{B}$ (Table II). Similarly, the basicity of the ring in $\text{CH}_3\text{BC}_5\text{H}_6$ is expected to be decreased if a favorable π interaction is disrupted by protonation. Although proton affinities vary significantly with substitution for homologous series, hydrogen affinities of the cations (homolytic bond dissociation energies) appear to be representative of the site of protonation (Table V).¹⁰ As noted above, the thermochemical properties derived for $\text{CH}_3\text{BC}_5\text{H}_6$ and the protonated species $\text{CH}_3\text{BC}_5\text{H}_7^+$, are consistent with protonation of an unperturbed alkene (Table V). Finally, both positive and negative ion reactions involving the boron moiety in $\text{CH}_3\text{BC}_5\text{H}_6$ are similar to those observed with alkyl boranes. The Lewis acidity proton affinity and ion chemistry of $\text{CH}_3\text{BC}_5\text{H}_6$ are all consistent with PES results,⁸ indicating that there is little interaction of the diene π system with boron.

Delocalization in Aromatic Anions. The proton affinity of an anion B^- , $\text{PA}(\text{B}^-)$, is related to the homolytic bond energy $D(\text{BH})$ and the electron affinity $\text{EA}(\text{B})$ by eq 32, in which the ionization potential of

$$\text{PA}(\text{B}^-) = D(\text{B}-\text{H}) - \text{EA}(\text{B}) + \text{IP}(\text{H}) \quad (32)$$

H, $\text{IP}(\text{H}) = 313.6 \text{ kcal/mol}$. Relative proton affinities or acidities are the result of differences in bond strength and electron affinities, which reflect the stability of the radical B and the anion B^- , respectively.

If two of the quantities in eq 32 are known, it is possible to assess how differences in radical and anion stabilities affect the acidity of a species.

By comparison to appropriate model compounds with known acidities, it is possible to quantify the resonance energy of aromatic anions. For example, in the gas phase $c\text{-C}_5\text{H}_6$ is only 7 kcal/mol more acidic than the open chain 1,4-pentadiene, C_5H_8 (Table I). Cyclopentadienyl radical has an electron affinity 22 kcal/mol higher than the open chain diene. The 15 kcal/mol higher bond strength in $c\text{-C}_5\text{H}_6$ compared to 1,4-pentadiene is responsible for the small acidity difference in the two dienes. This change in bond strength can be attributed for the most part to ring strain in the radical $c\text{-C}_5\text{H}_5$. The difference in electron affinities $\text{EA}(c\text{-C}_5\text{H}_5) - \text{EA}(\text{C}_5\text{H}_7)$ does not directly measure the delocalization energy in $c\text{-C}_5\text{H}_6$, since it ignores structural changes required to form the strained planar anion. If it is assumed that the strain in the anion is equal to that in the radical, 15 kcal/mol, a delocalization energy of 37 kcal/mol is calculated for $c\text{-C}_5\text{H}_5^-$.

Neither the electron affinity of the borabenzene radical $\text{EA}(\text{CH}_3\text{BC}_5\text{H}_5)$ nor the strength of the ring C-H bond in the neutral have been measured. An $\text{EA}(\text{CH}_3\text{BC}_5\text{H}_5) = 58$ kcal/mol is estimated, however, by assuming that the C-H bond strength is equal to that in 1,4-cyclohexadiene (74 kcal/mol).²⁰ The delocalization energy is the quantity needed for comparison to other aromatic systems. By the same analysis used for cyclopentadienyl anion, comparisons of relative bond strengths and electron affinities of $\text{CH}_3\text{BC}_5\text{H}_6$ and 1,4-pentadiene yield a delocalization or resonance energy of 40 kcal/mol for $\text{CH}_3\text{BC}_5\text{H}_5^-$. Although admittedly dependent on the assumptions made, this indicates little difference in delocalization energies of the 5-center 6π -electron cyclopentadienyl anion and the 6-center 6π -electron

dihydroborabenzene anion. Interestingly, the delocalization energies in both anions is approximately equivalent to that generally accepted for benzene which is determined (36 kcal/mol) from heats of hydrogenation. Simple Hückle molecular orbital theory²¹ predicts the equivalence of resonance energy in benzene and cyclopentadienyl anion. However, the extension of these principles to borabenzene anion is not straightforward. These results indicate that the presence of the heteroatom boron has little effect on π delocalization in the 6-member ring.

Acknowledgments. This research was supported in part by the Energy Research and Development Administration under Grant No. AT(04-3)767-8.

References and Notes

- (1) M. Taagepera, W. G. Henderson, R. T. C. Brownlee, J. L. Beauchamp, D. Holtz, and R. W. Taft, J. Amer. Chem. Soc., 95, 1369 (1972).
- (2) A. J. Ashe III, E. Meyers, P. Shu, T. von Lehmann, and J. Bastide, J. Amer. Chem. Soc., 97, 6865 (1975).
- (3) A. J. Ashe III, private communication.
- (4) See discussion in J. March, "Advances in Organic Chemistry Reactions, Mechanisms, and Structure", McGraw-Hill, New York, N.Y., 1968, Chapter 8.
- (5) T. B. McMahon and P. Kebarle, J. Amer. Chem. Soc., 98, 3399 (1976).
- (6) J. R. Durig, R. O. Carter, and J. D. Odom, Inorg. Chem., 13, 701 (1974).
- (7) L. W. Hall, J. D. Odom, and P. D. Ellis, J. Amer. Chem. Soc., 97, 4527 (1975).
- (8) A. K. Holliday, W. Reade, K. R. Seddon, and I. A. Steer, J. Organomet. Chem., 67, 1 (1974).
- (9) M. K. Murphy and J. L. Beauchamp, J. Amer. Chem. Soc., in press.
- (10) J. L. Beauchamp, Ann. Rev. Phys. Chem., 22, 527 (1971).
- (11) T. B. McMahon and J. L. Beauchamp, Rev. Sci. Instrum., 43, 509 (1972).
- (12) K. Jaeger and A. Heinglein, Z. Naturforsch A, 222, 700 (1967).

- (13) R. W. Odom, D. L. Smith, and J. H. Futrell, Chem. Phys. Lett., 24, 227 (1974) and M. S. Foster and J. L. Beauchamp, Chem. Phys. Lett., 31, 482 (1975).
- (14) A review of electron attachment processes is given in J. G. Dillard, Chem. Ref., 73, 641 (1973).
- (15) S. A. Sullivan and J. L. Beauchamp, J. Amer. Chem. Soc., 98, 1061 (1976).
- (16) W. E. Farneth and J. I. Brauman, J. Amer. Chem. Soc., 98, 7891 (1976).
- (17) M. K. Murphy and J. L. Beauchamp, J. Amer. Chem. Soc., 98, 1433 (1976).
- (18) Proton transfer reactions observed in mixtures of moderate acids with CD_3ONO suggest $\text{PA}(\text{DNO}^-) \cong 365 \pm 5 \text{ kcal/mol}$ (see Appendix II).
- (19) Since other measurements are not available, $\text{IP}(\text{CH}_3\text{BC}_5\text{H}_6) < 9.0 \pm 0.5 \text{ eV}$ is used, determined from $\text{CH}_3\text{BC}_5\text{H}_6^+$ intensity as a function of electron energy. In a similar way the appearance potential of the loss of hydrogen fragment $\text{AP}(\text{CH}_3\text{BC}_5\text{H}_5^+)$ was determined as $\sim 9.5 \pm 0.5 \text{ eV}$.
- (20) S. W. Benson, J. Chem. Ed., 42, 503 (1965).
- (21) C. J. Ballhausen and H. B. Gray, "Molecular Orbital Theory", Benjamin, New York, N.Y., 1964 and J. D. Roberts, A. Streitweiser, Jr. and C. M. Regan, J. Amer. Chem. Soc., 74, 4579 (1952).

CHAPTER III

Positive and Negative Ion Chemistry
of Sulfuryl Halides

S. A. Sullivan and J. L. Beauchamp

Contribution No. 5635 from the Arthur Amos Noyes
Laboratory of Chemical Physics, California Institute
of Technology, Pasadena, California 91125

ABSTRACT

Ion cyclotron resonance techniques are employed in the investigation of positive and negative ion formation and ion molecule reactions in sulfuryl halides SO_2XY ($\text{X}, \text{Y} = \text{Cl}, \text{F}$). Positive ion reactivity is discussed in terms of the relative Cl and F bond strengths in these species and possible structures of ionic intermediates and products. Electron attachment processes generate halide ion donors such as F_2^- , Cl_2^- , SO_2F^- and SO_2Cl^- from sulfuryl halides. Negative ion reactivity is dominated by halide transfer reactions. Halide transfer reactions in mixtures with HCN and HCl are examined in an attempt to quantify $\text{D}(\text{SO}_2-\text{F}^-)$ and $\text{D}(\text{SO}_2-\text{Cl}^-)$.

INTRODUCTION

Electron attachment processes generate fluoride ion donors SO_2F^- and F_2^- in SO_2F_2 and chloride ion donors SO_2Cl^- and Cl_2^- in SO_2Cl_2 [1]. Facile halide transfers from these ions to a variety of neutrals have been observed. Reactions of this type have been employed to quantify Lewis acidities [2] and hydrogen bond strengths [1] in proton bound dimer ions, i.e., ClHF^- . In addition, halide transfer reactions may result in generation of unusual ions such as $\text{CH}_3\text{COCl}_2^-$ which model solution reaction intermediates [3]. Halide donor ions may also be important for use in negative chemical ionization techniques to provide methods of soft ionization [4]. The characterization of negative ion chemistry in sulfuryl halides is important in relation to these applications. Negative ion formation in SO_2ClF has not been previously examined.

Other uses of sulfuryl halides are related to the relatively weak halide bonds in the neutral. There has been some interest recently in these species as possible reactants for rare gas halide excimer lasers [5]. Laser activity is generally induced by electron beam pumping [6] or electrical discharge [7]. Under such conditions, gaseous mixtures are highly ionized. Consequently, positive and negative ion processes may significantly modify the species present, and thereby affect lasing efficiency.

The present study describes positive and negative ion formation and ion molecule reactions in sulfuryl halides as determined by ion cyclotron resonance spectroscopy. Previous investigations have

considered only the electron impact ionization of SO_2F_2 [8] and negative ion generation from SO_2F_2 and SO_2Cl_2 [1]. In an attempt to quantify the halide bond strengths in SO_2F^- and SO_2Cl^- , halide ion transfers are examined in mixtures with HCN and HCl, for which halide binding energies are known [1, 9].

EXPERIMENTAL

Experiments were performed employing an ICR spectrometer built in this laboratory incorporating a 15" magnet, capable of observing up to m/e 800. Instrumentation and experimental techniques of ICR spectroscopy have been described in detail [10, 11]. Pressure measurements were made using a Schulz-Phelp ion gauge, calibrated against an MKS Baratron, Model 90-H1 capacitance manometer, at higher pressures.

Positive ion appearance potentials were estimated using the vanishing current method from the variation of ion intensity as a function of electron energy. The energy scale was calibrated using the known ionization potential of SO_2F_2 from photoelectron spectra [12]. These data can only be considered accurate to ± 0.5 eV [13]. All compounds were obtained from commercial sources and used without further purification except for multiple freeze-pump-thaw cycles to remove noncondensable impurities. Sulfuryl chloride decomposes readily on introduction into the ICR inlet system to produce SO_2 and presumably Cl_2 . The amount of SO_2 impurity was minimized by repeated flushing of the inlet system with SO_2Cl_2 . Large drifts in SO_2Cl_2 pressure prevented trapping studies and decreased the reliability of pressure studies of this molecule.

For simplicity, only the mass of the most abundant isotopic ion is included in figures and tables. In all cases, the expected natural abundance isotopic ratios were observed. Calculated ion intensities consider isotopic contributions.

RESULTS

Electron Impact Mass Spectra and Positive Ion Chemistry

SO₂F₂. Table 1 lists normalized relative intensities of fragment ions produced on 70.0 eV electron impact on SO₂F₂ (1×10^{-6} torr). The good agreement between these results and previous mass spectra measured under different conditions [8, 14] indicates that SO₂F₂ does not decompose in the ICR inlet. As SO₂F₂ pressure is raised to $\sim 10^{-4}$ torr and 30.0 eV electron energy, no other ions appear and the relative intensities of the initial fragment ions remain unchanged. Double resonance experiments indicate that no ion molecule reactions occur, in particular SO₂⁺ does not react to form SO₂F₂⁺.

SO₂Cl₂. The decomposition of SO₂Cl₂ is reflected by the variation of SO₂⁺ intensity with SO₂Cl₂ sample age and the length of time that the sample is exposed to the inlet system. Decomposition is minimized by repeated flushing of the inlet system with SO₂Cl₂. The 70.0 eV electron impact mass spectrum of SO₂Cl₂ described in Table 1, represents a sample in which a minimum amount of decomposition (~ 15 -20%) occurs. As SO₂Cl₂ pressure is increased, product ions (SO₂)₂Cl⁺ (m/e 163), SO₂Cl₃⁺ (m/e 169) and (SO₂Cl₂)SO₂Cl⁺ (m/e 233)

TABLE 1

Electron Impact (70.0 eV) Mass Spectra of Sulfuryl Halides

Ion	SO ₂ Cl ₂ ^a		SO ₂ FCI		SO ₂ F ₂			
	Relative Intensity	IP or AP ^b	Relative Intensity	IP or AP ^b	Relative Intensity			
					This Study	Previous Studies ^f		
parent	19.7	12.05 ^c , d	11.4 ^e	90.8	12.3 ^e	74	13.0 ^c , d	13.3 ^f
loss of Cl	100.0	11.8 ^e		100.0	13.0 ^e	- -	- -	
loss of F	- -	- -		13.7	- -	100.0	100	14.8 ^e
SOCl ⁺	4.5	- -		- -	- -	- -	- -	15.1 ^f
SOF ⁺	- -	- -		23.5	- -	25.9	30	
SO ₂ ⁺	29.5	- -		19.5	- -	11.2	4	
SO ⁺	10.5	- -		12.4	- -	5.7	9	

^aSome decomposition of SO₂Cl₂ occurs, resulting in larger amounts of SO₂⁺ and SO⁺. Decomposition is estimated as ~ 20%, see text.

^bIonization potentials and appearance potentials in eV at 298 °C.

^cIP(SO₂Cl₂) and IP(SO₂F₂) taken from ref. 12.

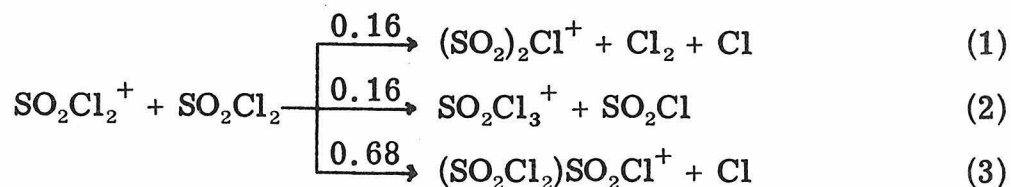
TABLE 1 - Continued

^dFor IP(SO₂Cl₂) in ref. 12, the vertical ionization potential is assigned a value (12.45 eV) equal to the peak maximum of the broad first band of the pes spectrum. This band represents ionization out of at least three orbitals. The band onset is taken as the adiabatic ionization potential.

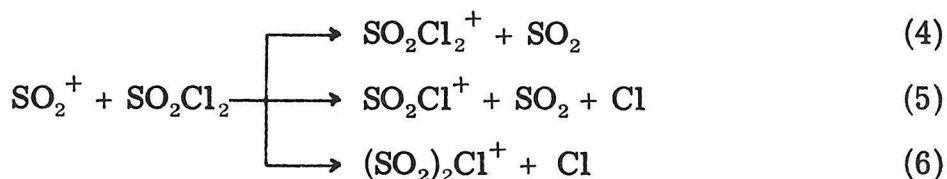
^eIonization and appearance potentials measured from the variation of ion intensity as a function of electron energy. The electron energy scale is calibrated using IP(SO₂F₂) = 13.0 eV from ref. 12. Values measured in this way can be considered accurate only to ± 0.5 eV.

^fFrom ref. 8. The mass spectrum is also consistent with that presented in ref. 14.

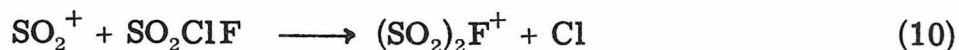
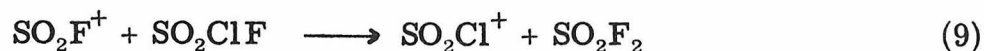
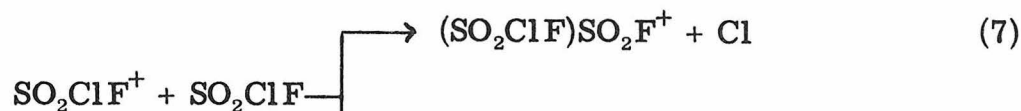
appear. Double resonance experiments indicate that SO_2Cl_2^+ reacts with SO_2Cl_2 to form each of these ions, eqn. (1-3). Product



distributions are determined from relative ion intensities at 1.0×10^{-4} torr SO_2Cl_2 . At this pressure, ionic products represent only 11% of total ionization, indicating moderately slow reactions ($\sim 5 \times 10^{-11} \text{ cm}^3 \text{ molecule}^{-1} \text{ s}^{-1}$). Double resonance further indicates that SO_2^+ reacts to produce both SO_2Cl_2^+ , eqn. (4), and SO_2Cl^+ , eqn. (5). The enhanced intensity of $(\text{SO}_2)_2\text{Cl}^+$ only when large amounts of SO_2^+ are present suggest that reaction 6 occurs but must proceed quite slowly.



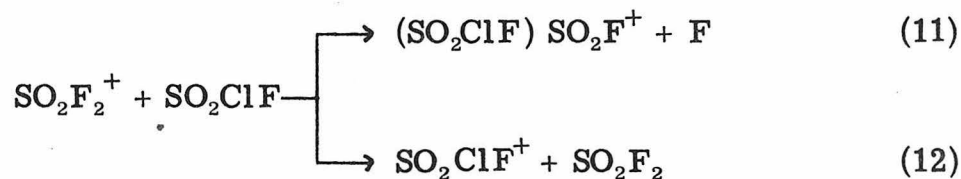
SO_2ClF . Table 1 presents the 70.0 eV electron impact mass spectrum of SO_2ClF . Cleavage of the S-Cl bond to form SO_2F^+ predominates over formation of SO_2Cl^+ . Although SO_2ClF samples decompose slowly over several weeks, there is no indication that rapid decomposition occurs on addition of the sample to the inlet system. As SO_2ClF pressure is increased at 30.0 eV electron energy, SO_2Cl^+ (m/e 99), $(\text{SO}_2)_2\text{F}^+$ (m/e 147) and $(\text{SO}_2\text{ClF})\text{SO}_2\text{F}^+$ (m/e 201) increase in intensity as SO_2F^+ (m/e 83) and SO_2ClF^+ (m/e 118) decrease. Reactions 7-10, are consistent with observed double resonance spectra. A small



contribution of SO_2ClF^+ to the formation of $(\text{SO}_2)_2\text{F}^+$ suggests a somewhat slow reaction 8.

Figure 1 presents the temporal variation of normalized positive ion intensity in SO_2ClF at 1.68×10^{-6} torr (30.0 eV). Rates for reactions 7, 9 and 10 are determined (Table 2) from semilog plots of normalized ion intensity, by neglecting the contribution of reaction 8.

$\text{SO}_2\text{F}_2/\text{SO}_2\text{ClF}$ and $\text{SO}_2\text{F}_2/\text{SO}_2\text{Cl}_2$ Mixtures. The reactions of SO_2F_2^+ with SO_2ClF were examined by increasing SO_2ClF pressure in a mixture with 1.5×10^{-6} torr SO_2F_2 . Reactions 11 and 12 are



consistent with double resonance experiments.

Similar reactions of SO_2F_2^+ are observed in mixtures with SO_2Cl_2 , eqn. (13, 14). The molecular ion SO_2ClF^+ reacts with SO_2F_2 to

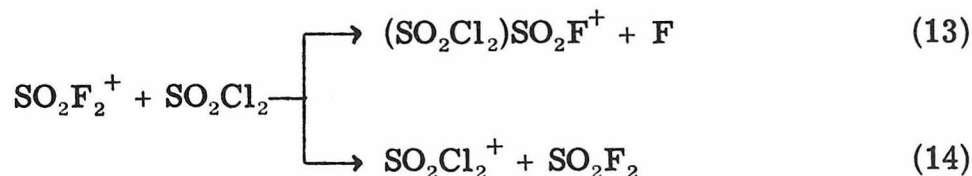


FIGURE 1

Temporal variation of normalized positive ion intensity
in 1.68×10^{-6} torr of SO_2ClF at 30.0 eV electron energy.

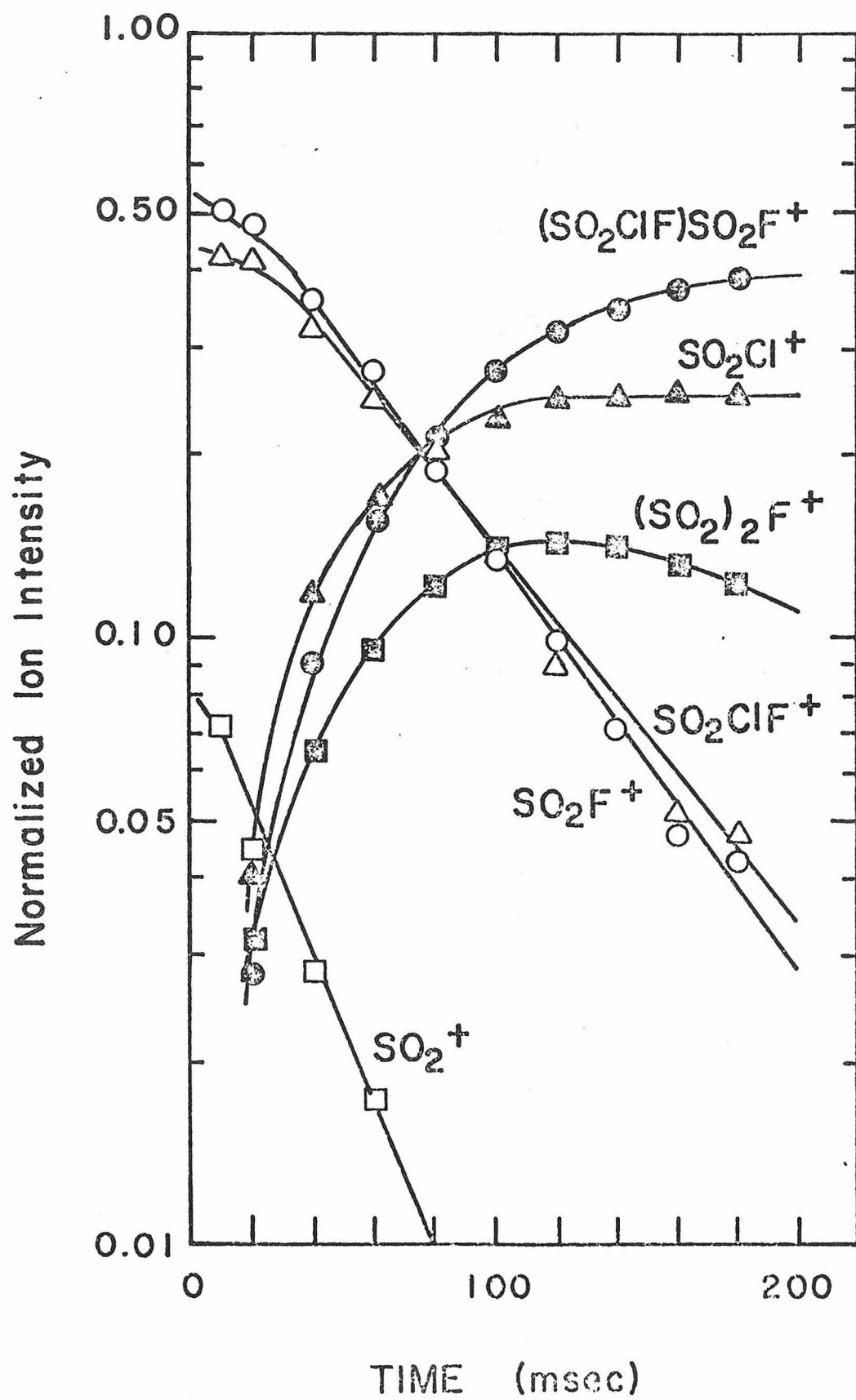


TABLE 2
Summary of the Ion Molecule Reactions of Sulfuryl Halides

	k_{ex}^a	Thermochemical Inferences, $\Delta H_{\text{reaction}}^b$
<u>Positive Ion Reactions</u>		
$\text{SO}_2\text{Cl}_2^+ + \text{SO}_2\text{Cl}_2$	$\xrightarrow{0.16} (\text{SO}_2)_2\text{Cl}^+ + \text{Cl}_2 + \text{Cl}$ $\xrightarrow{0.16} \text{SO}_2\text{Cl}_3^+ + \text{SO}_2\text{Cl}$ $\xrightarrow{0.68} (\text{SO}_2\text{Cl}_2)\text{SO}_2\text{Cl}^+ + \text{Cl}$	$\Delta H_f [(\text{SO}_2)_2\text{Cl}^+] < 79.2$ $D(\text{SO}_2\text{Cl}_2^+ - \text{Cl}) < D(\text{SO}_2\text{Cl} - \text{Cl})$ $\Delta H_f [(\text{SO}_2\text{Cl}_2)\text{SO}_2\text{Cl}^+] < 79.2$
$\text{SO}_2^+ + \text{SO}_2\text{Cl}_2$	$\xrightarrow{\quad} \text{SO}_2\text{Cl}_2^+ + \text{SO}_2$ $\xrightarrow{\quad} \text{SO}_2\text{Cl}^+ + \text{SO}_2 + \text{Cl}$ $\xrightarrow{\quad} (\text{SO}_2)_2\text{Cl}^+ + \text{Cl}$	-7 $\Delta H_f [(\text{SO}_2)_2\text{Cl}^+] < 100$ -13
$\text{SO}_2\text{ClF}^+ + \text{SO}_2\text{ClF}$	$\xrightarrow{\quad} (\text{SO}_2\text{ClF})\text{SO}_2\text{F}^+ + \text{Cl}$ $\xrightarrow{\quad} (\text{SO}_2)_2\text{F}^+ + \text{Cl}_2 + \text{F}$	2.98^c $\Delta H_f [(\text{SO}_2\text{ClF})\text{SO}_2\text{F}^+] < -10.9$ $\Delta H_f [(\text{SO}_2)_2\text{F}^+] < 0$
$\text{SO}_2\text{F}^+ + \text{SO}_2\text{ClF}$	$\xrightarrow{\quad} \text{SO}_2\text{Cl}^+ + \text{SO}_2\text{F}_2$	-31
$\text{SO}_2^+ + \text{SO}_2\text{ClF}$	$\xrightarrow{\quad} (\text{SO}_2)_2\text{F}^+ + \text{Cl}$	$\Delta H_f [(\text{SO}_2)_2\text{F}^+] < 52$
$\text{SO}_2\text{F}_2^+ + \text{SO}_2\text{ClF}$	$\xrightarrow{\quad} (\text{SO}_2\text{ClF})\text{SO}_2\text{F}^+ + \text{F}$ $\xrightarrow{\quad} \text{SO}_2\text{FCl}^+ + \text{SO}_2\text{F}_2$	$\Delta H_f [(\text{SO}_2\text{ClF})\text{SO}_2\text{F}^+] < -33$ ~ -16

TABLE 2 - Continued

	k_{ex}^a	Thermochemical Inferences, $\Delta H_{\text{reaction}}^b$
$\text{SO}_2\text{F}_2^+ + \text{SO}_2\text{Cl}_2 \begin{cases} \longrightarrow (\text{SO}_2\text{Cl}_2)\text{SO}_2\text{F}^+ + \text{F} \\ \longrightarrow \text{SO}_2\text{Cl}_2^+ + \text{SO}_2\text{F}_2 \end{cases}$		$\Delta H_f [(\text{SO}_2\text{Cl}_2)\text{SO}_2\text{F}^+] < 15$ ~ -22
$\text{SO}_2\text{ClF}^+ + \text{SO}_2\text{F}_2 \longrightarrow (\text{SO}_2\text{F}_2)\text{SO}_2\text{F}^+ + \text{Cl}$		$\Delta H_f [(\text{SO}_2\text{F}_2)\text{SO}_2\text{F}^+] < -59$
<u>Negative Ion Reactions</u>		
$\text{SO}_2\text{F}^- + \text{SO}_2\text{ClF} \longrightarrow \text{SO}_2\text{Cl}^- + \text{SO}_2\text{F}_2$	~ 0.1	~ -22
$\text{Cl}^- + \text{SO}_2\text{ClF} \longrightarrow \text{SO}_2\text{F}^- + \text{CL}_2$	1.05	~ 12
$\text{SO}_2\text{F}^- + \text{HCl} \longrightarrow \text{SO}_2\text{Cl}^- + \text{HF}$	$\sim 1.5^d$	~ -13
<u>Halide Transfer Reactions</u>		
$\text{SO}_2\text{F}^- + \text{HCl} \longrightarrow \text{FHC}l^- + \text{SO}_2$	$\sim 1.5^d$	$D(\text{SO}_2-\text{F}^-) < D(\text{HCl}-\text{F}^-)$
$\text{SO}_2\text{F}^- + \text{HCN} \longrightarrow \text{FHCN}^- + \text{SO}_2$		$D(\text{SO}_2-\text{F}^-) < D(\text{HCN}-\text{F}^-)$
$\text{SO}_2\text{Cl}^- + \text{HCl} \longrightarrow \text{ClHC}l^- + \text{SO}_2$	1.64	$D(\text{SO}_2-\text{Cl}^-) < D(\text{ClH}-\text{Cl}^-)$
$\text{FHC}l^- + \text{HCl} \longrightarrow \text{ClHC}l^- + \text{HF}$	1.40	$D(\text{FH}-\text{Cl}^-) < D(\text{ClH}-\text{Cl}^-)$
$\text{FHCN}^- + \text{HCl} \longrightarrow \text{CNHC}l^- + \text{HF}$		$D(\text{FHCN}^-) < D(\text{ClH}-\text{CN}^-)$
$\text{FHCN}^- + \text{HCN} \longrightarrow \text{CNHCN}^- + \text{HF}$		$D(\text{FH}-\text{CN}^-) < D(\text{CNH}-\text{CN}^-)$
$\text{CNHC}l^- + \text{HCl} \longrightarrow \text{ClHC}l^- + \text{HCN}$		$D(\text{CNHC}l^-) < D(\text{ClH}-\text{Cl}^-)$

TABLE 2 - Continued

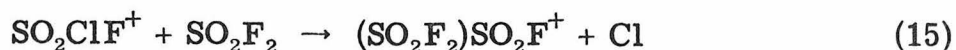
^a k_{ex} in units $10^{-10} \text{ cm}^3 \text{ molecule}^{-1} \text{ s}^{-1}$.

^bBased on heats of formation in Table 3. All values in kcal/mol at 298°K.

^cCalculated assuming that concomitant reaction 8 is slow.

^dTotal rate of decay of SO_2F^- in reaction with HCl is $3 \times 10^{-10} \text{ cc/molecule sec}$. Rates noted in table are approximate since product distribution could not be accurately determined.

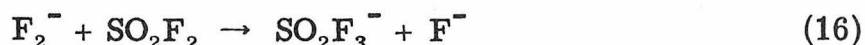
form $(\text{SO}_2\text{F}_2)\text{SO}_2\text{F}^+$ as in eqn. (15). Reactions 11-15 are moderately



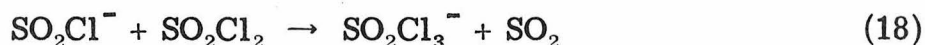
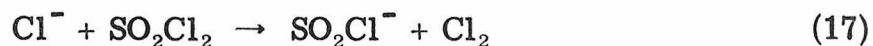
slow ($< 10^{-10} \text{ cm}^3 \text{ molecule}^{-1} \text{ s}^{-1}$) with product ions detected only at higher pressures ($> 5 \times 10^{-5} \text{ torr}$).

Negative Ion Chemistry

SO_2F_2 . The generation and reactivity of negative ions have been examined previously in SO_2F_2 and SO_2Cl_2 [1]. Negative ions are formed by attachment of scattered thermalized electrons provided by impact of a 70.0 eV electron beam. The ions F^- (60%), F_2^- (11%), and SO_2F^- (29%) are formed by electron attachment to SO_2F_2 at moderate pressures ($\sim 10^{-5} \text{ torr}$). Small amounts of SO_2F_2^- , presumably formed by similar processes, appear at high pressures ($\sim 10^{-4} \text{ torr}$) of SO_2F_2 . The only observed reaction is F^- transfer from F_2^- to SO_2F_2 , eqn. (16).

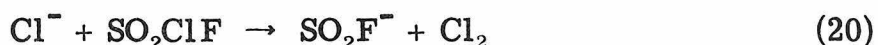
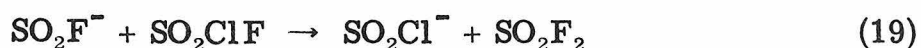


SO_2Cl_2 . Attachment processes from Cl^- (49%), Cl_2^- (8%), and SO_2Cl^- (43%) from SO_2Cl_2 . Reaction of Cl^- with SO_2Cl_2 occurs forming SO_2Cl^- , eqn. 17, which further reacts to generate SO_2Cl_3^- , eqn. (18).

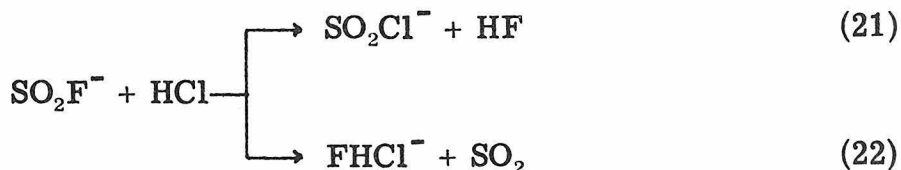


SO_2ClF . Negative ions Cl^- (16%) and SO_2F^- (84%) are produced by electron attachment to SO_2ClF at 70 eV electron energy. No other

abundant negative ions, in particular ClF^- , were detected. As SO_2ClF pressure is raised to 1.74×10^{-4} torr, no reactions are apparent. However, trapped ion studies of SO_2ClF (Fig. 2) reveal the very slow reaction of SO_2F^- to form SO_2Cl^- , eqn (19), with $k \simeq 1 \times 10^{-11} \text{ cm}^3 \text{ molecule}^{-1} \text{ s}^{-1}$. A somewhat faster reaction of Cl^- with SO_2ClF to form SO_2F^- , eqn (20) is also observed with $k = 1.05 \times 10^{-10} \text{ cm}^3 \text{ molecule}^{-1} \text{ s}^{-1}$.



SO₂ClF/HCl Mixture. Temporal variation of normalized negative ion intensity in a mixture of 6.98×10^{-7} torr SO₂Cl and 1.66×10^{-6} torr HCl is presented in Fig. 3. Ions FHC1⁻ (m/e 55), ClHCl⁻ (m/e 71) SO₂Cl⁻ (m/e 99) appear as SO₂F⁻ (m/e 83) decays with time. Initially formed Cl⁻ reacts away very slowly. The larger amount of SO₂Cl⁻ produced in this mixture compared to that generated in SO₂ClF by reaction 19, suggests that another mechanism is responsible for its formation. Double resonance experiments indicate that SO₂F⁻ is the only precursor to SO₂Cl⁻, therefore reaction 21 must occur. Concomitant F⁻ transfer to HCl, eqn. (22), is also confirmed by double



resonance results. Both SO_2Cl^- , eqn. (23) and FHC l^- , eqn. (24) further react with HCl to form ClHCl^- . Rates of reactions 21 and 22 are summarized in Table 2.

FIGURE 2

Temporal variation of normalized negative ion intensity
in 1.40×10^{-6} torr SO_2ClF at 70.0 eV electron energy.

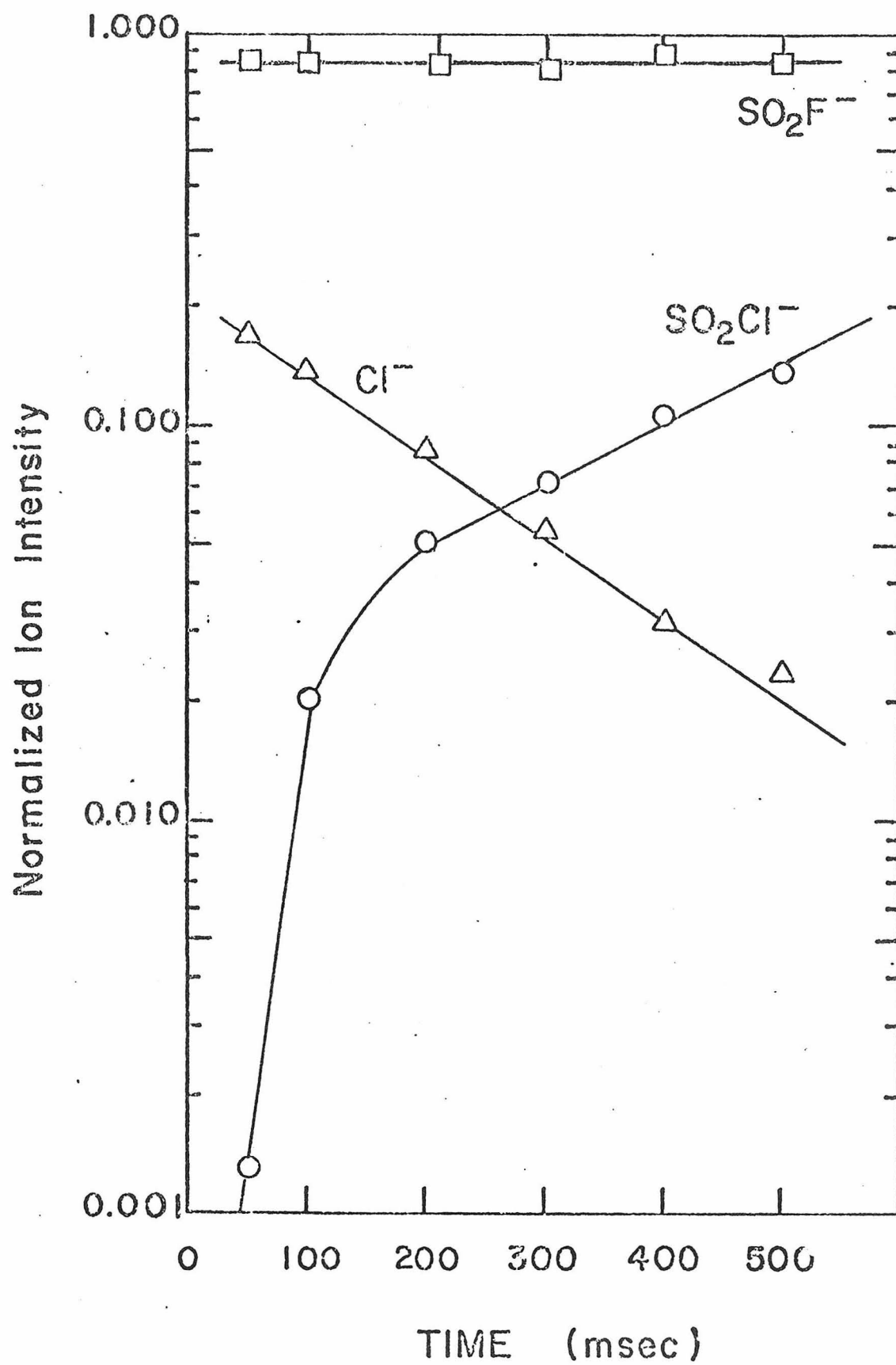
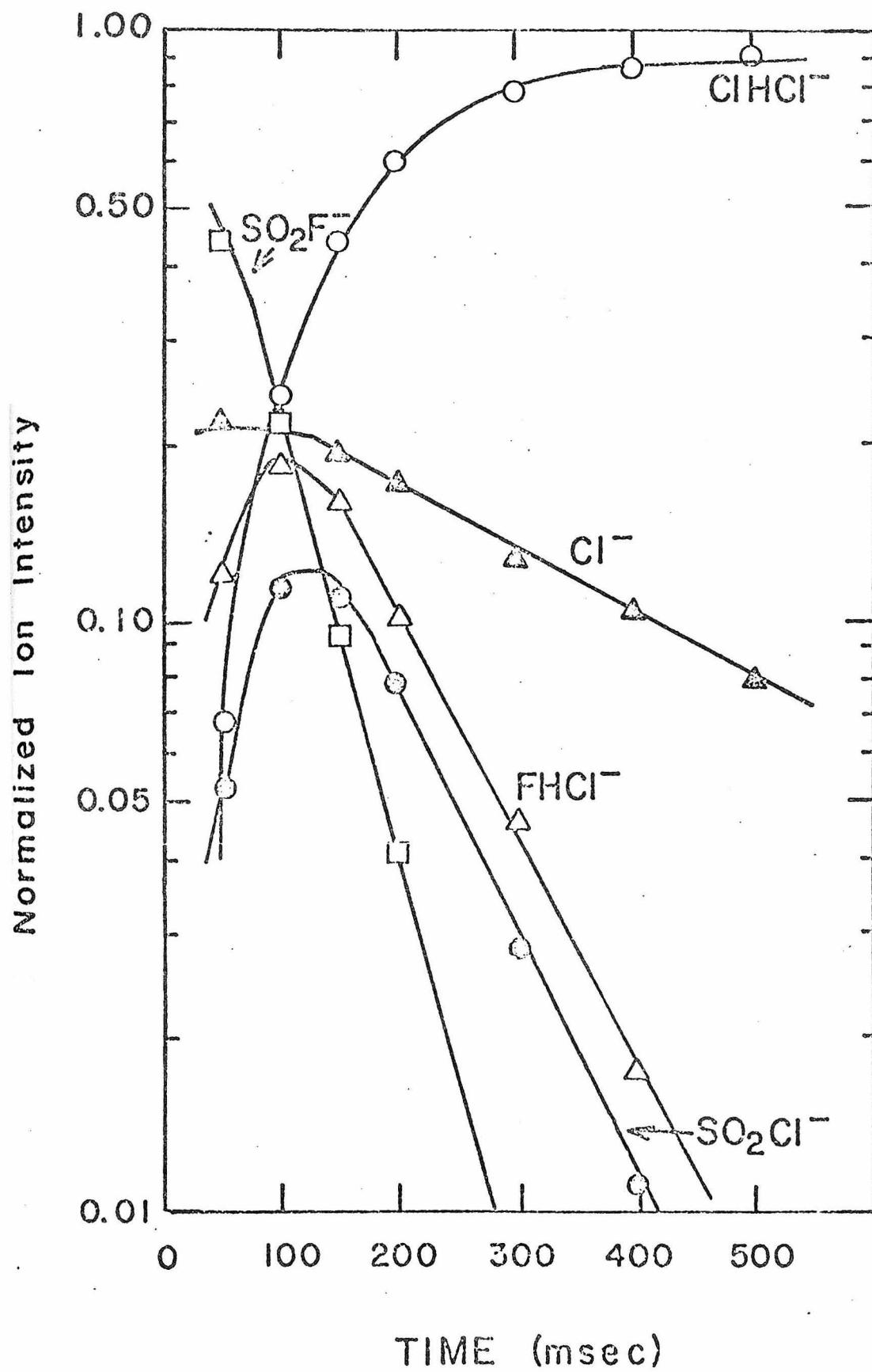
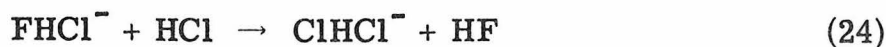
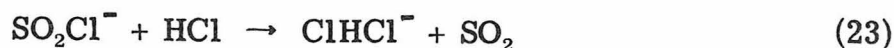


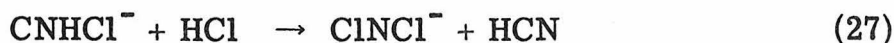
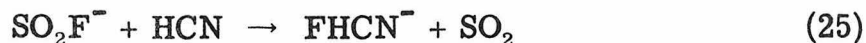
FIGURE 3

Temporal variation of normalized negative ion intensity in a mixture of 6.98×10^{-7} torr SO_2ClF with 1.66×10^{-6} torr HCl at 70.0 eV electron energy.





SO₂ClF/HCN Mixture. In a mixture of 3.49×10^{-7} torr, SO₂ClF and 2.35×10^{-6} torr HCN, ions FHCN⁻ (m/e 46), CNHCl⁻ (m/e 62) and ClHCl⁻ (m/e 71) appear as SO₂F⁻ decays with time. The sole precursor to FHCN⁻ is SO₂F⁻, presumably through F⁻ transfer, eqn. (25). The production of CNHCl⁻ from FHCN⁻, eqn. (26) and its further reaction, eqn. (27), to form ClHCl⁻ can be explained only by



the presence of HCl impurities. Although not directly detected under these conditions, double resonance of ClHCl⁻ indicates the presence of FHCN⁻ in this mixture, possibly formed by reaction 22. At lower pressures of HCN, FHCN⁻ is directly detected. On initial addition of HCN to the ICR spectrometer, the positive ion mass spectrum indicates less than 2% HCl impurity. However, HCl signal increases with exposure of the HCN sample to the inlet system. A similar problem results on addition of HBr to the inlet system. Since the amount of HCl present cannot be accurately determined, rate measurements are not possible in this mixture. The predominance of chlorinated products does indicate that Cl⁻ and CN⁻ transfer reactions to HCl are very fast relative to transfer to HCN. Small amounts of CNHCN⁻ produced by reaction 28 are detected at low pressures of SO₂ClF and HCN. No

double resonance was observed between CNHCN^- and ClHCN^- .



Thermochemical Considerations

Ionization potentials for the sulfonyl halides are listed in Table 1. While acknowledging the inaccuracies in their measurement, ionization potentials derived in this study are consistent with those for SO_2F_2 and SO_2Cl_2 derived from photoelectron spectra [12]. The electron impact $\text{IP}(\text{SO}_2\text{ClF}) = 12.4 \pm 0.5$ eV noted in Table 1 is intermediate between those of the other halides as expected from previous studies of the effects of chlorine and fluorine substitution on ionization potentials [15]. Data listed in Table 1 have been used to calculate heats of formation of some of the positive ions involved in ion molecule reactions (Table 3). Where possible heats of reaction have been calculated (Table 2) using these thermochemical data. In all cases, the observed reactions are predicted to be exothermic. For other reactions the assumption that only exothermic reactions will be observed allows upper limits to be set for ΔH_{f298}° of positive ions as noted in Table 2.

Observed F^- transfer reactions indicate that $D(\text{SO}_2-\text{F}^-) < D(\text{FH}-\text{F}^-) \sim 45 \pm 5$ kcal/mol and $D(\text{SO}_2-\text{Cl}^-) < D(\text{ClH}-\text{Cl}^-) \sim 24$ kcal/mol [1]. Estimates of $\Delta H_{f298}^\circ(\text{SO}_2\text{F}^-)$ and $\Delta H_{f298}^\circ(\text{SO}_2\text{Cl}^-)$ derived from these limits (Table 3) are consistent with other negative ion reactions observed in SO_2ClF , eqn. (19-21), Table 2. It is further possible to limit $\text{EA}(\text{SO}_2\text{F}) < 2.34$ eV and $\text{EA}(\text{SO}_2\text{Cl}) < 3.17$ eV using data in Table 3.

TABLE 3

Thermochemical Properties of Sulfuryl Halides^a

	$\Delta H_f(M)$	$\Delta H_f(M^+)^b$	$\Delta H_f(M^-)$
SO ₂ F ₂	-181.3	118.5	- -
SO ₂ Cl ₂	- 84.9	193.0	- -
SO ₂ FCl	$\leq -133^c$	≥ 151	- -
SO ₂ F	-122.2 ^d	141 (138)	$> -177^e$
SO ₂ Cl	- 77.8 ^d	158	$> -151^e$
SO ₂	- 70.9	214	- -
SO	1.17	246	- -
Cl	28.9	- -	- 55.9
F	18.86	- -	- 61.0

^aAll values in kcal/mol at 298°K. Unless otherwise noted, all values taken from D. R. Stull and H. Prophet, "JANAF Thermochemical Tables", U.S. Printing Office, Washington, D.C., 1971.

^bCalculated using appearance potentials in Table 1 and ref. 8.

^cEstimate assuming that D(SO₂F-Cl) and D(SO₂Cl-F) are equal to those in SO₂F₂ and SO₂Cl₂. This study indicates that D(SO₂F-Cl) > D(SO₂Cl-Cl), see text.

^dCalculated using average bond strengths D(SO₂F-F) = 74 kcal/mol, D(SO₂Cl-Cl) = 36 kcal/mol, which are derived from the heats of formation in this table.

^eEstimates based on observed halide transfers using D(FH-F⁻) ~ 45 ± 5 kcal/mol and D(ClH-Cl⁻) ≅ 24 kcal/mol. See S. A. Sullivan and J. L. Beauchamp, J. Amer. Chem. Soc., 98 (1976) 1160 and ref. 9.

DISCUSSION

Positive Ion Chemistry

Positive ion reactions of sulfuryl halides can be classified as charge transfer processes, halogen atom, or anion transfer reactions and condensation reactions which are generalized in eqn. (29) for

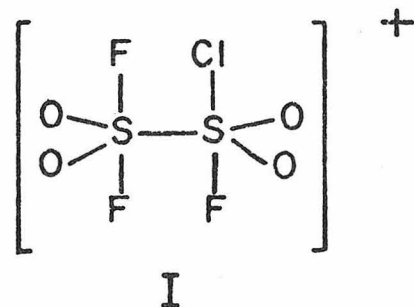


X = Cl or F. As noted above, and shown in Table 2, the observed charge transfer reactions are consistent with the relative ionization potentials of the neutrals involved.

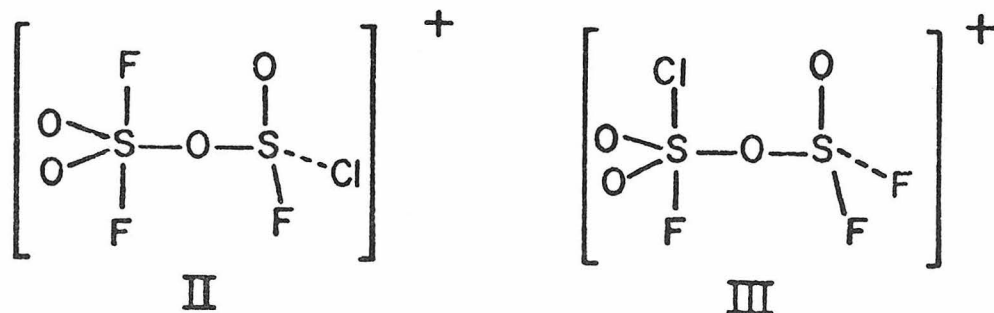
The chlorine transfer reaction 2 indicates that $D(\text{SO}_2\text{Cl}_2^+ - \text{Cl}) > D(\text{SO}_2\text{Cl} - \text{Cl}) = 36 \text{ kcal/mol}$ (Table 3). In contrast, SO_2FCl^+ does not transfer Cl to the neutral SO_2FCl , suggesting that $D(\text{SO}_2\text{FCl}^+ - \text{Cl}) < D(\text{SO}_2\text{F} - \text{Cl})$. This may result from an increase in $D(\text{SO}_2\text{F} - \text{Cl})$ compared to $D(\text{SO}_2\text{Cl} - \text{Cl})$. Qualitative theoretical descriptions of bonding in hypervalent sulfur indicate that the more electronegative F should contract the sulfur d orbitals allowing better overlap and stronger bonds [12, 16]. This idea is consistent with the observed shortening of O—S bonds in SO_2F_2 compared to SO_2Cl_2 [17].

Parent ions SO_2F_2^+ , SO_2ClF^+ and SO_2Cl_2^+ each react with the neutral sulfuryl halides by eqn. (29). Only in the case of SO_2F_2^+ reacting with SO_2F_2 is this process not observed. Preferential loss of Cl is observed on reaction of SO_2ClF^+ with SO_2F_2 for which the only product of reaction 29 is $(\text{SO}_2\text{F}_2)\text{SO}_2\text{F}^+$, eqn. 15. This is consistent with the weaker S—Cl bond. Interestingly when SO_2F_2^+ reacts with

SO₂ClF, exclusive cleavage of the S—F bond produces (SO₂FC1)SO₂F⁺, eqn. (11). The formation of a symmetric ionic reaction intermediate as in I for both reaction 11 and 15, should result in identical ionic



products. The observation of different reaction products suggests that attack may occur at oxygen, as in II and III, for reactions 11 and 15, respectively. Loss of the more weakly bonded halogen from the penta coordinate sulfur may then predominate.



Negative Ion Chemistry and Halide Binding Energies

The negative ions SO_2F^- and SO_2Cl^- formed in sulfonyl halides are unreactive or react only slowly with their neutral precursors. Chloride transfer from SO_2Cl^- to SO_2Cl_2 suggests that $D(\text{SO}_2-\text{Cl}^-) < D(\text{SO}_2\text{Cl}_2-\text{Cl}^-)$. In contrast, SO_2F^- does not transfer F^- to SO_2ClF , suggesting $D(\text{SO}_2-\text{F}^-) > D(\text{SO}_2\text{ClF}-\text{F}^-)$. This ion reacts only very slowly with SO_2ClF to form SO_2Cl^- , eqn. (19). Similarly, Cl^- reacts

with SO_2ClF and SO_2Cl_2 to form SO_2F^- , eqn. (20), and SO_2Cl^- , eqn. (17), respectively.

In mixtures of HCN and HCl with SO_2ClF , SO_2F^- transfers F^- to form the hydrogen bonded anions FHCN^- and FHCl^- . The further transfers of CN^- , Cl^- and F^- in these mixtures allow the ordering of anion binding energies in Table 2. This order is consistent with that in Table 4 which had been proposed by Yamdagni and Kebarle [9]. Anion binding energies $D(\text{YH}-\text{X}^-)$ increase with gas phase acidity of HY and the gas phase basicity of X^- .

In conclusion, the generation of large amounts of SO_2F^- by electron attachment in low pressures of SO_2FCl and the inertness of the ion toward the precursor halide, suggest that these compound would be a good reagent for negative chemical ionization. The mixed sulfonyl halide also appears to be an excellent choice for further study in excimer laser investigations because of the expected weakness of the chloride bond and the chemical inertness of the neutral compared to other halogen atom donors.

ACKNOWLEDGMENTS

This research was supported in part by the Energy Research and Development Administration under Grant No. E(04-3)767-8.

TABLE 4

Anion Bond Energies in Proton Bound Ions^a

$D(\text{FH}-\text{F}^-) \sim 45 \text{ kcal/mol}^b$	$< D(\text{CNH}-\text{F}^-)$	$< D(\text{ClH}-\text{F}^-) \sim 50 \text{ kcal/mol}^c$
∇	∇	∇
$D(\text{FH}-\text{CN}^-)$	$< D(\text{CNH}-\text{CN}^-)$	$< D(\text{ClH}-\text{CN}^-)$
∇	∇	∇
$D(\text{FH}-\text{Cl}^-) \sim 13 \text{ kcal/mol}^d$	$< D(\text{CNH}-\text{Cl}^-)$	$< D(\text{ClH}-\text{Cl}^-) \sim 24 \text{ kcal/mol}^c$

^aOrdering based on halide and anion transfers in references 1 and 9.^bS. A. Sullivan and J. L. Beauchamp, J. Amer. Chem. Soc., 98, (1975) 1066.^cReference 9.^dCalculated from $D(\text{ClH}-\text{F}^-)$.

REFERENCES

- 1 M. S. Foster and J. L. Beauchamp, Inorg. Chem., to be published.
- 2 M. K. Murphy and J. L. Beauchamp, J. Amer. Chem. Soc., 98 (1976) 1433; M. K. Murphy and J. L. Beauchamp, Inorg. Chem., submitted for publication.
- 3 O. I. Asubiojo, L. K. Blair and J. I. Brauman, J. Amer. Chem. Soc., 97 (1975) 6685; W. N. Olmstead and J. I. Brauman, J. Amer. Chem. Soc., 99 (1977) 4219.
- 4 H. P. Tannenbaum, J. D. Roberts and R. C. Dougherty, Anal. Chem., 47 (1975) 49.
- 5 J. E. Velazco, J. H. Kolts and D. W. Setser, J. Chem. Phys., 65 (1976) 3498.
- 6 J. J. Ewing and C. A. Brau, Appl. Phys. Lett., 27 (1975) 350; E. R. Ault, R. S. Bradford and M. L. Bhaumik, Appl. Phys. Lett., 27 (1975) 413.
- 7 D. G. Dutton, S. H. Suchard, O. L. Gibb and C. P. Wang, Appl. Phys. Lett., 28 (1976) 522.
- 8 R. M. Reese, V. H. Diebler and J. L. Franklin, J. Chem. Phys., 29 (1958) 880.
- 9 R. Yamdagni and P. Kebarle, J. Amer. Chem. Soc., 93 (1971) 7139.
- 10 J. L. Beauchamp, Ann. Rev. Phys. Chem., 22 (1972) 527.
- 11 T. B. McMahon and J. L. Beauchamp, Rev. Sci. Inst., 43 (1972) 509.
- 12 D. Chadwick, D. C. Frost, F. G. Herring, A. Katrib, C. A. McDowell and R. A. N. McLean, Can. J. Chem., 51 (1975) 1893.

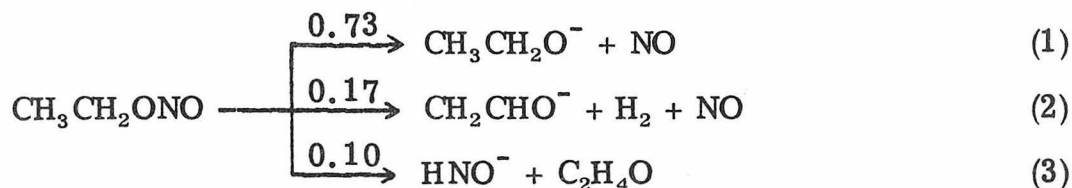
- 13 H. M. Rosenstock, Int. J. Mass Spectrom. Ion Phys., 20 (1976) 139.
- 14 W. H. Beattie, Appl. Spectrosc., 29 (1975) 334.
- 15 M. R. Litrow and T. R. Spalding, Mass Spectrometry of Inorganic and Organometallic Compounds, Elsevier, New York, 1973.
- 16 There is much controversy as to the role of d orbitals in bonding of hypervalent sulfur. None of the theoretical treatments adequately describes reactivity. I. H. Hillier and V. R. Saunders, J. Chem. Soc. D, 1183 (1970); I. H. Hillier and M. F. Guest, Int. J. Quant. Chem., 6 (1972) 967; P. J. Hay, J. Amer. Chem. Soc., 99 (1977) 1003.
- 17 R. M. Fristrom, J. Chem. Phys., 20 (1952) 1; I. Hargittai, Acta Chem. Acad. Sci. Hung., 57 (1968) 403.

Appendix I

Negative Ion Formation and Ion-Molecule Reactions in Alkyl Nitrites

Alkyl nitrites have been used extensively in recent gas phase studies¹ as an abundant source of alkoxide ions. These species are useful in the determination of gas phase acidities and in the investigation of negative ion-molecule reaction mechanisms. It is therefore important that negative ion generation and reactivity with the precursor nitrites are well understood. For this reason, we have examined negative ion formation and reactivity in CD_3ONO , $\text{CH}_3\text{CH}_2\text{ONO}$, $i\text{C}_3\text{H}_7\text{ONO}$ and $t\text{C}_4\text{H}_9\text{ONO}$ employing ion cyclotron resonance spectroscopy.²

Negative Ion Generation. Negative ion generation in alkyl nitrites can be summarized by the electron attachment processes observed in $\text{CH}_3\text{CH}_2\text{ONO}$. Thermalized electron attachment to $\text{CH}_3\text{CH}_2\text{ONO}$ results in $\text{CH}_3\text{CH}_2\text{O}^-$ (eq 1), CH_2CHO^- (eq 2) and HNO^- (eq 3).³ The major



process (1) results from dissociation of the very weak O-NO bond.

Alkoxide formation is the major process observed for each of the alkyl nitrites examined as seen in Table 1. Enolate anion formation, process (2), is observed only in $\text{CH}_3\text{CH}_2\text{ONO}$ and $i\text{C}_3\text{H}_7\text{ONO}$. Only 3% of $\text{CH}_3\text{CH}_2\text{CO}^-$ (m/e 57) is observed in $i\text{C}_3\text{H}_7\text{ONO}$, consistent with the

Table I. Negative Ion Formation in Alkyl Nitrites^a

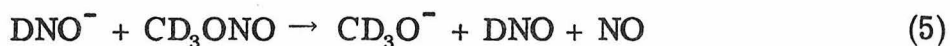
Nitrite	<u>Electron Attachment Product Distribution</u>		
	Alkoxide	Enolate	HNO ⁻
CD ₃ ONO	0.75	--	0.25
CH ₃ CH ₂ ONO	0.73	0.17	0.10
i-C ₃ H ₇ ONO	0.91	0.03	0.07
t-C ₄ H ₉ ONO	1.00	--	--

^aNegative ions are formed by attachment of thermalized electrons provided by impact of a 70.0 eV electron beam. In each case, product distributions were determined, after the Schulz-Phelp gauge was turned off and allowed to cool (see text).

greater energy required to eliminate H_2 from $iC_3H_7O^-$ ($\Delta H_{elim} \cong 9 \text{ kcal mole}^{-1}$) than $CH_3CH_2O^-$ ($\Delta H_{elim} \cong 1 \text{ kcal mole}^{-1}$). Formation of HNO^- apparently results from cleavage of the α -H in the nitrite, since no HNO^- is detected in $t\text{-}C_4H_9ONO$ (Table 1).

Negative Ion Reactions in Alkyl Nitrites .

CD_3ONO . The deuterated nitrite is employed to distinguish between HNO^- and CH_3O^- both appearing at m/e 31. Figure 1 presents the temporal variation of ion intensity in 3.7×10^{-6} torr of CD_3ONO . The product ion NO_2^- (m/e 46) appears as both CD_3O^- (m/e 34) and DNO^- (m/e 32) decrease with time. Double resonance links production of NO_2^- to CD_3O^- (eq 4) and indicates that DNO^- reacts to form CD_3O^- (eq 5).^{4,5} Rates determined from semilog plots of the disappearance



of CD_3O^- and DNO^- are listed in Table 2.

CH_3CH_2ONO . The temporal variation of ion intensity in 2.0×10^{-6} torr CH_3CH_2ONO is presented in Figure 2. As initially formed $CH_3CH_2O^-$ (m/e 45) and HNO^- (m/e 31) decrease, NO_2^- (m/e 46) appears and there is a small increase (9%) in CH_2CHO^- (m/e 43). Double resonance confirms that NO_2^- is formed by reaction of $CH_3CH_2O^-$ (eq 6). As discussed below, the increase in CH_2CHO^- may result from the reaction of $CH_3CH_2O^-$ with the pyrolysis impurity CH_3CHO or from reaction (7) with the nitrite. Data presented in Figure 2 were obtained with the ion pressure gauge off to avoid pyrolysis. Reaction products of HNO^-

Figure 1

Temporal variation of normalized ion
intensity in 3.7×10^{-6} torr of CD_3ONO .

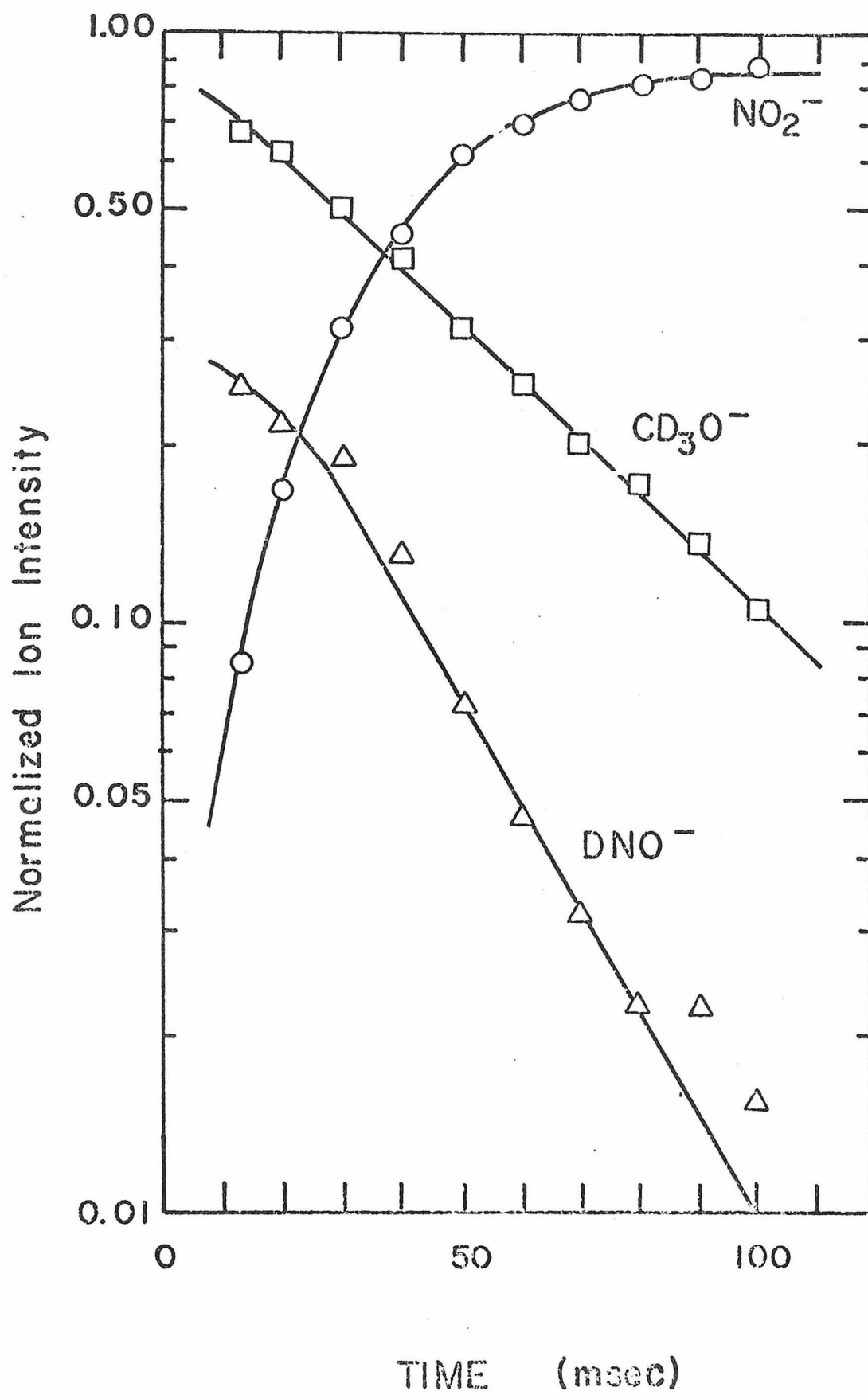
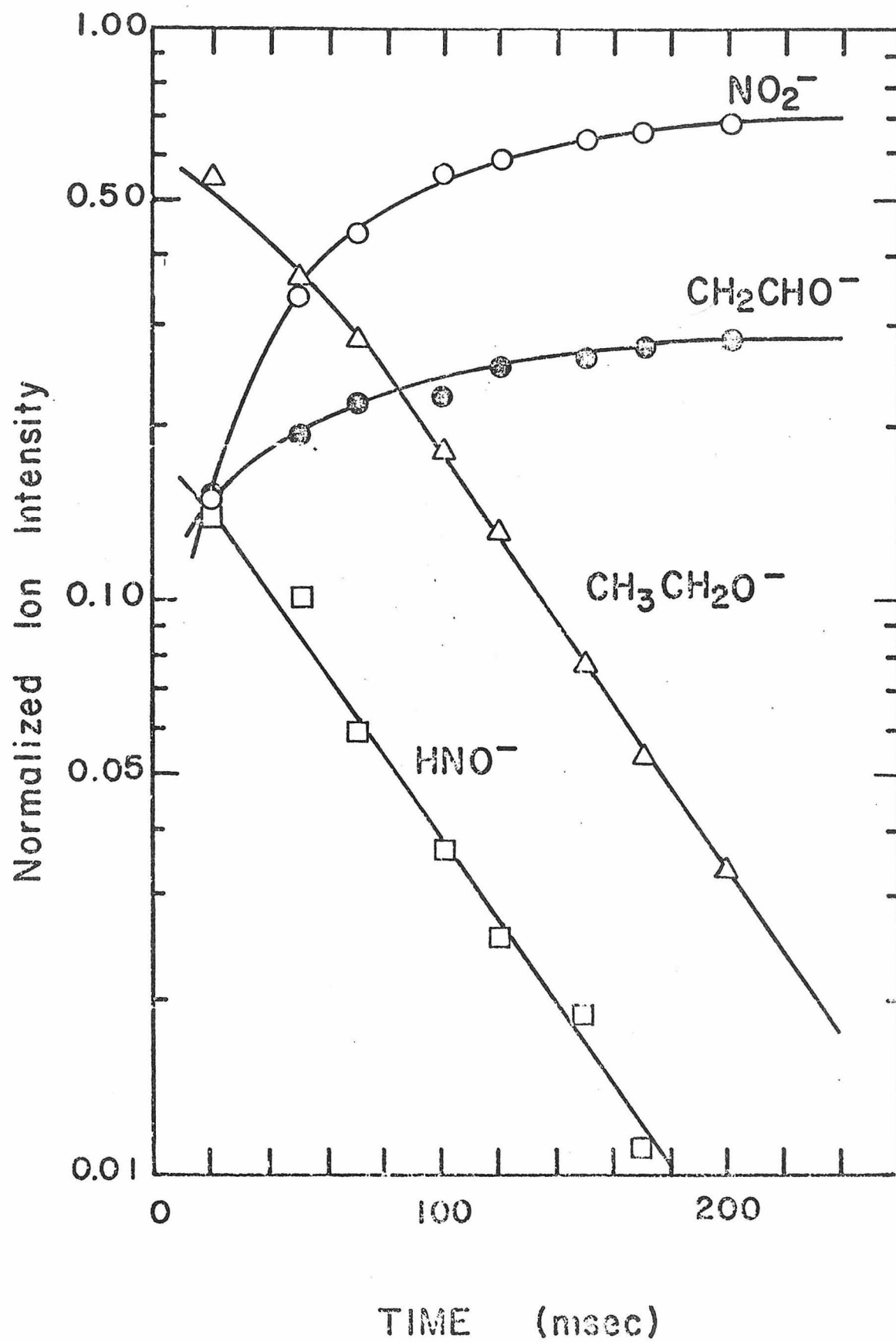
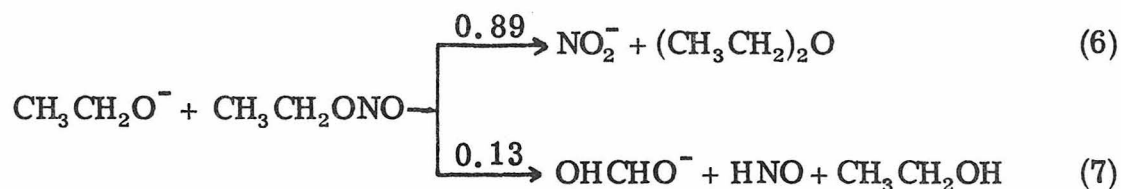


Figure 2

Temporal variation of normalized ion
intensity in 2.0×10^{-6} torr of $\text{CH}_3\text{CH}_2\text{ONO}$.

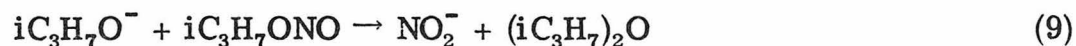




could not be identified by double resonance.⁵ The ion, HNO^- may react with $\text{CH}_3\text{CH}_2\text{ONO}$ forming $\text{CH}_3\text{CH}_2\text{O}^-$ (eq 8), analogous to reaction (5). Rates listed in Table 2 were calculated assuming that CH_2CHO^- is produced only by reaction (7) and that HNO^- reacts only through process (8).



$\text{iC}_3\text{H}_7\text{ONO}$ and $\text{tC}_4\text{H}_9\text{ONO}$. Isopropoxide reacts to form both NO_2^- and $\text{CH}_3\text{CHCHO}^-$ (m/e 57), presumably by reactions (9) and (10). Reaction



(10) is indicated by a large decrease in the intensity of $\text{CH}_3\text{CHCHO}^-$ relative to NO_2^- when the S-P pressure gauge is turned off. Reaction to form $\text{CH}_3\text{CH}_2\text{CO}^-$ is negligible under these conditions, suggesting that reaction (11) does not occur or is very slow. The rate for



reaction (9) is determined with minimum pyrolysis of the nitrite. Again double resonance cannot identify the fate of HNO^- .⁵ By analogy with reaction (5), $\text{iC}_3\text{H}_7\text{O}^-$ may be formed (eq 12).



The only reaction detected in $\text{tC}_4\text{H}_9\text{ONO}$, is formation of NO_2^- from $\text{tC}_4\text{H}_9\text{O}^-$ (eq 13).



Reactions are summarized in Table 2 along with rates determined under conditions of minimum pyrolysis. Since the extent of pyrolysis has not been determined, rates of reactions of HNO^{-4} and reaction (7) may be effected by the presence of impurities. Formation of NO_2^- is not subject to these problems.

Pyrolysis of Alkyl Nitrites. It is well established that alkyl nitrites are easily decomposed by heating⁶⁻⁸ or photolysis.⁹ The initial step in the pyrolysis is cleavage of the weak $\sim 40 \text{ kcal mole}^{-1}$ O—NO bond, to form alkoxy radicals ($\text{RO}\cdot$). Neutral products then result from radical decomposition.^{7, 8} For example, $\text{CH}_3\text{CH}_2\text{O}\cdot$ produced in the pyrolysis of $\text{CH}_3\text{CH}_2\text{ONO}$ (eq 14), will lose CH_3 to form CH_2O (eq 15).



Similarly, $\text{CH}_3\text{CH}_2\text{CHO}$ is formed in pyrolysis of $\text{i-C}_3\text{H}_7\text{ONO}$.

It has recently been determined⁸ that an elimination of HNO from all nitrites except $\text{t-C}_4\text{H}_9\text{ONO}$ occurs in competition with $\text{RO}\cdot$ formation. For example, $\text{CH}_3\text{CH}_2\text{ONO}$ decomposed to HNO and $\text{CH}_3\text{CH}_2\text{O}$ (eq 16).

Table 2. Summary of Reactions and Rates

Reaction	k ^a	ΔH ^b
$\text{CD}_3\text{O}^- + \text{CD}_3\text{ONO} \rightarrow \text{NO}_2^- + (\text{CD}_3)_2\text{O}$	1.90	-40
$\text{CH}_3\text{CH}_2\text{O}^- + \text{CH}_3\text{CH}_2\text{ONO} \rightarrow \text{NO}_2^- + (\text{CH}_3\text{CH}_2)_2\text{O}$	2.24	-39
$\text{iC}_3\text{H}_7\text{O}^- + \text{iC}_3\text{H}_7\text{ONO} \rightarrow \text{NO}_2^- + (\text{i-C}_3\text{H}_7)_2\text{O}$	1.82	-33
$\text{tC}_4\text{H}_9\text{O}^- + \text{tC}_4\text{H}_9\text{ONO} \rightarrow \text{NO}_2^- + (\text{t-C}_4\text{H}_9)_2\text{O}$	1.47	-24
$\text{HNO}^- + \text{CH}_3\text{ONO} \rightarrow \text{CD}_3\text{O}^- + \text{HNO} + \text{NO}$	4.5	~ 0
$\text{HNO}^- + \text{CH}_3\text{CH}_2\text{ONO} \rightarrow \text{CH}_3\text{CH}_2\text{O}^- + \text{HNO} + \text{NO}$	3.9	-4
$\text{HNO}^- + \text{iC}_3\text{H}_7\text{ONO} \rightarrow \text{iC}_3\text{H}_7\text{O}^- + \text{HNO} + \text{NO}$	2.1	-5
$\text{CH}_3\text{CH}_2\text{O}^- + \text{CH}_3\text{CH}_2\text{ONO} \rightarrow \text{CH}_2\text{CHO}^- + \text{CH}_3\text{CH}_2\text{OH} + \text{HNO}$	0.50	-9
$\text{iC}_3\text{H}_7\text{O}^- + \text{iC}_3\text{H}_7\text{ONO} \rightarrow \text{CH}_3\text{CHCHO}^- + \text{iC}_3\text{H}_7\text{OH} + \text{HNO}$	--	-2

^aExperimental rates in units $10^{-10} \text{ cm}^3 \text{ molecule}^{-1} \text{ sec}^{-1}$.

^bHeats of reactions in kcal mole^{-1} at 298°K , calculated using heats of formation in Table 3.

Table 3. Thermochemical Data of Anions and Neutrals Involved in Nitrite Reactions^a

Anion	$\Delta H_f 298^\circ{}^b$	Neutral	$\Delta H_f 298^\circ{}^c$
CD_3O^-	-36.9	NO	21.58 ± 0.04
$CH_3CH_2O^-$	-48.0	HNO	23.8
$i-C_3H_7O^-$	-58.8	CH_3ONO	-15.79 ± 0.25
$t-C_4H_9O^-$	-69.2	CH_3CH_2ONO	-22.3 ± 0.50
CH_2CHO^-	-47 ± 5.0^c	$i-C_3H_7ONO$	-32.7 ± 0.50
CH_3CHCHO^-	-52 ± 5.0^c	$t-C_4H_9ONO$	-42.4 ± 0.50
NO_2^-	-48.45	$(CH_3)_2O$	-43.99 ± 0.12
HNO^-	24^d	$(CH_3CH_2)_2O$	-60.62 ± 0.19
		$(i-C_3H_7)_2O$	-76.20 ± 0.59
		$(t-C_4H_9)_2O$	-87.1 ± 0.40
		CH_3OH	-48.07 ± 0.05
		CH_3CH_2OH	-56.24 ± 0.07
		$i-C_3H_7OH$	-65.5 ± 0.50^f
		$t-C_4H_9OH$	-75.1 ± 0.50^f

^aUnless otherwise noted, values are in kcal mole⁻¹ at 298°C and are taken from J. D. Cox and G. Pilcher, "Thermochemistry of Organic and Organometallic Compounds", Academic Press, New York, 1970 and D. R. Stull and H. Prophet, "JANAF Thermochemical Tables" NSRDS-NBS37, 1971.

^bAlkoxide ion ΔH_f are calculated using $PA(RO^-)$ from J. S. Miller and R. T. McIver, J. Amer. Chem. Soc., 96, 4323 (1974), with correc-

Table 3 (continued)

tions to original data, J. S. Miller, private communication.

^cSee reference 10.

^dSee Appendix II.

^e $\Delta H_f 298^\circ$ for nitrites are calculated using Benson's group additivities and by comparison to known ΔH_f of alkyl nitro compounds. See S. W. Benson, "Thermochemical Kinetics", Wiley, New York, 1976. See also reference 2.

^fEstimated using group additivities, see ref. e.



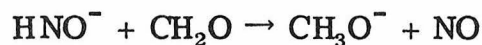
Kinetic studies indicate that for the most part, these eliminations result from heterogeneous surface reactions (pyrex vessel). In only one case, $\text{CH}_3\text{CH}_2\text{ONO}$, was homogeneous elimination expected to contribute significantly to the products formed.

The pyrolysis of nitrites is important to ion-molecule chemistry because of the presence of heated surfaces within the icr cell. Both the heated electron filament and the Schulz-Phelp gauge filament and its shield may induce nitrite decomposition. In $\text{CH}_3\text{CH}_2\text{ONO}$ and $\text{iC}_3\text{H}_7\text{ONO}$, it was found that the amount of enolate anion formed is greatly decreased when the pressure gauge filament is turned off and allowed to cool. Since both CH_3CHO and $\text{CH}_3\text{CH}_2\text{CHO}$ are more acidic than the alcohols,¹⁰ alkoxide ions are expected to abstract protons from them to form the corresponding enolate anions.

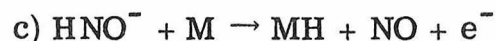
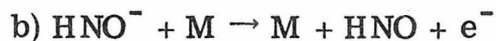
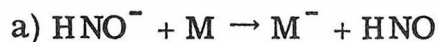
In conclusion, the observed reactivity of the nitrites especially $\text{CH}_3\text{CH}_2\text{ONO}$ and $\text{iC}_3\text{H}_7\text{ONO}$ are strongly moderated by concomitant neutrals reactions. Recent results¹¹ suggest that the generation and reactions of negative ions in other systems may also be affected by surface processes of the neutrals present. Since neutral products can not be routinely detected under icr conditions, such processes are not readily detectible. Therefore care must be taken to consider the possibility of such interfering reactions when ion-molecule chemistry is investigated.

References

1. S. A. Sullivan and J. L. Beauchamp, J. Amer. Chem. Soc., 98, 1066 (1976). S. M. J. Briscese and J. M. Riveros, J. Amer. Chem. Soc., 97, 230 (1975), and J. S. Miller and R. T. McIver, J. Amer. Chem. Soc., 96, 4323 (1974).
2. Techniques of icr spectroscopy are detailed in J. L. Beauchamp, Ann. Rev. of Phys. Chem., 22, 527 (1972).
3. K. Jaeger and A. Heinglein, Z. Naturforsch A, 222, 700 (1967).
4. It should be noted that HNO^- may react with the possible pyrolysis products to form alkoxides. For example:



5. A number of processes may be responsible for decay of HNO^- . Recent studies suggest that $\text{EA}(\text{HNO}) \sim 0$, so that electron transfer (a), collisional detachment (b) and associative detachment (c) may all be favorable.



These processes are discussed by F. H. Paulson in "Ion-Molecule Reactions", Vol. 1, J. L. Franklin, ed., Plenum Press, New York, 1972, p. 77. See also Appendix II.

6. J. B. Levy, J. Amer. Chem. Soc., 78, 1780 (1956) and references therein.

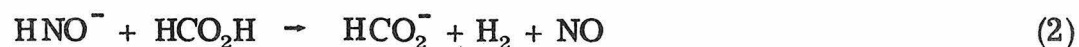
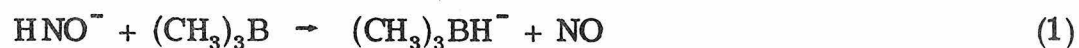
References (continued)

7. L. Batt, K. Christie, R. T. Milne and A. J. Summers, Inter. J. Chem. Kinetics, 6, 877 (1974).
8. L. Batt, R. D. McCulloch and R. T. Milne, Inter J. Chem. Kinetics, 1st Symposium, 441 (1975).
9. For example, P. Kabasakalian and E. R. Townley, J. Amer. Chem. Soc., 84, 2711 (1962).
10. $\text{PA}(\text{CH}_3\text{CHCHO}^-)$ and $\text{PA}(\text{CH}_2\text{CHO}^-)$ are both estimated at $\sim 360 \pm 5$ kcal/mole, B. S. Freiser, unpublished results.
11. S. A. Sullivan and J. L. Beauchamp, Chem. Phys. Lett., in press and this thesis, Chapter I.

Appendix II

Reactions of HNO^-

The unusual ion HNO^- (m/e 31) is generated by electron attachment in alkyl nitrites.¹ Two types of reactions of HNO^- are observed in mixtures of nitrites with neutrals, hydride transfer and apparent proton transfer. For example, HNO^- reacts to transfer H^- to $(\text{CH}_3)_3\text{B}$ (eq 1) while with HCO_2H , only HCO_2^- (m/e 45) is observed. Reaction 2 may proceed directly or by energetic hydride transfer forming



$[\text{H}_2\text{CO}_2\text{H}^-]^*$, which then decomposes to products. Observed reactions are summarized in Table 1 along with thermochemical inferences. In mixtures of CD_3ONO and fluorinated alkanes and alkenes proton transfer to DNO^- is not observed. Considering the reactions listed in Table 1, HNO^- does not abstract a proton from species less acidic than $\text{CF}_3\text{CH}_2\text{OH}$. An approximate $\text{PA}(\text{HNO}^-)$ is then estimated as 365 ± 5 kcal/mole⁻¹. From this, $\Delta\text{H}_f(\text{HNO}^-) = 24 \pm 5$ kcal/mole⁻¹ is calculated, and the electron affinity $\text{EA}(\text{HNO})$ is estimated as ~ 0 . Since HNO^- is involved in H^- transfers, the $\text{D}(\text{NO}-\text{H}^-)$ is of interest. The bond strength is calculated to be a quite weak 31 kcal mole⁻¹.

Table I. Summary of the Reactions of HNO^-

Reaction	Thermochemical References ^f
$\text{HNO}^- + (\text{CH}_3)_3\text{B} \rightarrow (\text{CH}_3)_3\text{BH}^- + \text{NO}^{\text{a}}$	—
$\text{HNO}^- + \text{CF}_3\text{CH}_2\text{OH} \rightarrow \text{CF}_3\text{CH}_2\text{O}^- + \text{H}_2 + \text{NO}^{\text{b}}$	$\text{PA}(\text{HNO}^-) \sim 365 \text{ kcal mole}^{-1}$
$\text{HNO}^- + \text{AsH}_3 \rightarrow \text{AsH}_2^- + \text{H}_2 + \text{NO}^{\text{b}}$	$\text{PA}(\text{HNO}^-) > 356 \text{ kcal mole}^{-1}$
$\text{HNO}^- + \text{HCO}_2\text{H} \rightarrow \text{HCO}_2^- + \text{H}_2 + \text{NO}^{\text{b}}$	$\text{PA}(\text{HNO}^-) > 342 \text{ kcal mole}^{-1}$
$\text{HNO}^- + \text{CH}_3\text{BC}_5\text{H}_6 \rightarrow \text{CH}_3\text{BC}_5\text{H}_5^- + \text{H}_2 + \text{NO}^{\text{c}}$	$\text{PA}(\text{HNO}^-) > 337 \text{ kcal mole}^{-1}$
$\text{HNO}^- + \text{CH}_3\text{ONONO} \rightarrow \text{CH}_3\text{O}^- + \text{HNO} + \text{NO}^{\text{d}}$	$\Delta H_f(\text{HNO}^-) < 24.3 \text{ kcal mole}^{-1}$
$\text{HNO}^- + \text{OPF}_3 \rightarrow \text{OPF}_2^- + \text{HF} + \text{NO}^{\text{e}}$	—
$\text{HNO}^- + \text{PF}_3 \rightarrow \text{NOPF}_2^- + \text{HF}^{\text{e}}$	—

^aM. K. Murphy and J. L. Beauchamp, *J. Amer. Chem. Soc.*, **98**, 1433, 1976.

$\text{PA}[(\text{CH}_3)_2\text{BCH}_2^-] \sim 365 \text{ kcal mole}^{-1}$

^bS. A. Sullivan and J. L. Beauchamp, unpublished results.

^cSee Chapter II.

^dSee Appendix I.

^eSee Chapter I.

^fA table of acidities is given in Appendix III.

Appendix III

Tables of Gas Phase Acidities




The following tables list gas phase proton affinities of anions, which are defined as the enthalpy for reaction 1 or the heterolytic



bond dissociation energy. These values are inversely related to the acidity of BH. These tables present representative values, and as such are not comprehensive lists of all known gas phase proton affinities. The references following the tables represent major contributions to gas phase acidity measurements in the last few years.

Table 1	Hydrocarbons
Table 2	Substituted Alkanes
Table 3	Organic Oxygen Compounds
Table 4	Organic Nitrogen Compounds
Table 5	Inorganic Acids


Table 1. Gas Phase Proton Affinities - Hydrocarbon Acidities^a

MH	PA(M ⁻)	References
CH ₄	>403.8	12
CH ₂ CH ₂	>403.8	12
C ₆ H ₆	395 ± 5	14, 12
CH ₃ CHCH ₂	<390	14, 12
CH ₃ C ₆ H ₄ CH ₃	384 ± 7	15
C ₆ H ₅ CH ₃	373 ± 3 ^b	12
C ₂ H ₂	373.2	15, 12, 8
C ₆ H ₅ CH ₂ C ₆ H ₅	360.6	4
	359.7	4
	352.6	4, 5
	348.5	4

^aAll values in kcal/mole at 298°K. Unless otherwise noted error limits can be considered $\leq \pm 2.0$ kcal/mole.

^bElectron affinity measurements suggest $\text{PA}(\text{C}_2\text{H}_5\text{O}^-) > \text{PA}(\text{C}_6\text{H}_5\text{CH}_2^-) > \text{PA}(\text{t-C}_4\text{H}_9\text{O}^-)$ see Table 3 and J. H. Richardson, L. M. Stephenson and J. I. Brauman, J. Chem. Phys., **63**, 74 (1975).

Table 2. Gas Phase Proton Affinities - Acidities of Substituted Alkanes^a

MH	PA(M ⁻)	References
CH ₃ F	> 390 ^b	-
CH ₂ F ₂	384 ± 7 ^b	-
CHF ₃	377 ± 3 ^c	-
C ₆ H ₅ CH ₃	376 ± 3	12
CH ₃ CH ₂ F	374 ± 3 ^d	-
CH ₃ CN	366.3 ^e	4
CHCl ₃	<363	12
CH ₂ Cl ₂	>366.3	12
CH ₃ NO ₂	>350	12
CF ₃  CH ₃	347	4, 5
(CN) ₂ CH ₂	330.8	4

^aAll values in kcal/mole at 298°K. Unless otherwise noted error limits can be considered ≤ ± 2.0 kcal/mole.

^bS. A. Sullivan and J. L. Beauchamp, unpublished results.

^cB. S. Freiser and J. L. Beauchamp, unpublished results.

^dS. A. Sullivan and J. L. Beauchamp, J. Amer. Chem. Soc., 98, 1060 (1976).

^eNote a footnote correction to PA(CH₂CN⁻) in reference 4.

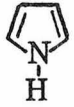
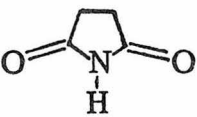
Table 3. Gas Phase Proton Affinities - Acidities of Organic Oxygen Compounds⁹

MH	PA(M ⁻)	References
H ₂ O	390.7 ^b	13, 12
H ₂ CO	>378.3 ^c	
CH ₃ OH	378.3 ^d	} 16, 8
C ₂ H ₅ OH	375.4	
i-C ₃ H ₇ OH	373.5	
t-C ₄ H ₉ OH	372.7	
CH ₃ CHO	<370.1 ^c	
CH ₃ COCH ₃	363.6	4
C ₆ H ₅ OH	347	10
CH ₃ CO ₂ H	345.8	9
HCO ₂ H	342.6	9
CH ₃ COCH ₂ COCH ₃	341.6	4
C ₆ H ₅ CO ₂ H	337.1	7

^aAll values in kcal/mole at 298°K. Unless otherwise noted error limits can be considered $\leq \pm 2$ kcal/mole.

^bCalculated from electron affinity data, see Table 5.

Table 4. Gas Phase Proton Affinities - Acidities of Organic Nitrogen Compounds^a

MH	PA (M ⁻)	References
NH ₃	403.8 ^b	
CH ₃ NH ₂	402 ± 3 ^c	15
(CH ₃) ₂ NH	395 ± 5 ^c	15
	355.4	4, 5
CH ₃ CONHCOCH ₃	343.7	4, 5
	341.3	4, 5

^aAll values in kcal/mole at 298°K. Unless otherwise noted error limits can be considered $\leq \pm 2$ kcal/mole.

^bSee Table 5.

^cJ. I. Brauman, private communication.

Table 5. Gas Phase Proton Affinities - Acidities of Inorganic Hydrides^a

M	PA(M ⁻) ^b	References
NH ₃	403.8	13, 12
H ₂	400	
H ₂ O	390.7	13, 12
HF	370.1	13
PH ₃	370 ^c	13
HCN	350.3	
H ₂ S	351	13
H ₂ Se	343 ^d	
HNO ₂	337	
HCl	333.3	13
HNO ₃	324.5	
HBr	323.6	13
HI	314.4	13

^aAll values in kcal/mole at 298°K. Unless otherwise noted error limits can be considered $\leq \pm 2$ kcal/mole.

^bUnless otherwise noted these values are calculated from data in D. R. Stull and H. Prophet "JANAF Thermochemical Tables" U.S. Government Printing Office, Washington, D.C., 1971.

^cPrivate communication, J. S. Miller and R. T. McIver.

^dElectron affinity EA(HSe) = 2.21 ± 0.03 eV from K. C. Smyth and J. I. Brauman, J. Chem. Phys., 56, 5993 (1972).

References

1. J. E. Bartmess, W. J. Hehre, R. T. McIver, Jr., and L. E. Overman, J. Amer. Chem. Soc., 99, 1976 (1977).
2. J. E. Bartmess and R. T. McIver, Jr., J. Amer. Chem. Soc., 99, 4163 (1977).
3. T. B. McMahon and P. Kebarle, J. Amer. Chem. Soc., 99, 2222 (1977).
4. T. B. McMahon and P. Kebarle, J. Amer. Chem. Soc., 98, 3399 (1976).
5. P. Kebarle, R. Yamdagni, K. Hiraoka and T. B. McMahon, Int. J. Mass Spectrom. Ion Physics, 19, 71 (1976).
6. R. Yamdagni and P. Kebarle, Can. J. Chem., 52, 861 (1974).
7. R. Yamdagni, T. B. McMahon and P. Kebarle, J. Amer. Chem. Soc., 96, 4035 (1974).
8. R. T. McIver and J. S. Miller, J. Amer. Chem. Soc., 96, 4323 (1974).
9. R. Yamdagni and P. Kebarle, J. Amer. Chem. Soc., 95, 4050 (1973).
10. R. T. McIver, Jr., and J. H. Silvers, J. Amer. Chem. Soc., 95, 8463 (1973).
11. K. Hiraoka, R. Yamdagni and P. Kebarle, J. Amer. Chem. Soc., 95, 6833 (1973).
12. D. K. Bohme, E. Lee Ruff and L. B. Young, J. Amer. Chem. Soc., 94, 5153 (1972).

References (continued)

13. J. I. Brauman, J. R. Eyler, L. K. Blair, M. J. White,
M. B. Comisarow and K. C. Smith, J. Amer. Chem. Soc.,
93, 6360 (1971).
14. D. K. Bohme and L. B. Young, Can. J. Chem., 49, 2918
(1971).
15. J. I. Brauman and L. K. Blair, J. Amer. Chem. Soc., 93,
3911 (1971).
16. J. I. Brauman and L. K. Blair, J. Amer. Chem. Soc.,
93, 4315 (1971).
17. J. I. Brauman and L. K. Blair, J. Amer. Chem. Soc.,
92, 5986 (1970).